ALMA MATER STUDIORUM – UNIVERSITÀ DI BOLOGNA
SCHOOL OF ENGINEERING AND ARCHITECTURE

Master degree in
CHEMICAL AND PROCESS ENGINEERING
SUSTAINABLE TECHNOLOGIES AND BIOTECHNOLOGIES FOR ENERGY AND MATERIALS

A MEMBRANE PROCESS TO EXTRACT CITRUS LEMON DERIVED EXTRACELLULAR VESICLES

Master thesis on
BIOREACTORS AND DOWNSTREAM PROCESSES

SUPERVISOR:
Prof.ssa Cristiana Boi

PRESENTED BY:
Zubin Kunhi Mahin

CO-SUPERVISOR:
Prof.ssa Serena Bandini

ACADEMIC YEAR 2020/21

ACKNOWLEGMENT

I would like to express my immense gratitude towards my supervisor Prof.ssa Cristiana Boi for introducing me to this topic and offering advices and suggestions every step of the way from the very beginning. Prof.ssa Boi's expertise in the field has been indispensable for the development of the methodology for this thesis. I would like to thank Prof.ssa Serena Bandini for offering extra assistance and feedback for this work.

Additionally, I thank Prof. Francesco Francia and Stefano Cerini for allowing me to use their laboratories. The help of Ricardo Onesti has been of immense importance for setting up of experiments and analyses. I thank Thomas Fabiani for valuable advices he offered me at the beginning of this study. I also express my deep gratitude towards my lab partner Sara Giancaterino for always brainstorming with me and sometimes challenging me for the best of this project.

I would like to thank UNIBO and the STEM department for accepting my application two years ago and the DICAM laboratories for welcoming me for carrying out my work.

I would like to thank my parents, my brothers and my dear friends for undying support and love without which I would not be here. Thank you all.

TABLE OF CONTENTS

ACKNOWLEGMENT **1**

ABSTRACT **4**

INTRODUCTION **5**

LITERATURE REVIEW **7**

2.1. CLASSIFICATION OF VESICLES 7

2.1.1. EXOSOMES 7

2.1.2. MICROVESICLES 8

2.1.3. APOPTOTIC BODIES 9

2.2. CONSTITUENTS OF VESICLES 10

2.2.1. PROTEINS 10

2.2.2. LIPIDS 11

2.2.3. RNA 11

2.2.4. DNA 12

2.3. POTENTIAL APPLICATIONS OF EVs 13

2.3.1. EVs FOR DRUG DELIVERY 13

2.3.2. NEUROLOGICAL DISEASES 14

2.3.3. CARGO LOADING 14

2.3.4. AS A DIAGNOSTIC TOOL 15

2.3.5. REGENERATIVE MEDICINE 16

2.4. ISOLATION OF EXTRACELLULAR VESICLES 17

2.4.1. BASED ON SIZE AND DENSITY. 18

2.4.2. BASED ON SOLUBILITY 25

2.4.3. BASED ON CHARGE 28

2.4.4. BASED ON AFFINITY INTERACTIONS 31

2.4.5. BASED ON MICROFLUIDICS 33

2.5. EXTRACELLULAR VESICLES FROM PLANTS 38

2.5.1. CONSTITUENTS 40

2.5.2. APPLICATION 41

2.6. CITRUS LEMON 42

2.7. CITRUS LEMON VESICLES 44

2.8. STORAGE 45
MATERIALS AND METHODS 47
3.1. MATERIALS 47
3.2. INSTRUMENTS 48
RESULTS AND DISCUSSION 67
4.1. PRE-TREATMENT 68
4.2. STAGE WISE DIAFILTRATION 69
4.3. MEMBRANE GEL LAYER 71
4.4. MEMBRANE SELECTION 72
4.5. MODEL FOR STAGE DIAFILTRATION 77
4.6. THE EFFECT OF BUFFER USED 78
4.7. TANGENTIAL FLOW FILTRATION 80
4.7.1. TFF WITH 0.5 DIAVOLUMES 82
4.7.2. TFF WITH 1.5 DIAVOLUMES 83
4.7.3. FINAL PROTOCOL WITH RESUSPENSION OF CAKE WITH EVERY DIA VOLUME 85
4.8. MICROSCOPIC ANALYSIS OF MEMBRANE GEL LAYER. 88
4.9. MODEL OF TANGENTIAL FLOW FILTRATION 89
4.10. ULTRACENTRIFUGATION 90
4.11. DYNAMIC LIGHT SCATTERING 92
4.12. BCA ASSAY 96
4.13. STORAGE TEST 98
4.14. QUANTIFICATION OF EVs 101
CONCLUSION AND FUTURE PROSPECTS 104
REFERENCES 107
LIST OF FIGURES 113
LIST OF TABLES 115
APPENDIX I 116
APPENDIX II 117
APPENDIX III 119

ABSTRACT

Extra cellular vesicles are membrane bound and lipid based nano particles having the size range of 30 to 1000 nm released by a plethora of cells. Their prime function is cellular communication but in the recent studies, the potential of these vesicles to maintain physiological and pathological processes as well as their nano-sized constituents opened doors to its applications in therapeutics, prognostics, and diagnostics of variety of diseases such as cancer. Their main constituents include lipids, proteins, mRNAs and micro-RNAs. They are categorized into subtypes such as exosomes (30 to 150nm), micro-vesicles (100 to 800nm) and apoptotic bodies (800 to 5000nm). In mammalian cells, EVs are found in bodily secretions such as milk, urine, semen, and saliva and they have different properties with respect to the source of origin.

In recent studies, extracellular vesicles that are derived from plants such as ginger, grapefruit, broccoli, and lemon are gaining high regard due to their variety of advantages such as safety, non-toxicity, and high availability which promotes large scale production.

EVs are isolated from mammalian and plant cells using multitude of techniques such as Ultracentrifugation, Membrane filtration, Size Exclusion Chromatography, Precipitation and so on. Ultracentrifugation is considered the benchmark for EV purification. But due to the variety in the sources as well as shortcomings arising from the isolation method, a scalable and inexpensive EV isolation method is yet to be designed.

This study focusses on isolation of EVs from citrus lemon juice through membrane diafiltration. Lemon is a promising source due to its broad biological properties to act as antioxidant, anticancer, and anti-inflammatory agents. Lemon derived vesicles was proven to have several proteins analogous to mammalian vesicles. A diafiltration could be carried out for successful removal of impurities and more importantly it is a scalable, continuous technique with potentially lower process times than ultracentrifugation. The concentration of purified product and impurities are analysed using Size Exclusion Chromatography in analytical mode. It is also considered imperative to compare the results from diafiltration with gold standard UC. BCA is proposed to evaluate total protein content and DLS for size measurements. Finally, the ideal mode of storage of EVs to protect its internals and its structure is analysed with storage tests.

CHAPTER 1

INTRODUCTION

Extracellular vesicles (EVs) were first discovered in the mid-20th century by Chargaff, Erwin, and Randolph West [1] in the human plasma. They are released by a variety of cells of prokaryotes, eukaryotes, and plants [2]. The structure of vesicles involves biological entities such as proteins, RNAs, lipids and metabolites enclosed by a phospholipid bi-layer membrane [3]. Therefore, the cellular information from EVs can be transmitted by all these biomolecules making it suitable for delivery as well as protection of information even at longer distances from the origin [2]. In humans, EVs are observed in variety of body fluids such as serum, plasma, saliva etc.

There exists a huge discrepancy in the morphology and properties of the constituents such as proteins in the EVs with respect to the source of extraction as well as the method. There is also variation in the contents between a healthy and a sick person or in the case of intense physiological changes, for instance, in pregnancy. So, EVs can also be regarded as a marker for many diseases such as cancer. Cancer progression involves extensive communication between cells which in turn involves EVs. Hence, both the healthy and the sick cells can be used for diagnostics as well as treatment as drug delivery vehicles specifically targeted at the cancer cells [4]. Furthermore, EVs have high bioavailability. If a drug is loaded into the interior of the vesicles, the immune system will not reject it and more importantly, EVs have the distinct ability of crossing the blood-brain barrier which potentially makes it a unique drug delivery vehicle for rare neurological diseases [5]. Also, their potential to alter the recipient cells can point towards their use in regenerative medicine [6] to replace and replenish the recipient cell.

Very recently, nanovesicles with similar morphology and diameters as that of mammalian vesicles were found to be released by plants through fruits and vegetables such as grape, grapefruit, carrot, ginger, broccoli, and lemon [7]. This opened new doors in EV research for large scale production. Since plants are involved in diets, human immune systems are accustomed to them. Therefore, plant derived EVs can be considered non-toxic and non-immunogenic. They are proven to have tissue specific binding properties and high internalization rate with mammalian cells [8]. Moreover, plant vesicles are not limited by

availability. Due to this, plant vesicles are an interesting source for application that are established for mammalian vesicles such as targeted drug delivery.

Lemon juice vesicles have striking similarity with mammalian vesicles regarding size and proteomics [2]. Because of the abundant components such as flavonoids and phenolic acids, they house wide mammalian friendly biological properties. They are also proven to proliferate tumour cells and hence can be ideal for drug delivery. They are proven to have high internalization with human cells, hence boosting its therapeutic potential. Previously lemon vesicles were isolated using ultracentrifugation [9]. This project applies diafiltration to purify lemon vesicles. Diafiltration can remove smaller proteins and impurities and purify large EV volumes in a fast and cost-effective manner. The resulting retentate and permeates are analysed using size exclusion chromatography with HPLC and FPLC to interpret the extent of purification done. Additionally, the EV fraction are analysed with DLS for its size and zeta potential and with BCA for its total protein contents.

For the efficient application of vesicles, it is essential to understand the method of storage and maintenance of physical structure and biological characteristics for long time. EVs are known to aggregate and alter its morphology and lose its biological activity with time. The general model of storage is to freeze EVs at -80°C which is considered a major bottleneck due to the economic disadvantage. Sugars like trehalose are usually used as a cryoprotectant to protect EVs from the effects of freezing. In this project storage at different temperatures are studied with and without the use of trehalose to elucidate the effects.

CHAPTER 2

LITERATURE REVIEW

2.1. CLASSIFICATION OF VESICLES

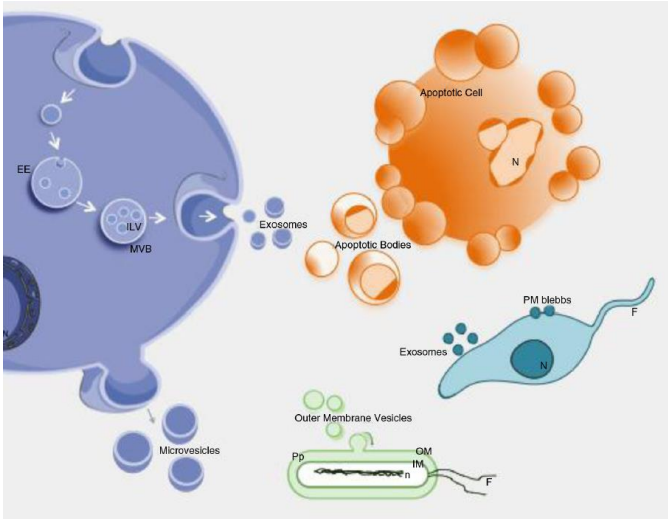

Figure 1: Classification of EVs and their release [10]
EE: early endosome; MVB: multi-vesicular body; N: Nucleus;

Extracellular vesicles can be broadly classified into 3 main classes according to the consensus in International Society for Extracellular vesicles (ISEV) [3]:

2.1.1. EXOSOMES

Exosomes are the smallest sub-type of EVs with a diameter ranging from 30 to 150 nm secreted by all types of cells. They are formed due to the inward budding of the membrane of an early endosome as it evolves into Multi vesicular bodies (MVBs) as shown in figure 2. The function of early endosome and such MVBs are storage, transport, and release of cellular materials. When fused with the plasma membrane of the cell, they release its constituents into the outer cellular space. The exosome is one of the constituents released in this fashion.

The formation of exosomes is controlled by the endosomal sorting complexes required for transport (ESCRT) proteins such as Alix, TSGG101 etc. These proteins are generally identified as exosomal markers since they are expected to be found in almost all exosomes. There exists another pathway which is independent of ESCRT using certain enzymes and tetraspanin proteins such as CD63 to cause the inward budding and hence the release of exosomes [2]. There is a discrepancy in understanding these pathways as these are not universal for all types of cell sources. Additionally, these proteins were found also in other vesicular subtypes [4].

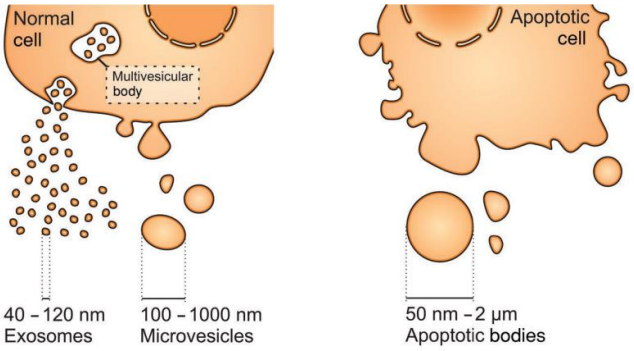

Figure 2: Figure 2: Formation of EVs subtypes [10].

Initially these exosomes were considered as nothing more than cellular debris but in the past two decades they have held high regard due to their cellular communication, maintenance of homeostasis, disease detection, and drug delivery. For example, they have a major role in cancer metastasis [11] and urinary exosomes can reveal kidney damage [4]. So, these exosomes can be applied for 'liquid biopsy' which is a non-invasive and non-risky way of detecting diseases using markers such as exosomes. As mentioned before, exosomes are ideal drug delivery vehicles since they are bio-compatible and bio-available. So, exosomal drug delivery can be useful for diseases like cancer which is usually treated with chemotherapeutic drugs with very poor bioavailability [10].

2.1.2. MICROVESICLES

Microvesicles, sharing similar functions as that of exosomes, on the other hand, are formed when the plasma membrane of the parent cells is budding outwards as shown in figure 2. They have the average diameter ranging from 100 nm to 1 µm. They share the similar functions as that of exosomes. They also carry the ability for inter cellular communication hence changing

the conditions in the parent and recipient cells. This rises from the innate ability of EVs to carry and encapsulate its constituents such as proteins and nucleic acids and deliver it with pathways elucidated in figure 3.

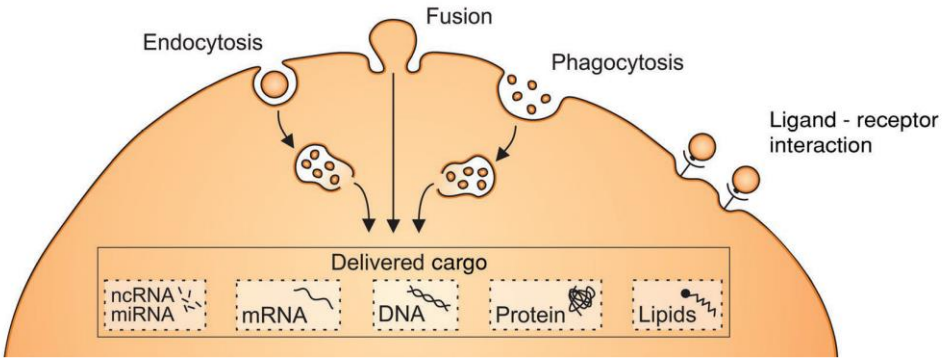

Figure 3: Cells recieving EVs [10]

Cells take up EVs by endocytosis which is the budding off of the EVs into the recipient cell, the fusion of both cellular and EV membrane, or by (phagocytosis). Besides, ligand–receptor interaction can also cause this transport of cargo. Due to their similarity in origin as well as functions, the potential uses of microvesicles are similar to that of exosomes.

2.1.3. APOPTOTIC BODIES

Apoptotic bodies are released to the extracellular space after apoptosis (cell death). The average diameter ranges from 50nm to 5000nm. As shown in figure 2, they form by cutting away or blebbing from the plasma membrane. In contrast to other subtypes, apoptotic bodies vary in their proteomic and biological constituents. As they are result of cell death, the constituents include cell organelles and proteins associated to such organelles such as mitochondria, nucleus, golgi apparatus and endoplasmic reticulum. They also contain tetraspanins such as CD63, just like their smaller counterparts. On the contrary, glycoproteins are absent from apoptotic bodies in comparison with the other subdivisions [6]. Apoptotic bodies are found in large concentration and are usually removed for processing exosomes or microvesicles [10].

2.2. CONSTITUENTS OF VESICLES

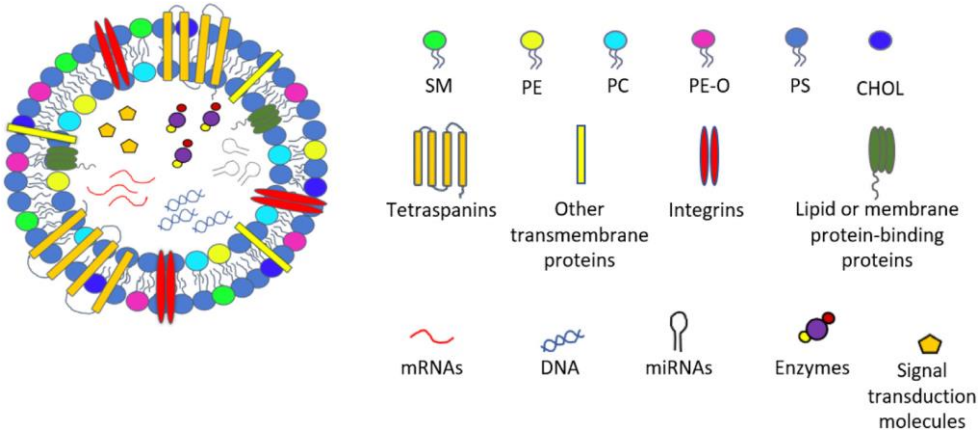

Figure 4: EV composition

SM: Sphingomyelin; PE: phosphatidylethanolamine; PC: phosphatidylcholine;

PE-O: alkyl-ether substituted phosphatidylethanolamine PS: phosphatidylserine; CHOL: cholesterol [3]

2.2.1. PROTEINS

The protein content and its composition in vesicles vary according to the parent cell where it is derived from and the type of isolation [12]. Proteins composition can elucidate the functions, origin, and biogenesis of the EVs. Proteins are not only a relevant cargo of EVs but also an important factor in defining the structure of EVs [12]. The three different classifications of EV have a clear variation in the protein composition. In exosomes there is a high concentration of tetraspanins such as CD37, CD53, CD63. Due to the involvement of ESCRT proteins in the biogenesis of exosomes, there exists a high concentration of ESCRT proteins as well as the proteins such as Alix and TSG101 due to its role in the ESCRT pathway with which exosomes are produced [3]. On the other hand, micro vesicles, being formed due to the outward budding of plasma membrane contains high concentration of proteins such as glycoproteins and phosphoproteins. Finally, since apoptotic bodies contain cell organelles that undergo cell-death, there is a high concentration of DNA-binding histones and contains no glycoproteins as opposed to the smaller vesicles [12]. EVs in general are abundant in heat shock proteins such as HSC70, HSP84 and HSPA8 [2]

Despite the differences, some proteins like tetraspanins, ESCRT, Alix are found in all EV subdivisions and are generally regarded as EV protein markers [3]. Consequently, since the differences are minute, it is tedious to differentiate the subdivisions of EVs based on their

proteins. Furthermore, there is no singular marker that is only specific to EV in general for identification either [2].

Mass spectrometry-based proteomics are the most abundantly used technique for profiling [2]. There are online databases that constantly update and report the proteins identified in EVs, one such is Vesiclepedia (http://microvesicles.org/index.html. The best technique would be to compare the top identified proteins from such dynamic databases to analyse the different proteins in different subdivisions of EVs.

2.2.2. LIPIDS

Lipids are important EV cargo which has substantial role in the biogenesis and functions of EVs [2]. They are also an integral to the structure of EVs since the membrane enclosure consists of a phospholipid bilayer. This bilayer is responsible for stability of EVs in different types of environments and consequently lipids play a key role in stability [3]. Like proteins, there exists a disparity in the content and composition depending on the source of extraction but generally, all EVs contain lipids such as sphingomyelin, cholesterol, and glycol-sphingolipids. The fact that EVs contains lipids is further proof that lipids play key role in structural rigidity as well as resistance to shocks upon transfer to different environments [10]. Besides, the concentration of these lipids is higher than that of cell membranes which indicates that the rigidity of EV bilayer could be even higher than that of cell [2]. Furthermore, cholesterol has been found to be important for the release of EVs since they have the innate ability to cause apoptosis of the cell. Consequently, lipids can cause alterations in the recipient cell and could be key to cell-to-cell communication [3].

Major identified lipids belonging to EVs can be found in databases such as Vesiclepedia mentioned in the previous section. Unfortunately, the lipidomic of EVs are still a growing research field albeit a fascinating one.

2.2.3. RNA

RNA is regarded as critical biomolecules in EVs for their ability for cell-to-cell communication. EV RNAs are noticed in free form, as EV enclosed or as protein bound complexes [10]. Generally, the research is focussed on micro-RNA (miRNA) even though other species such as mRNA and fragments of r-RNA, Y-RNA as well as t-RNA is found in

vesicles [2]. In comparison with RNAs in cellular environment, EV RNAs are shorter and has about 200 nucleotides in comparison with 400-12000 nucleotides in cells, although this typically depends on the cell of origin [2].

There is evidence that suggests EVs are capable of transferring mRNAs to the recipient cells. This transferred RNA can be taken up by the cell and translated hence suggesting their role in altering the recipient cell. mRNA can also help in maintaining homeostasis in the recipient cell since the mRNA cont,ent is controlled by the stress condition inside the cell [2].

Similarly, miRNAs have the capability to alter and regulate gene expression upon translation in the recipient cell. Also, miRNAs perform an important role in the immune response system [10]. The list of identified RNAs in vesicles can be found in online databases like Vesiclepedia.

It is becoming clear that RNAs play a role in intracellular communication. But the characterisation technique and the isolation technique can influence RNA detection and quantification [2]. Besides, it is difficult to deduce what percentage of the detected RNA in EVs remain functional and what percent is fragmented from the cellular RNA during biogenesis. This is crucial to understand since RNA is one of the cargos that EVs can transport and deliver to recipient cells even at longer distances [10].

2.2.4. DNA

DNA in EVs is perhaps the least explored biomolecule. Although their presence and amount vary with respect to the subclass of EVs, DNA is abundantly found in apoptotic bodies. Identified EV DNAs include Mitochondrial DNA single-stranded DNA and double-stranded DNA (dsDNA) [13]. The size of DNAs ranges from 100 base pairs to 2500 base pairs in EVs [6].

Studies have suggested that EV DNAs can be used as a translational marker to identify mutations in tumour cells [2]. It is also possible to deduce the stage of development of tumour using this DNA. Despite these promising developments, the functional and the physiological significance of EV DNAs are yet to be explored.

2.3. POTENTIAL APPLICATIONS OF EVs

Extracellular vesicles have the innate ability to transfer biomolecules such as proteins, lipids, and nucleic acids to long and short distances. These biomolecules can include important genetic and physiological information of the origin cell and is well protected owing to its strong lipid bilayer. Since diseased and normal cells have clear distinction in EV morphology and constituents, its potential as a biomarker for diseases are being broadly explored [14]. Extensive research proves its role in regulating the immune system and stem cell maintenance. Furthermore, they can prevail deep inside tissues while maintaining their biostability. Hence, EVs are promising in the field of regenerative medicine [5]. Recently, the study has been focussed on the involvement of EVs in the pathology and progression of various diseases such as cancer [13] and several neurological diseases [6]. These focussed studies on cancer include promising aspects such as liquid biopsy for detection, treatment through usage as drug delivery, and live monitoring of the prognosis [5]. These stands out from the usual method of treatment and detection since it is completely non-invasive and non-toxic. Since EVs are cell-free and their application are not influenced by the tumour cells and they do not undergo a transformation and hence they maintain stability during its employment. Given EVs' association with the immune system, they also have been explored as vaccines in recent studies [4]. Neurological diseases on the other hand are emphasized due to the capability of EVs to cross the blood-brain barrier (BBB) to deliver drugs to the site in the human brain [15]. The treatment methods for such diseases are stagnant due to the inability of other drug delivery vehicles to do so. This budding field of study is however impeded by the inexistence of standardization in isolating and characterising the vesicles. Since clinical trials require EVs of high purity and consistent source of origin, it is difficult to standardize this as well. Most of the techniques used are size based and hence it is difficult to differentiate between different subtypes such as exosomes and micro vesicles due to their overlapping size ranges [4].

2.3.1. EVs FOR DRUG DELIVERY

The most prominent nano drug delivery system in past decades is liposomes which shares the similarity with EVs with respect to size and the employed drug loading method. So, it is interesting to make that comparison. Liposomes also contain a phospho-lipid bilayer surrounded by an aqueous core. Both vehicles can transport hydrophilic and hydrophobic

agents on the lipid membrane or in the interior [5]. Since nanoparticles share similar dimensions with bacteria and viruses, it can be recognized by the immune system. EVs offer a unique advantage of circumventing the immune system and can last longer in the system with higher stability. Additionally, EVs can target specific cells to undergo the uptake mechanism [5]. However, the similarity with liposomes is taken advantage of when exploring the research into drug loading method and range of application.

2.3.2. NEUROLOGICAL DISEASES

EVs stands out from the prevalent drug delivery systems in their ability to cross the blood brain barrier (BBB) [4]. BBB is a diffusion barrier that selectively permeates small molecules. This barrier impedes drug delivery systems for delivering the drugs to the brain for neurological disorders. Further, EVs can last longer without detection from the immune system. In addition to drug delivery, EVs can regenerate cells and tissues and have therapeutic effects. Hence, they serve a dual purpose in the case of neurological disorders since central nervous system has poor self-regeneration [4]. Even though the potential is undeniable, these drug delivery systems need to efficiently load the cargo and have components which boost targeting and selectivity.

2.3.3. CARGO LOADING

Depending on the intended purpose, EVs can intrinsically carry molecular cargo across biological barriers. They can be loaded with several drugs, small molecules, nucleic acids, and proteins, without causing immuno-toxicity [16]. The loading efficiency, however, is influenced by the type of cargo loaded, EV source, type of isolation and the loading method.

Loading methods can be categorized as pre-loading and post loading. Pre-loading is done during the EV biogenesis while post loading is after EV isolation [16].

Components like proteins can be simply loaded into the parent cells of EVs during its biogenesis. The drawback however is the random loading and expression of these proteins. Pre-loading methods are time consuming and can have low loading efficiency. This method is preferred for small hydrophobic molecules like the chemotherapeutic drug Doxorubicin which has been successfully loaded onto EVs [16]. Despite that, pre-loading methods are not detrimental to the surface integrity of the membrane bilayer and are easy to carry out.

Post loading involves mixing of drugs with isolated EVs. The lipid membrane in EVs is hydrophobic hence post loading is easier with hydrophobic drugs.

Nucleic acids are loaded to EVs for mainly RNA based therapies. Electroporation is a general post loading strategy used to load RNAs to EVs wherein the lipid membrane permeability is increased using an electric field across it [4]. Nucleic acids possess the same negative charges as that of vesicles so the loading is a strenuous procedure [4]. Sonication has been previously used to load proteins onto EVs. Sonication can disrupt the rigidity of EV membranes [16]. Freeze-thaw cycles is a post loading strategy since the thermal energy is proven to interfere with the lipid membrane but these methods are found to be harsh towards EV morphology and cause aggregation [4]. Some small molecules like steroids were previously loaded by simple mixing in the EV medium.

EV surfaces are sometimes engineered to be coupled with targeting ligands, stimuli responsive agents or immune evasive agents to improve targeting capacity, specificity, and long-term distribution [4]. This can be advantageous since tumours with acidic pH can be selectively targeted by using pH sensitive functional groups. So, upon the introduction in the vicinity of the tumour, the loaded drugs will specifically release at the tumour site. Additionally, immune evasive agents are added to help EVs in alleviating immunotoxicity [14]. Previously PEG has been used to avoid the detection of immune system upon the inception of EVs in the system. However, most of these strategies, albeit being effective are very expensive and at present only viable in small or laboratory scale.

2.3.4. AS A DIAGNOSTIC TOOL

The majority of EV application in both diagnostics and treatment is applied to the abominable disease of cancer. Cancer is usually treated with chemotherapy which has the downsides of low bioavailability, low specificity, and the apparent side effects [13]. In addition to the role of EVs in drug delivery for cancer treatment, they will have a major role to play in cancer detection and progression monitoring in the future. Normal cells and diseased cells possess distinct characteristics. EVs derived from diseased cells are known to deliver cargo that can control the progression of diseases such as colon cancer [14] and can elucidate information that reveals their response to treatment. These vesicles contain specific proteins or nucleic acids that is absent in a normal cell derived EVs [14]. Besides, tumour cells always communicate with each other. The fact that EVs are considerably involved in cellular communication, further proves that EVs are a critical component of tumour metastasis. Moreover, EVs are also known to be involved in tumour growth and survival [6]. As a result, research has been growing for the application of EVs in cancer research as seen in figure 5. The chart is obtained by using key word search for exosomes and cancer.

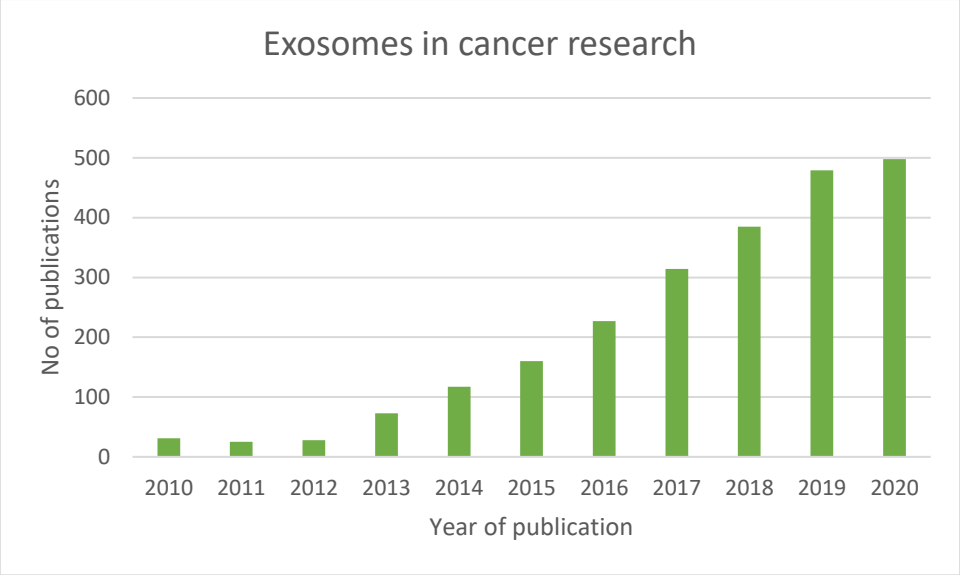

Figure 5: No of publications based on cancer and EVs research in the past decade (PubMed)

Recent studies have revealed that certain tumour cells release an altered version of EVs termed as large oncosomes [13]. These are significantly larger than most EV subtypes with a size range of 1-10 µm. It is an attractive field of study since this detection can be obtained even at very early stages of cancer in a completely non-invasive way. Consequently, EVs are gaining popularity in liquid biopsy field which is the analysis of certain biofluids such as serum and blood for disease detection. This is also an effective tool for relapse monitoring [6].

2.3.5. REGENERATIVE MEDICINE

Regeneration is the natural ability of cells and tissues to replenish and restore itself following a damage. Their inherent function of cellular communication further revealed their role in tissue repair, immune system modulation and stem cell maintenance. Application of the same in regenerative medicine is possible since they can mimic the natural repair process and implicate a therapeutic effect [17]. It has been postulated that this cell free delivery can offer the same advantages of a stem cell replacement [18].

As an inference, the potential of EVs in diagnostics and treatment is a fast-developing field. This growth however is slowed down due to the absence of standardization in isolating and characterizing the vesicles. EVs required in clinical trials need to be of high purity and should ideally have less variability regarding the source of extraction. Most conventional methods are

not able to achieve this and hence different isolation techniques must be discussed and evaluated for these undoubtedly beneficial applications.

2.4. ISOLATION OF EXTRACELLULAR VESICLES

Despite the advances in their potential uses, a universally accepted isolation method is not available for EVs. Even though ultracentrifugation is considered the benchmark, the long process times, and low recovery rates and more importantly the lack of scalability and automation has led to the research in other isolation techniques such as membrane filtration, precipitation with crowding reagent, size exclusion chromatography etc.

An overview of average number of publications according to PubMed the isolation of vesicles since the turn of the century is given in figure 6. Ultracentrifugation, precipitation, and SEC can be considered as conventional method in this time frame. Very recent developments revealing the physical and biological characteristics of EVs have led to the advent of advanced technologies such as microfluidics, electrophoresis, field flow fractionation, and affinity-based separation to be applied in EV research to obtain EVs of superior quality with lower process times. Most of these advanced techniques are inexpensive and does not require a skilled professional. There are also commercially available reagents that can precipitate EVs overnight like Exoquick from System Biosciences which are expensive but convenient. Despite such efforts, ultracentrifugation remains the primary focus of researchers and is considered the gold standard.

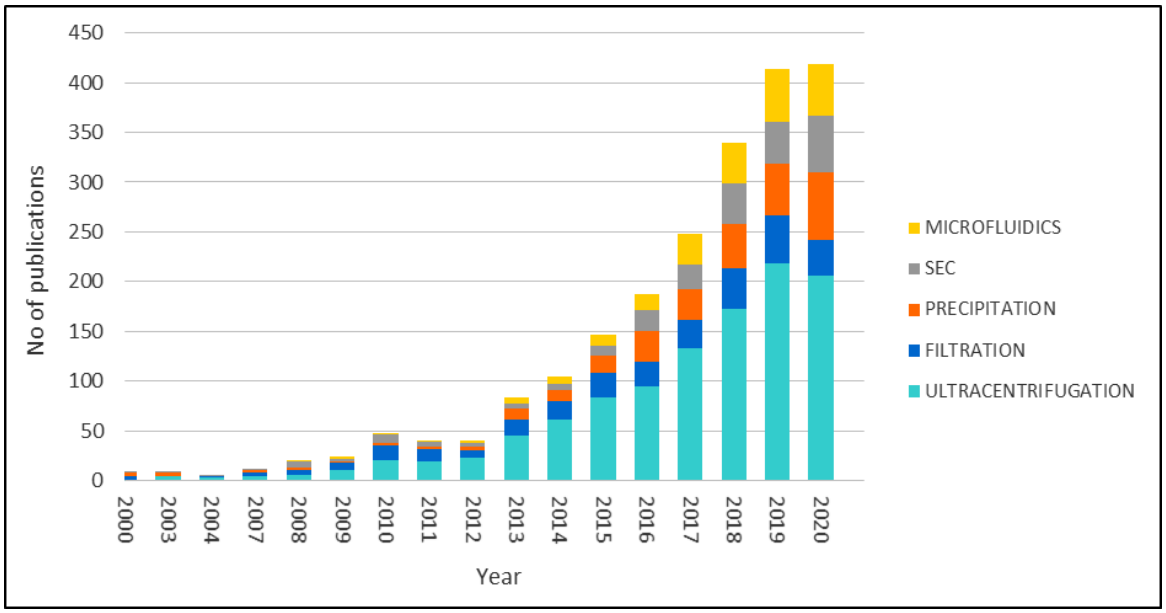

Figure 6: Number of publications of EV isolation methods in the last 2 decades

The various methods are elucidated below.

2.4.1. BASED ON SIZE AND DENSITY.

2.4.1.1. ULTRACENTRIFUGATION (UC)

Centrifugation is the most popular and prevalent technique for the isolation of extracellular vesicles. The widely used technique's principle is that, the particles in the solution separate according to their density differences under a centrifugal force [19].

The protocol involves a low-speed centrifugation to remove high density cell debris and apoptotic bodies and then the supernatant is centrifuged at high speed to remove larger debris. The new supernatant is then followed with a high-speed ultracentrifugation and the EVs are obtained in the pellet as represented in figure 7 [20]. This pellet is resuspended in a buffer, usually PBS and then stored as a concentrated product. As represented, the protocol is rather long and the ultracentrifugation alone takes two hours for a small amount of sample.

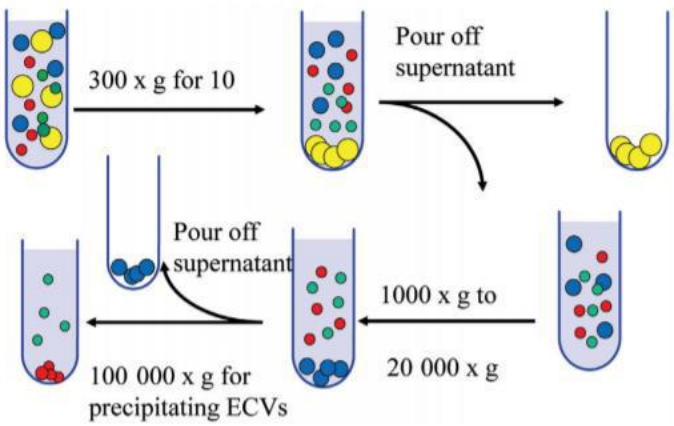

Figure 7: UC protocol [20]

EV solation utilizes two main rotors namely, swinging bucket and fixed angle as shown in figure 8 [21]

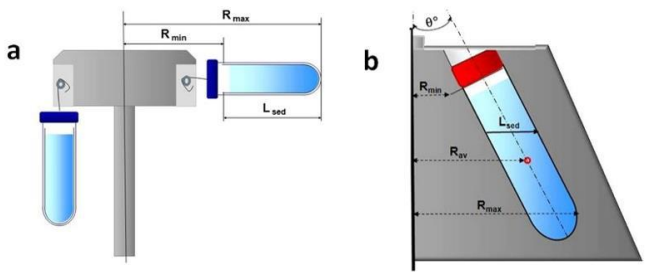

Figure 8: Figure 3: (a) "swinging bucket" and (b) "fixed angle" rotors of a centrifuge [17]

The swinging bucket changes its angle of rotation during the use while the fixed angle as the name suggests maintains its initial position. A swinging bucket offers a higher length of sedimentation and subsequently lower efficiency and is better at separating particles of a similar size range.

UC requires only centrifuge and the corresponding tubes which are available in most laboratories. The downside is the low yield and purity. Due to the variations in the sources and since the principle of separation is based on size, it is difficult to reproduce the results. EVs can have high viscosity depending on the source of extraction and this is a determining factor for the efficiency of the centrifuge. Additionally, obtained EVs in many cases are seen to be aggregated due to the high shear force employed during high-speed ultracentrifugation [17]. Most evident drawback however is the long process time and small starting volume and consequently the inability to scale up.

Density gradient UC addresses the drawbacks of conventional UC by using a medium with a graduating density gradient inside the centrifuge tube [17]. The tube is most dense at the bottom as shown in figure 9. The particles are aided in separating more efficiently due to this density gradient along which particles settle according to their individual densities. Therefore, once this step is coupled with traditional UC, higher purity can be achieved.

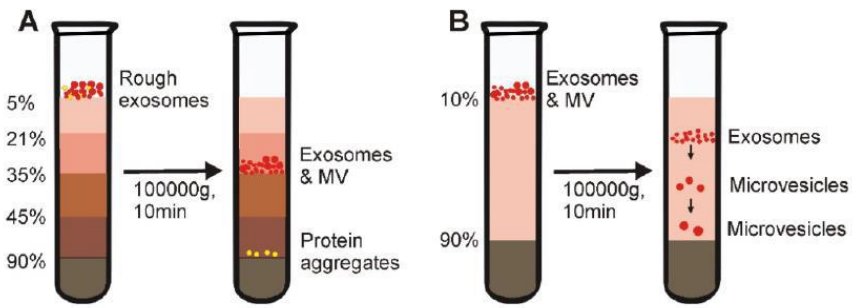

Figure 9: A.Isopycnic density-gradient UC and B.Moving-zone gradient UC [17]

Differential gradient ultracentrifugation has two subtypes, isopycnic and moving gradient [18]. In isopycnic, high density gradients are used and particles arrange themselves in a wide range of density gradients. Hence, the separation is based on density alone and cannot differentiate between particles of similar size range [17]. This is a major drawback since subtypes of EVs are in the same range of diameters.

Moving gradient or zonal UC separates particles with respect to both size and density and consists of only two density gradient sections as in the figure. The bottom layer is a very high-density cushion and sucrose and iodixanol are usually used for EVs separation [18]. As a result of these zones, particles not only separate with respect to their densities but also size and mass. Consequently, moving gradient UC is very time consuming unless properly controlled [17]. In addition, due to the presence of the gradient, sample load is lowered even further [22]. However, the aggregation and co-contamination is reduced from conventional UC and hence higher purity can be attained.

2.4.1.2. SIZE EXCLUSION CHROMATOGRAPHY

Chromatography is a highly efficient separation method based on the differential distribution of the constituents in a mixture between a mobile and a stationary phase. The mixture is dissolved in the mobile phase and it passes through the stationary phase fixed inside a system. In size exclusion chromatography however, this distribution is with respect to the size and shape of the constituents. The mobile phase is a buffer and the stationary phase consists of packed beads inside a column. The beads consist of pores of specific size ranges. Larger particles do not pass through these pores and are eluted first meanwhile small particles that pass through the pores elutes later [SEC Handbook]. The separated components exiting the column enters a detector which displays the volume of the components that eluted and the retention time of elution in the form of a peak as shown in figure 10.

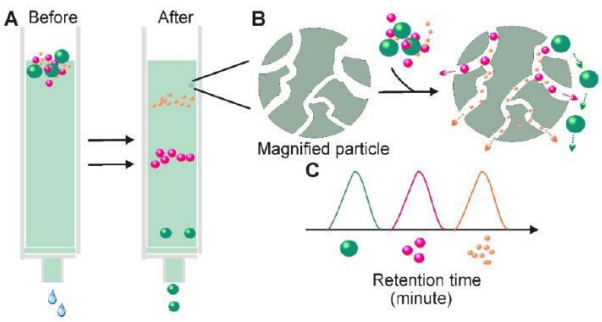

Figure 10: EV isolation using SEC [17]

In EVs the small particles are the proteins and EVs are the ones that exists early from the column. This method is gaining popularity due to its non-invasiveness and prevention of phenomena such as aggregation which is detrimental to the vesicle structure and biological activity [23]. Additionally, there is almost no interaction of exosomes with the stationary phase which suggest high recovery of samples. Recently, commercially available EV isolation columns such as qEV and PURE-EVs are gaining popularity as well [23]

Most common stationary phase for EV isolation includes agarose beads such as Sepharose® and Sephacryl®. However, the selection of the medium is highly dependent on the size exclusion limit which is a function of the impurities in the sample to be separated and cannot be universally applied across all EVs [24]. The packing must be efficient and homogenous for efficient resolution of the peaks and this is usually dependent on the personnel in charge and can lead to human errors [17]. The role of column height in separation was analyzed by Arntz et al. [25] using plasma-derived EVs with two different Sepharose®CL-2B SEC columns with different heights (56 mm vs. 222 mm). It was concluded that with the longer column, the contamination was reduced by 90%. However, longer columns lead to longer process times. Flowrate is another determining factor for the optimization. Lower flowrates are preferred for better separation but of course, this means longer process times. Therefore, it is crucial to diligently control and optimize these variables to utilize the maximum potential of this method. Nevertheless, there is a limit in the sample volume that can be fed to the column. Due to this, it is common to couple SEC with a membrane process where the feed is pre-treated to remove a significant number of impurities before sending it to the column. However, this step can affect EV purity [26].

Despite these shortcomings, SEC retains the structural and biological properties of the EVs. Moreover, SEC can separate lipoproteins which are in the same size range of the vesicles and are difficult to separate with conventional UC [27]. So, higher purity with high reproducibility can be attained.

2.4.1.3. FILTRATION TECHNIQUES

Membrane filtration for separating mixtures with respect to their sizes have been in use for decades. Liposomes that are similar to EVs have been previously purified by membrane filtration [28]. These processes are growing in popularity for EV isolation because of their

cheap and simple operation and scalability. Microfiltration membranes with a pore size of 0.1 to 3 μm as well as ultrafiltration membranes with high molecular weight cut off (100-600 kDa) has been previously used for EV separation and concentration. Usually, the filtration is carried out in series using first, a microfiltration membrane to remove larger cell debris in a concentration step and then this permeate is sent to an ultrafiltration membranes of small pore size to purify the EVs and remove impurities smaller than EVs.

In a study by Merchant et. al. [28] urinary exosomes were isolated by polyvinylidene difluoride (PVDF) membrane if 0.1 μm pore size. Proteomic analysis indicated that the proteins are retained at a higher purity and recovery in comparison with UC.

Heinemann et al. [29] coupled MF and UF sequentially using polyether sulfone (PES) membranes of 0.11 μm and 500 kDa MWCO in tangential flow filtration mode. These step guarantees the removal of cells and its debris along with small proteins. Finally, a 0.1 μm membrane filtration is done to remove larger micro vesicles and concentrate exosomes and small vesicles.

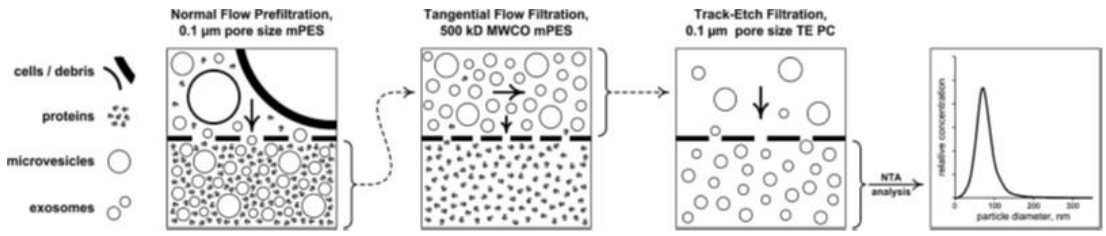

Figure 11: Coupled MF-UF protocol developed by Heinemann et. al [30]

To have a dual effect, membrane filtration can be coupled with centrifugation in the form of centrifugal concentrators. The centrifugal force helps to speed up the removal of small molecules through the membrane. Cheruvanky et. al. [31] utilized such a concentrator with 100 kDa membranes at a low centrifugal speed of 3000 x g which is milder towards EVs. Unlike normal pressure driven filtration, this method is limited by the small sample volume loading ranging from 100 μl to 100 ml. Despite this, a study by Lobb et. al. [32] concluded that centrifugal filters perform better and recover more particles than pressure driven processes regarding exosomes isolation. This is since the susceptibility of exosomes to get attached and fouled on the surface of the membrane is higher in pressure driven process. However, concentrators are preferred only if the starting volume is less than 200 ml and hence not suitable for large scale application.

Like in all membrane processes, fouling is the major issue. The various components of the input fluid get accumulated at the membrane surface, resulting in the blocking of the pores. The modified pores result in reduction in permeate flux, contamination of products, as well as some loss of the product. This can be controlled by controlling the membrane type and size. Usually, PES or PVDF membranes with lower affinity towards proteins are selected.

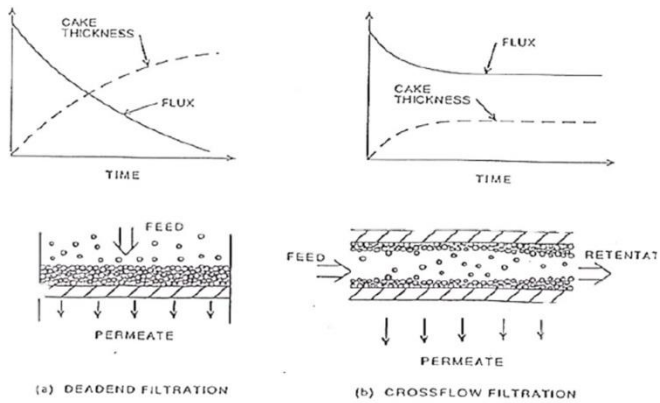

Figure 12: Dead end filtration vs crossflow filtration

Besides, use of tangential flow filtration is preferred to dead-end filtration due to the lower tendency to foul. The feed flowing in a direction tangential towards the membrane avoids or limits the cake formation on the membrane surface as in the case of dead-end filtration. Ideally, the driving force of pressure and flux through the membrane can be correlated to find ideal operating condition where these factors remain constant with time which indicates constant filtration with limited fouling. Additionally, TFF can be scaled up easily in a continuous manner and offers shorter process time.

A comparison of TFF with UC was made by Bussato et. al. [33] using a 500 kDa PES membrane which signified that TFF offers faster isolation with higher purity and recovery rate. The yield is found to be 5 times higher with merely 1 hour of process time. Contrastingly, by Heath et al. [23] found that the final product is TFF is highly co-contaminated even though the other advantages are concurrent. However, TFF recovers EVs with lower alteration to their morphology since the shear forces in UC can be controlled by controlling the driving force of pressure [23].

2.4.1.4. FIELD FLOW FRACTIONATION (FFF)

Field-flow fractionation is a size-based isolation technique with a scale of operation ranging from a few nanometres to a few hundred micrometres. Hence, this technique has been applied for the purpose of EV isolation. The principle of separation is guided by the diffusion coefficients of the particles as it flows a narrow channel made by two plates separated by a spacer. The upper plate is impermeable while the bottom plate is made permeable with a semi-permeable membrane. The feed flows in a parabolic shape as a constant laminar flow is employed. A force field is applied perpendicular to the laminar flow which drives the particle towards the semi permeable, ultrafiltration membrane which selectively permeates according to the size [34]. This crossflow can be controlled and altered even between runs making this process very flexible since the flow controls the elution and eventually the separation efficiency. Contrary to the elution in SEC, the smaller particles elute first followed by the larger ones. This is because smaller particles have higher diffusion coefficient. Asymmetric Flow Field-Flow Fractionation (AF4) is the most abundantly used sub-technique of FFF. This method stands out from SEC due to the absence of shear forces in comparison, which could be detrimental to the EVs. Additionally, this method offers the possibility to change the buffer which is important for therapeutic applications. Furthermore, as in the previous section, AF4 can successfully separate EVs from lipoproteins. The major disadvantage in comparison is the low sample volume since the field and the membrane could get overloaded at high volumes [35]. Usually, these devices are coupled with a detector such as UV and multi-angle light scattering (MALS) detector for the in-line detection of size and size distribution of the molecules. This is easier because a wide variety of buffers are compatible with AF4 systems. The AF4 system used in most of the studies is Eclipse 3+ system (Wyatt Technology Europe, Germany).

The cross flowrate is the determining factor for separation efficiency. The separation is achieved with the equilibrium between the crossflow rate and the counter-acting Brownian movement of the particle. Bowen et.al. [36] implemented a AF4 system to control and optimize the separation efficiency. This study showed that EVs from a small amount of plasma (150 μL) can be isolated in less than an hour. If properly controlled, the method is completely non-invasive and highly reproducible. Another study done by Sitar et.al. [23] carried out the separation and quantification of exosomes with the intention of optimizing the parameters such as cross flow rate. The ideal crossflow rate is obtained through trial and error. The study

revealed that the deciding factor for efficiency of separation is only cross flow rate and channel thickness rather than this focussing time. The channel thickness is defined by the thickness of spacer used and more the thickness, higher is the feed that can be loaded into the system.

In another pioneering study by Zhang et.al. [23] AF4 was utilized to separate EVs into exosomes and large EVs and additionally, a new EV subpopulation was discovered which was termed as exomeres with an average size of 35 nm. The three subpopulations had distinct bio-physical and proteomic features. The newly discovered exomeres were proven to be taken up by human cells such as liver which shows its potential in diagnostics and therapeutics. This further proves that AF4 can successfully separate and characterize heterogenous and complex nanosized populations.

2.4.2. BASED ON SOLUBILITY

2.4.2.1. PRECIPITATION WITH CROWDING REAGENTS

Crowding reagents have previously been used to precipitate virus particles and proteins out of a solution. Since viruses and exosomes have certain similarities, precipitation has evolved into an accepted isolation protocol [37]. The protocol includes the simple mixing of the biological fluid containing EVs with a polymer containing the crowding reagent. This mixture is incubated at 4°C and then centrifugated at low speed (<2000g) resulting in lower effect on the EVs due to the much higher speeds in ultracentrifugation. They can also process larger volumes in comparison to ultracentrifugation and requires no specialized equipment. The principle is that the crowding agent gets attached to the larger molecules such as cellular debris in a cluster while smaller molecules such as EVs and lipoproteins remains in the solution.

The most used crowding reagent is Polyethylene glycol (PEG) since they had been previously used for virus precipitation. PEG is also attractive due to their use in neutral pH which results in milder effects on EVs biological activity. Although loss of biological activity should be expected since precipitation with PEG could take hours [19]. A notable disadvantage of this method is the presence of the polymeric materials which should be separated from EVs [38]. Since the precipitation works to concentrate the EVs, this does not mean that the EVs are separated from proteins and RNAs which are not associated with EVs are hence making the resulting mixture high in contaminants. Furthermore, since PEG can interfere with molecular

imaging techniques such as TEM, SEM as well as proteomic analyses, the PEG solution must be removed from the cell culture sample which further augments the downstream cost and post processing load [39].

Mark et al. [39] devised a new protocol called as ExtraPEG which is a rapid, inexpensive way to precipitate vesicles using PEG. A comparative study with differential centrifugation was also carried out. In the protocol, 5-12% PEG solutions were added to the cell culture media and incubated in the refrigerated overnight. This mixture is centrifugated at low speed and then a small volume ultracentrifugation is carried out. The study revealed through nanoparticle tracking analysis that the concentration of PEG and number of particles recovered have a linear relationship but considering the purity of vesicles. Additionally, an analysis for the efficacy of ExtraPEG in retaining the desired properties of proteins and RNA content in the vesicles were evaluated. For protein, the proteomic experiment carried out revealed that 97% of the proteins associated with vesicles, according to Vesiclepedia database was found after purifying with Extra PEG. Another important factor is the mRNA and miRNA integrity which is of utmost importance in the ability of EVs to carry out cell-cell communication. The analysis interestingly revealed that the RNA of samples isolated with ExtraPEG has the structural integrity higher than the EVs isolated by differential centrifugation.

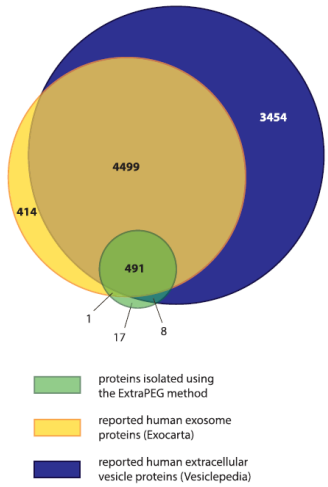

Figure 13: Proteins from ExtraPEG method [38]

2.4.2.2. COMMERCIAL PRECIPITATION REAGENTS

Recent studies in precipitation have led to the rise of user friendly and single step commercial precipitation reagents like ExoQuick from Systems Biosciences and Total Exosome Isolation (TEI) from Life Technologies.

Exoquick is a rapid, high yield EV isolation system that requires much lesser amount of sample volume (100 µl) in comparison with other methods. It contains a proprietary polymer that precipitates exosomes overnight after mixing with a biofluid. Upon refrigeration, the mixture is centrifuged at low speed and the exosomes are found in the pellet. Albeit being expensive, this method is scalable and retains the crucial miRNAs with higher quality and quantity better than chromatography and ultracentrifugation and additionally have higher purity than the others. [40]

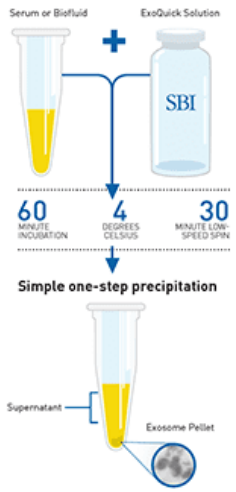

Figure 14: Exoquick protocol [System Biosciences]

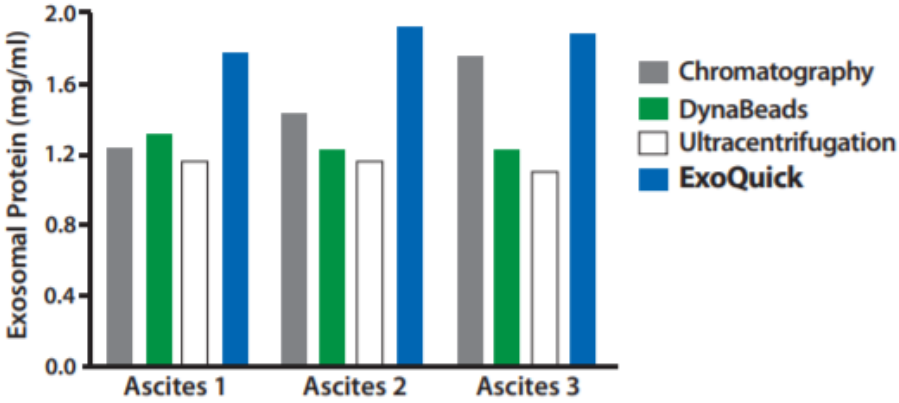

Figure 15: Comparison of different methods with Exoquick in terms of proteins recovered [24]

Another important factor for comparison with the golden standard of ultracentrifugation is reproducibility. Studies showed that the Exoquick method is more reproducible than ultracentrifugation since proteomic analysis suggests that Exoquick method shows more stability with variation in the sample volumes and purity [42]. This method also shows higher efficiency, close to 100% with respect to the number of nanoparticles in the sample culture in comparison to only 30% with UC. Therefore, co-contamination from non-exosomal protein is much lesser in Exoquick method.

Total Exosome Isolation is another isolation reagent from Thermo Fisher Scientific. The protocol is similar where the cell culture sample is added to the reagent, incubated at 2-8°C overnight and centrifugation at 10000 x g for 1 hour [Thermo Fisher Scientific]. Studies shows that this is one of the best commercially available reagents where the protein content as well

as the exosomal stability determined by comparing zeta potential is considerably higher than that isolated by UC [43],[43]. This method offers higher yield and high proteome recovery and shows no aggregation which is a major disadvantage of UC. Both studies showed that the particle mean diameter is higher and having more homogenous morphology in case of TEI. TEI is equally effective on viscous cell culture such as human serum and plasma. Despite being expensive, this process reduces the stress on downstream since there is no need of post processing unlike other isolation techniques which are usually coupled with size exclusion chromatography and density gradient centrifugation as a post processing step due to formation of aggregates or lower recovery rates.

Soares et al. [44] carried out a comparative study of the use of precipitation and column-based methods for exosome isolation from different cell cultures. The precipitation-based methods used the above mentioned Exoquick and TEI. The column-based methods outperformed the commercially available kits in terms of performance as well as purity and this study showcases the potential co-contamination resulting from use of a precipitating reagent with a biofluid. Due to precipitation, the downstream processes as well as analytical processes suffer heavily.

	Serum			Plasma			CSF		
	TEI	ExoQ	ExoS	TEI	ExoQ	ExoS	TEI	ExoQ	ExoS
Exosome yield (NTA)	**	**	***	**	**	***	*	*	*
Exosome yield (EXOCET)	*	***	***	*	**	**	-	-	*
Ratio (n° particles/µg protein)	**	**	***	**	**	***	*	*	*

*Low yield or purity
** Medium yield or purity
*** High yield or purity;—No yield.

Figure 16: Comparison of commercial precipitation reagents (TEI, Exoquick) with column-based methods (ExoS) in terms of exosome purity [44]

2.4.3. BASED ON CHARGE

2.4.3.1. ELECTROPHORESIS

The charge of the extracellular vesicles has been determined to be negative through zeta potential (-10 to -50 mV) [45]. This is the basis of charge-based separation of EVs such as anion exchange chromatography and electrophoresis. The electrophoretic mobilities of the different particles are different under the influence of an electric field due to their charge to size ratios. Agarose gel is commonly used as a non-conducting gel on which the sample is loaded with a buffer [44]. This is an emerging method for the separation of RNA, DNA, and

proteins. Since this is a quite novel technique, it is usually combined with other size-based processes to increase separation intensity and recovery rate. Yang et.al. [44] combined a membrane dialysis with electrophoresis to isolate exosomes from lemons. This provided for a quick separation with appreciable homogeneity in the size and morphology. The non-invasiveness of the method makes it ideal in clinical laboratories since there is no need of specific equipment or reagents.

The separation of EVs from certain biofluids such as plasma are difficult due to the presence of lipoproteins which have similar dimensions as that of EVs. Due to this, even the most accepted size-based techniques such as UC, SEC are usually unreliable in separating them. The presence of such lipoproteins can impede the subsequent proteomics after isolation. Zhang et.al. [45] evaluated the average diameters and zeta potentials of lipoproteins as well as EVs and formulated a protocol for agarose gel electrophoresis based on their ratios. Lipoproteins are classified with respect to their densities as very low density (VLDL), low density (LDL), and high density (HDL). Their migration is depicted in figure 17C.

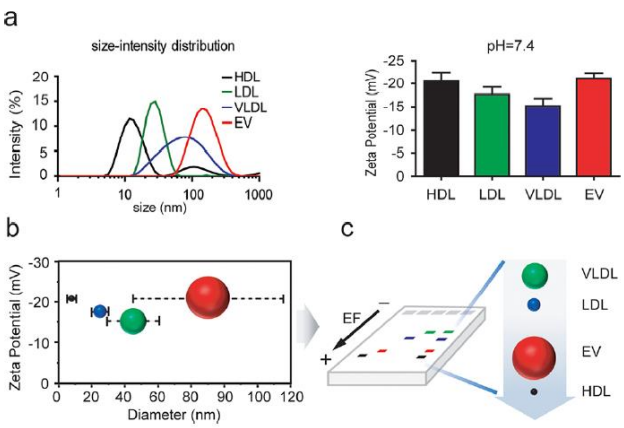

Figure 17: A) The size and B) zeta potential comparison of common lipoproteins with EVs. C) The migration of the lipoproteins and EVs under electric field on an agarose gel [46]

This method offers recovery rates close to 100% in a shorter window of time (3 hrs). As this is an emerging field, it has not been able to develop a correlation between the gel porosity and the velocities with which particles like EVs migrate under an electric field. Additionally, if this technology were to be used for therapeutical applications, the surface charges and the sizes vary from a healthy biofluids to one that is suffering from diseases [46]. Hence more research and standardization are needed to establish the apparent advantages of this process.

The drawback for electrophoretic separation in general is that huge amount of electric field needs to be generated for efficient separation which results in unnecessary heating of the feed

sample which could be detrimental to EVs. This undesired phenomenon was tackled by Marczak et. al. [32]. using an ion selective membrane simultaneously in the electrophoretic gel. The arrangement of the membrane is perpendicular to the flow of the feed over the agarose gel as in figure 18.

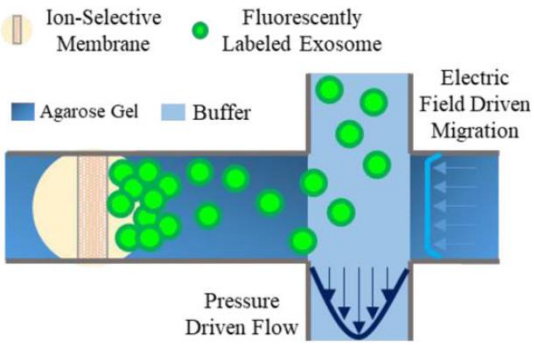

Figure 18: Microfluidic cell with electrophoresis and an ion selective membrane [47]

This membrane attracts the negatively charged EVs as it flows over the gel under the influence of a strong electric field. At the cation-selective membrane surface, the exosomes get attached and are continuously concentrated. A comparison was carried out with the golden standard ultracentrifugation as well as the commercial precipitation reagent Exoquick. The recovery rate with the present method was between 70-80% while UC and Exoquick had 6% and 11% respectively from the same source. Moreover, the input volume is considerably small and at the same time, EVs from a 200 µL feed can be isolated in one hour which is much lower than conventional protocols. Furthermore, the process does not require complex equipment or expensive reagents.

2.4.3.2. ANION EXCHANGE CHROMATOGRAPHY (AIEC)

Anion exchange chromatography is a widely employed charge-based technique used in the separation of proteins and viruses and thus can be used to separate EVs. The principle of separation is the interaction between the negatively charged EVs and an anion exchanger stationary phase containing positively charged functional groups. Due to this interaction, the EVs gets attached to the stationary phase and is progressively eluted by a buffer of high ionic strength.

This method offers high specificity and selectivity due to the charge-based interactions. In addition, these monolithic macro porous columns can be operated at higher flowrates than the prominent size exclusion chromatography hence diminishing the drawback of low sample

volume. Such a monolithic column with a strong positively charged quaternary amine stationary phase was tested by Heath et.al. [23]. A litre of sample was processed in 3 hours which is a substantial increase in process volume compared to conventional methods. In addition, the purity in comparison with UC and TFF is found to be higher in this study.

In another study by Kosanović et al. [17], diethylamino ethyl cellulose resin was used as the stationary phase to separate EVs from amniotic fluid. Elution buffer was sodium chloride. The study indicated that the concentration of NaCl is a determining factor for the size of the EVs obtained and higher concentration of NaCl yielded larger vesicles.

Although process time implies scalability, AIEC research has been only focussed on cell culture media derived EVs and not highly viscous biological fluids such as blood and serum [17]. These fluids contain many other components with negative charge and hence can affect the separation. At this point, this method is highly recommended as a concentration step after a conventional isolation method to further increase the purity.

2.4.4. BASED ON AFFINITY INTERACTIONS

2.4.4.1. IMMUNO AFFINITY CAPTURE

The biomolecules on the EV membrane surface such as lipids and proteins can be selectively attached to certain immobilized ligands. This attachment due to the consequence of a reversible interaction is the core principle of immunoaffinity capture. Ligands such as antibodies, lectins, and lipid-binding proteins have been previously used for EVs [23]. These ligands containing EV-markers are attached to a solid surface through which the biofluid is exposed to. EVs in the biofluid are attached onto the solid matrix and then eluted to remove the ligands as in the protocol given below.

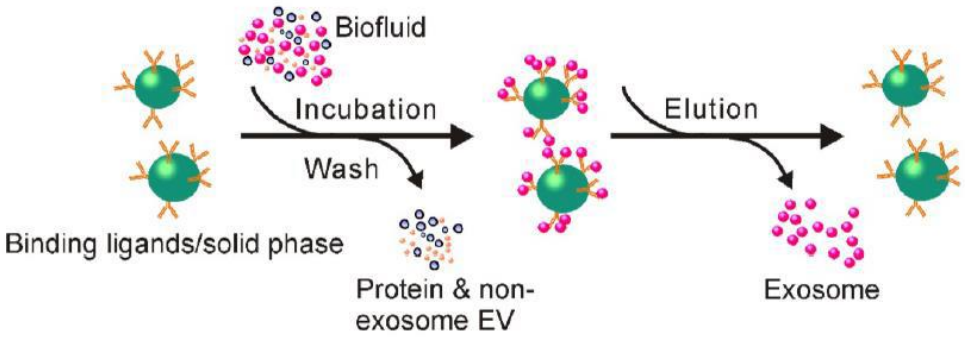

Figure 19: immunoaffinity-based exosome isolation by Yang et al. [48]

In EV research, this solid surface can be in form of a column as in affinity chromatography or simply beads or filters containing immunocapture ligands [49].

The most prominently used ligands are antibodies which uses proteins of the class tetraspanin proteins as EV specific markers. These proteins such as CD9, CD63, CD81, and CD82 are universally found in EVs from all sources [50].Magnetic beads containing CD9, CD81 and CD63 was successfully able to capture EVs from human plasma [51].

Heat shock proteins and heparins are other examples for EV markers used previously [52]. Interestingly Zhou et. al. [53] successfully used epithelial cellular adhesion molecule EpCAM as an EV marker which is a glycoprotein that are overexpressed in tumour cell derived EVs. This marker was used in another study by Rupp et. al. [53] in the form of a magnetic bead which isolated tumour EVs from different cell sources. This amplifies the use of immunocapture not solely for isolation but also for disease diagnosis.

Monolithic polymeric columns containing antibodies are another type of immuno-affinity capture as utilized by Multia et. al. [53]. They offer high flowrates and subsequently shorter separation time in comparison to conventional column-based processes. The protocol is given in figure 19. The process took about half an hour and the ligand used were tetraspanins.

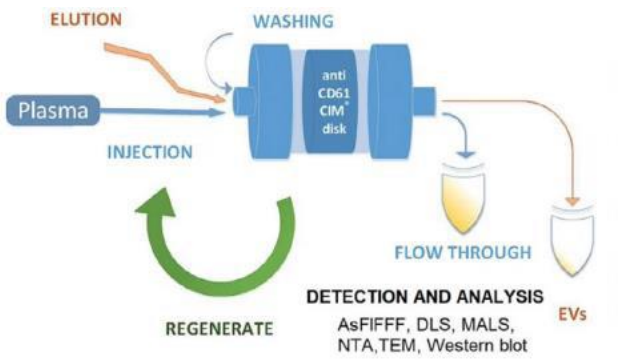

Figure 20: Immunoaffinity monolithic disk column for EV isolation from plasma developed by Multia et al. [53]

Aptamers are the latest type of ligands used for the selective capture of EVs [19]. Aptamers are cheaper than antibodies. They contain short single stranded DNA or RNA sequences, that can specifically recognize and bind to their target nucleic acids in EVs. They are better suited for scaling and are not limited by low shelf life like antibodies

2.4.5. BASED ON MICROFLUIDICS

Microfluidic separations aim to control the fluid flow in a microscale. The scale of operation starts from 100nm to a few 100 micrometres. Due to the recent rise in the use of such Lab on Chip (LOC) techniques which offer high selectivity and specificity with lower costs and lower sample volume, this technique has been applied to isolation of EVs [55]. The single step-high purity separation with remarkably low energy requirements makes it ideal for clinical applications. EV isolation through microfluidics can be classified into immuno-affinity based and size-based techniques [56]. The most used methods in the recent years are given below.

2.4.5.1. IMMUNO-AFFINITY-BASED TECHNIQUES

This technique captures the EVs using the antibodies that binds to the specific markers associated with EVs. The two approaches are modifying the surface of EVs or using beads which are functionalized with antibodies [57]. The protocol for both basically involves an EV-antibody binding step and the subsequent washing of the and recovery of the antibody coated device. The coated antibody binds only to the corresponding antigen in the EV which makes it highly specific to the identified antigen subpopulation but at the same time it has the disadvantage that not all the EVs in a population is isolated.

Chen et.al [57]devised a procedure for such isolation using CD63 antibody which belongs to the class of tetraspanins which are abundantly found in EVs from any source. The EV source is simply passed through a fabricated system and then washed with PBS. The procedure only takes an hour to isolate EVs from human serum with a volume of 100-400 μL. This procedure avails consistent size distribution which is crucial. This rapid procedure with high sensitivity and low cost can pave way for its use in the therapeutics and diagnostics field. As an example, the study also shows that, in this protocol it is possible to diagnose diseases such as cancer by isolating the EVs dissociated from cancerous cells due to the specificity of the binding procedure.

Functionalized beads coated with antibodies on the other hand be easily manipulated due to the structure hence makes downstream processes easier in comparison [58].

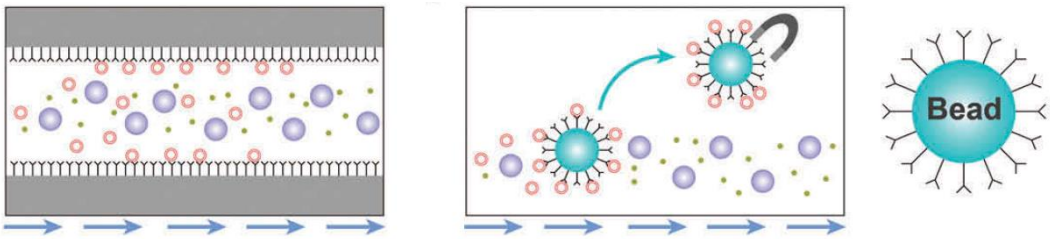

Figure 21: Microfluidic devices with surface coating and functionalized beads (red are vesicles while blue is impurities) [58]

2.4.5.2. SIZE AND DENSITY BASED TECHNIQUES

VISCOELASTIC SEPARATION

This method uses viscoelastic forces to separate EVs with respect to their size since these forces cause particle migration. Liu et al [59] devised a continuous protocol with the absence of any external fields to isolate exosomes from larger EVs. The protocol basically involves the addition of the feed as well as a sheath fluid (Eg: Polyoxyethylene) to induce viscoelastic flow. This induced viscoelastic flow employs lift forces which helps the feed to separate in the microchannel according to the cut off applied as shown in fig 19.

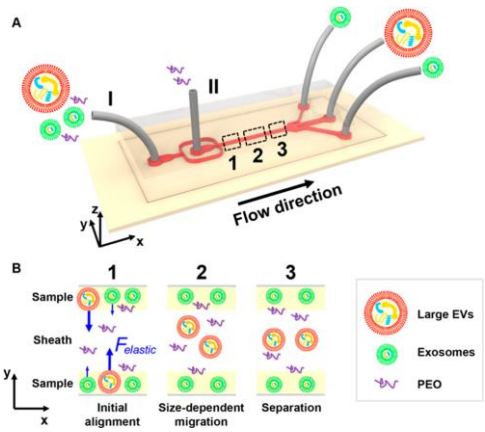

Figure 22: Viscoelastic separation [59]

Large EVs migrates faster and are taken out first from the central outlet while smaller exosomes with slower migration are collected in the side channels. The dimensions this channel is 50x20 µm. So, with low costs, minimal sample requirement and controllable cut off ranges, a separation efficiency above 90% and a recovery rate above 80% is reached with this process.

MICROFLUIDIC FILTRATION

Filtration with microfluidic devices consists of membranes consists of nano sized membrane polymer with adjustable cut off which can separate EVs from any sample culture [5]. Since it

is entirely size based, the driving force of the membrane is the prime variable. Stage filtration systems with subsequent reduction of pore sizes with each stage are used to classify exosomes and high efficiency removal of proteins. Higher recovery rates with the absence of intense pre-treatment steps are achieved in comparison with conventional process although low throughput and difficulty to fabricate is a bottleneck.

ACOUSTIC DEVICES

Acoustic devices have the capability to separate EVs based on their size and density. These devices are highly bio-compatible and allows contact free separation. Wu et.al [7] employed an acousto-fluidic device with a first step which removes large cell debris and a second step where EVs are isolated into their sub-groups. A purity of 98.4% is achieved after the second step. These 2 steps are combined in a microfluidic chip. This rapid, non-intrusive method offers continuous separation. The particle separation is caused due to the interaction between Stokes drag forces and acoustic radiation forces. The drag forces depend on the radius while acoustic radiation forces depend on volume. For larger EVs, the drag force is much lower and for smaller EVs it is higher in comparison. Hence, once particle move to the pressure nodes as in figure 20, they get separated at the nodes.

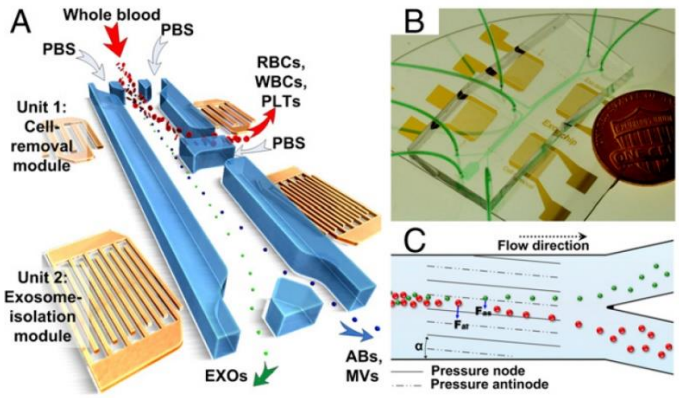

Figure 23: Separation using acoustofluidics. A) Protocol of 2 seperate units for cell removal and exosome separation. B) Setup. C) Pressure nodes separate larger and smaller particles [60]

The cut off can be adjusted by altering the power given to the system which in turn alters the acoustic radiation provided. The additional advantages include the reproducibility, ability to automate, single step separation, high speed (100 µL in 25 minutes) and gentleness. Despite these advantages, it is difficult to fabricate the micro-channels employed in microfluidic devices. Therefore. sufficient studies need to be done in-order to elucidate the efficiencies with different EV sources and at a larger scale.

The summary of the methods discussed is tabulated below

Table 1: EV Isolation methods summary

	Principle	**Process Time**	**Advantages**	**Disadvantages**	**Scalability**	**Cost**
DIFFERENTIAL CENTRIFUGATION (UC)	Sedimentation with respect to density using high g-force	140 - 600 min	• Easy to operate • Commonly available in labs	• Long process time • Small process volume • Non reproducible • Co-contamination	+	€€€€
DENSITY GRADIENT ULTRACENTRIFUGATION (DG UC)	Separation with respect to density in a density gradient medium	250 min – 2 days	• Higher yield and purity than UC	• Long process time • Small process volume • Complex machinery • Need skilled technician • Vesicle aggregation and damage due to shear force	++	€€€
SIZE EXCLUSION CHROMATOGRAPHY (SEC)	Separates by hydrodynamic volume	30 minutes to few hours	• Reproducibility • Low contamination • Gentle method • Reduces aggregation.	• Low sample volume • Long process time • Low resolution • Need to concentrate EVs again	++++	€€

FILTRATION (MF/UF)	Uses membranes with specific pore sizes	130 min	• Simple and cheap • Short process time and large volumes • Continuous process	• Membrane fouling • Vesicle aggregation	++++	€
FIELD FLOW FRACTIONATION	Flow modulated by a field applied perpendicular to the flow	45-60 mins	• Removal of lipoproteins • Easy to link with UV-MALS.	• Low sample volume • Non-invasive • Reproducible	+	€€
PRECIPITATION	Solubility changes in a crowding agent	8-12 hrs	• Inexpensive • Simplicity • Gentle method	• Need to remove PEG • Long procedure • Contamination	+++	€
COMMERCIAL PRECIPITATION REAGENTS	Solubility changes in a crowding agent	8-12 hrs	• Quick and easy to handle. • High purity and recovery • Low contamination	• Expensive • Need of downstream treatment	+++	€€€
AIEX	Separation based on charge	180 min	• Fast processing • Maintains EV integrity	• Co-contamination of molecules of similar charge • Requires additional concentration	++++	€€
ELECTROPHORESIS	Separation based on electrophoretic mobility in an electric field	60-120 mins	• Easy control • Fast and efficient • Non invasive	• Heating due to electric field • Co-contamination	+++	€

IMMUNO-AFFINITY TECHNIQUES	Capture EVs using antibodies	240 mins	• Fast and efficient • Very specific isolation	• Antibodies are expensive • Needs more EV markers • Only isolates specific EV population	++	€€€€
MICRROFLUIDICS	Flow manipulation in microscale	60-120 mins	• Specificity and selectivity • Low energy requirement • Quick and efficient	• Still a growing field • Low sample loading	+	€€

2.5. EXTRACELLULAR VESICLES FROM PLANTS

The plentiful applications of EVs in diagnostics and therapeutics demand a large scale and efficient mode of isolation. EVs from human beings however has finite quantities and is unsuitable for mass production and depending on the biofluid could lead to a monetary disadvantage. There is other mammalian source of isolation such as EVs from bovine serum but this is unquestionably restricted by moral and ethical grounds. So, it is of paramount importance to have a source of extraction that is abundant and cheap.

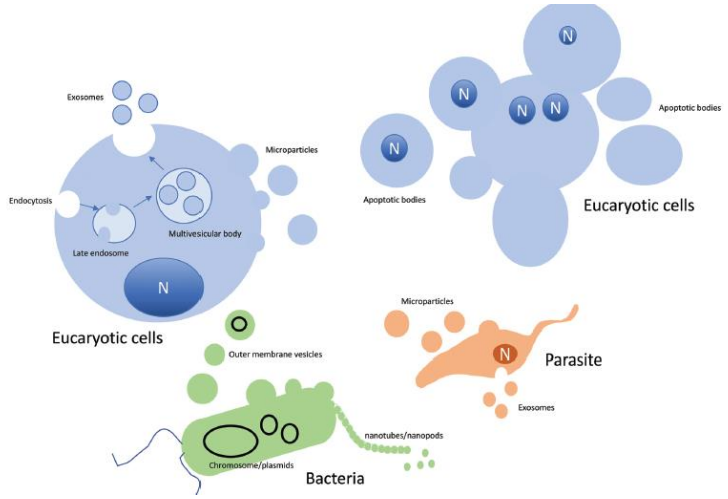

Figure 24: Extracellular vesicles in plants and lower organisms [61]

Very recently, nano-sized membrane vesicles were found to be released by fruits such as lemon, grape and grapefruit, tubers such as carrots and ginger, vegetables like broccoli and seeds of sunflower [8]. This alleviated the issues related to availability to employ EV mass production. Since they are food sources, they are environmentally friendly to produce, have low toxicity, low immunogenicity, high internalization rate and are completely non-hazardous. Studies have shown their ability to target specific tissues [9]. Plant EVs have the hydrodynamic size, morphology, and zeta potential adequately comparable to mammalian EVs [62]. So far, lemon vesicles are found to have closest size similarity with mammalian exosomes (70 nm) [61]. Ginger and grapefruit EVs are larger (~250-400 nm) while carrot EVs are found to be in a wide range of sizes (100 to 1000 nm). Zeta potential is in the range of -2.92 to -39.2 mV [62]. Like mammalian EVs, plant EVs are responsible for intracellular communication and the control of plant immunity [8].

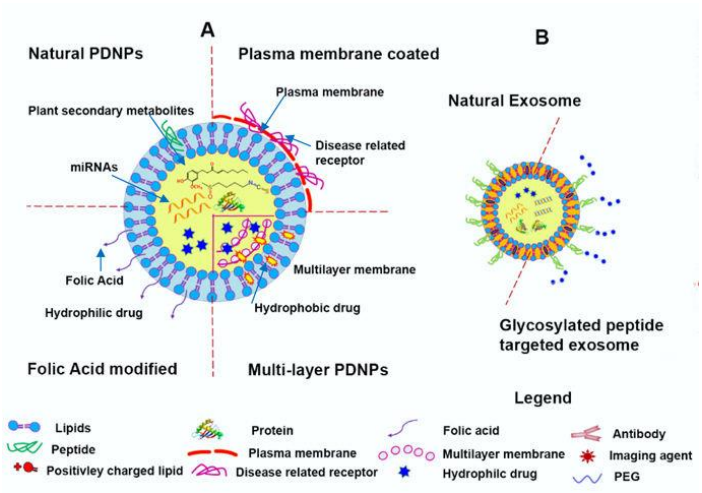

Figure 25: Structural comparison of A) Mammalian and B) Plant derived EVs [63]

In a study by Jingyao et. al. [8] vesicles from carrots, ginger, broccoli, and grapes were extracted and analysed. Since isolation of plants is in its infancy, most of the studies use the traditional, golden standard method of ultracentrifugation to isolate EVs. The juices of fruits or vegetables are extracted first using a blender or a mixer and is subjected to a sequence of centrifugation from low speed finally leading up to ultracentrifugation at 100000 to 200000 x g. The final pellet is resuspended in a buffer, usually PBS to obtain the vesicles. This study was mainly to investigate whether these plant vesicles can communicate with mammalian cells upon contact with intestinal cells after consumption. It was concluded that the cells carry out the uptake of these nano-vesicles revealing a novel mode of communication between plants and animals which can be exploited for therapeutics. Due to the presence of lipids, proteins and RNAs, it is postulated that the mode of action is like that of mammalian vesicles and upon contact they can alter the recipient cells. Additionally, studies revealed that these vesicles not only act locally in the intestinal environment but can also be transported via blood [9]. Even though it is hypothesized that EVs can protect its constituents due to the strong lipid bilayer, some studies proved that the diameter of plant EVs were altered in a stomach and intestine like microenvironment where the pH is acidic [64]. Therefore, plant EVs have evident correlation with the pH of the target cell.

2.5.1. CONSTITUENTS

Proteomic analyses have been applied to plant EVs from a variety of sources. There are no specific protein markers as of now as it has been difficult to elucidate protein families exclusive to plant EVs. Also, the total amount of proteins is found to be much higher in mammalian EVs. Heat shock proteins which are effective in protein homeostasis and found in mammalian EVs were also found in plant EVs. In a study by Raimondo et. al. [62] it was demonstrated citrus lemon derived EVs had almost 50% of proteins generically found in mammalian EVs. Specifically, HSP70 and HSP90 were found in such vesicles. Another protein hypothesized as a marker is Annexins which were again found in several citrus species, grape and broccoli [62].

Since lipids are responsible for the stability and the biological activity in EVs, the lipid profiling has been extensively carried out in plant vesicles. This has indicated that phospholipids and glycerol lipids are prominently detected. Contrary to mammalian EVs, cholesterol is found to be lacking in plant EVs. The role of cholesterol in mammalian EVs is

to stabilize the bilayer and to facilitate release of its constituents [64]. So, the mechanism of protection and release could be different in the lipid bilayer of plant vesicles.

In contrast, mammalian, and plant derived EVs have comparable number of mRNAs, miRNAs, and non-coding RNAs. Certain miRNAs exclusive to plants are found in human cells and it is theorized that once these miRNAs are ingested, they can travel within the organism's system. In addition, plant EVs also contain bioactive secondary metabolites which have inherent anti-inflammatory, anti-cancer, and antioxidant properties [65]. This suggests their unique therapeutic potential in comparison with mammalian vesicles.

2.5.2. APPLICATION

Like mammalian vesicles, plant EVs are suggested to have applications in therapeutics and drug delivery. Their low immunogenicity, non-toxicity and tissue targeting properties intensify this role. Plant vesicles are peculiar in the fact that they are constantly introduced to human bodies through diet. Due to this, human immune systems are acclimatized with them. This further amplifies the potential of these EVs for its applications. Due to the internalization through diet, most of the studies on plant EVs are on gastrointestinal tract, inflammatory bowel diseases, and several types of cancer [62]. Like mammalian vesicles, they have the advantage over synthetic drug delivery vehicles since they can cross blood brain barrier (BBB) and hence can be used for neurological and brain related diseases. This was demonstrated by Zhuang et. al [60] by using grapefruit derived vesicles to arrest brain tumour progression in mice. Also, their negative charge means that chemotherapeutic drugs like doxorubicin can be easily loaded into the plant EVs [9].

They are highly biocompatible and can be delivered orally or intranasally. It is also suggested to use coatings of membranes from mammalian EVs to further increase the compatibility. These membranes can contain specific receptors of the target cell to further the efficiency of delivery [65].

Although these applications are still emerging, many studies have discovered interesting implementations. A study by Raimondo et. al. [45] determined that nanovesicles from lemon prevented cancer cell proliferation in different tumour cell lines. In another study, vesicles isolated from grapefruit was applied for delivery of anti-inflammatory drugs to the intestines. Intestinal cells are found to take up these EVs at an impressive rate [8]

More recently, Yang et.al. [66] combined a membrane dialysis with electrophoresis to isolate exosomes from lemons. These EVs were found to be efficient in causing cancer cell death and concluded that these EVs could be orally administered with chemotherapeutic drugs

It is imperative to note that most of these tests are done in mouse models which have less than 10% similarity to human immune systems. Even though the prowess is remarkable, there needs to be further research. In addition, the apparent disadvantages of using UC for isolation needs to be addressed and novel techniques should be applied for efficient extraction of plant vesicles. There needs to be a standardization of isolation and characterisation methods just like what is called for in the case of mammalian vesicles. The question of variability in sources as well as time of extraction (fresh or store bought) needs to be addressed [67] to further improve the utility of these vesicles. Since these EVs stand out from mammalian in their availability and applicability they could be considered as the future for green nano drug delivery vehicles.

2.6. CITRUS LEMON

Citrus lemon of the family *Rutaceae* is one of the most vastly cultivated fruits worldwide. The medicinal and biological properties of lemons have been extensively used for centuries. There are shreds of evidence of the use of lemons in traditional medicine in Asian countries such as China, India, and Japan to treat blood pressure, sore throat, cold, and fever [68]. The biological activity had been characterized in the fruit extract, fruit juices and its seed essential oils. Due to the high concentration of Vitamin C (Ascorbic acid), lemon juice used to be a popular treatment method of scurvy or Vitamin C deficiency.

The significant biological activity of Citrus Lemon is owing to its phenolic compounds, alkaloids, limonoids, essential oils and especially flavonoids. Flavonoids such as eriodyctiol, hesperidin, naringenin, apigenin, and quercetin are detected in lemon, some of which are unique to citrus plants. Limonoids are a distinct family of compounds contained in several citrus fruits. Carboxylic acids, particularly citric acid is well established in lemon pulp and peel. Other important secondary metabolite of Lemon includes phenolic acids such as ferulic acid and synaptic acid which is predominant in the fruit juice. In addition, they are rich in Vitamin C, several coumarin compounds, carbohydrates, and amino acids. Lemon seed oils are abundant in fatty acids and carotenoids. Citrus fruits contain more of these biologically relevant carotenoids than any other fruit [69].

Among this extensive list of metabolites, citrus lemon juice predominantly contains flavonoids and phenolic acids. Due to these beneficial and active components, the juice possesses significant biological activities such as antioxidant, anti-inflammatory, anti-microbial, protection of cardiovascular and neurological systems, and anti-cancer.

2.6.1. Antioxidant

Many diseases such as cancer, inflammation, arthritis is correlated to the development of reactive oxidation species (ROS) [68]. These ROS arising due to oxidative stress can cause cellular damage. Cells limit their damage by employing compounds that acts as antioxidants. Citrus fruits contain phenolic acids and their poly-hydroxyl subtype which are regarded for their antioxidant properties [69]. A study carried out by Tong Zhou et. al [66] revealed that ROS is induced by liver damage due to alcohol use is suppressed by treatment with lemon juice.

2.6.2. Anti-inflammatory

Flavonoids and coumarin show the ability to suppress inflammatory cytokines. These cytokines are responsible for certain diseases such as Alzheimer's, Parkinson's, colon cancer etc. [69]. Hesperidin have been studied for their ability to reduce inflammation.

2.6.3. Anti-microbial

Lemon juice have been applied for the inhibition of both gram-negative and gram-positive bacteria [66]. They could inhibit pathogenic microorganisms such as Enterococcus faecium, Staphylococcus aureus, Pseudomonas aeruginosa, and Salmonella.

2.6.4. Protection of cardiovascular and neurological systems

Several studies suggest that flavonoid rich foods are ideal for reducing cardiovascular stress and related diseases by impacting mainly the blood pressure [9]. Additionally, lemon juice had been proven to ìmprove of memory in certain animals [9].

2.6.5. Anti-cancer

Flavonoids are also associated with lowering the risk of cancer such as gastric cancer, breast cancer, colon cancer etc. Raimondo et. al. [67] isolated nanovesicles from lemon juice thorough ultracentrifugation. This nanovesicles was found to be responsible for cancer cell proliferation in mice.

2.7. CITRUS LEMON VESICLES

The medicinal and biological relevance of citrus lemon is paramount. There has been evidence of innovative research done in the field of vesicles from the lemon. One such is the study by Raimondo et. al. [38]. The isolation method was the conventional ultracentrifugation with a 30% sucrose gradient. The dimensions of the nanovesicles were found to be in between 30 and 70 nm with similar morphology with mammalian exosomes. The proteomic profile revealed that the proteins matched with ExoCarta which is a database for exosomal proteins in mammals had a similarity of about 57%. The experiment successful in loading lemon vesicles to the interiors of human cancer cells from lungs, colon, and leukaemia. It was proven that these vesicles could specifically carry out the proliferation of cancer cells but at the same time did not have any effect on normal cells. Upon investigating the mechanism of the tumour cell apoptosis, TRAIL pathway was found to be the cause. TRAIL is a protein that functions as a ligand that causes cell death. This study was also carried out in vivo by using mice with chronic myeloid leukaemia. The nanovesicles were able to supress the cancer also in the mice.

Baldini et. al. [70] isolated lemon vesicles with a series of filtration and UC. To quantify, 250 ml of juice yielded approximately 920 µg of nanovesicles. The diameter range was from 30 to 100 nm. Similar to the previous study, uptake tests were done on human cells namely, mesenchymal stem cells (MSC). It was found that MSC were able to load lemon vesicles and were completely non-toxic towards normal human cells. The innate antioxidant ability of the constituents of lemon juice to was tested on human cells and it was revealed that these vesicles could reduce the secretion of reactive oxidation species (ROS) which are primarily responsible for oxidative stress. Furthermore, it was shown that these nanovesicles containing citrate and Vitamin C was protected from degradation due to their lipid bilayer, which can open doors in targeted delivery of bio cargo using lemon juice derived vesicles.

Yang et. al. [71] was among the first to diverge from the conventional UC method to extract lemon vesicles by combining electrophoresis and membrane filtration using a dialysis bag. The size and numbers were concurrent with UC isolation. It is however difficult to apply isolation methods that is diverse from the conventional ones. Since specific protein markers are not established, immuno-affinity methods are not possible. Same reason is valid for microfluidics which are not scalable either. This method uses size as well as electric charge and both are considered as well grounded for lemon EVs. Under the electric field, particles in lemon juices are migrated according to their charge and are carried across a 300 kDa dialysis bag which

removes smaller proteins and purifies the exosomal fraction. To evaluate the therapeutic potential, the EVs were subjected to internalization by gastric cancer cells. The cancer cells not only carried out the uptake but also was subjected to apoptosis. Additionally, even in the acidic pH found in gastric cells, vesicles maintained their activity and morphology. These EVs were also sent in vivo to major organs in mice such as heart, liver, spleen, lung, and kidney to investigate whether EVs are safe towards normal cells and this hypothesis was found to be true.

Analysis of lemon vesicle constituents encourages its intended mammalian vesicle applications. Lipidomic profiling and nucleic acid analyses are barely at its emergence. But proteomic profiling has resulted in encouraging outcomes. Although plant vesicles in general do not have a specific protein marker, several proteins are analogous to mammalian vesicles. In an extensive study carried out on protein cargo in citrus fruit derived vesicles, Pocsfalvi et. al. [72] identified 600-800 proteins in citrus lemon. Heat shock proteins (HSP70, HSP80) which are homologous with mammalian vesicles are identified in lemon. Aquaporin which are also abundantly found in mammalian vesicles are found in lemon as well, and they were previously found to help in mediating vesicle stability. On the other hand, *Patellin-3-like* and *clathrin heavy chain* are the highly specific to plants. The former was a novel discovery in this study and it is interesting because *Patellins* are known for enabling vesicle mediated transport like many proteins in mammalian vesicles. These proteins were suggested by this study as potential markers in citrus or plant vesicles in general. It is also compelling to know that 1/3rd of the proteins detected were related to vesicle trafficking hence indicating that lemon vesicles, like mammalian vesicles can be applied in drug delivery and targeted transport.

2.8. STORAGE

Extracellular vesicles with all their therapeutic and diagnostic capabilities are hindered by several factors, storage being one of them. Due to the plethora in its components, EVs are sensitive to several factors. Moreover, it is not always possible to sequentially isolate and use EVs immediately after collection of the sample source. Hence, preserving the morphological and biological characteristics is a crucial for large scale and extended use of EVs. Lower temperatures are favourable for maintaining life activities of several biological materials [72]. Most common method of storing mammalian EVs is at -80°C and EVs from serum, plasma, and urine were conserved at this temperature [71]. This is highly unfavourable towards the costs related to maintain as well as transport EVs.

Even at this temperature, it is discovered that EVs lose their structural integrity, stability, and biological activity [71]. The effects of storage comprise increase or decrease in diameter, fusion of vesicles together leading to aggregation and intensifying the heterogeneity, and reduction in total number of vesicles. Furthermore, the loss of structural integrity means that the internal proteins and RNAs can exit the lipid bilayer. Regarding proteins, the prominent heat shock proteins that are regarded as markers will be sever severely affected due to temperature changes during operation and storage [71]. As far as stability is concerned, it is very apparent that vesicle stability is lowered since between before and after storage, the zeta potential is lowered by a considerable amount [38]. When the zeta potential is lowered, aggregation will evidently follow.

One of the most salient cause of these effects during storage is identified as freeze-thaw cycles. During freezing, ice crystals are formed on the surface of vesicles. The lipid bilayer can get damaged or teared due to these ice crystals. Once the protective membrane is penetrated, EVs lose their stability and their internal components. To lower these consequences, it is common to add cryoprotectants such as glycerol, dimethyl sulfoxide, PEG, and several sugars such as trehalose and sucrose [71]Click or tap here to enter text.. Sugars are preferred from the alternatives since it is tedious to remove the other permeable cryoprotectants.

Trehalose is a disaccharide which is proven to maintain protein stability and previously used for storage of liposomes which have striking similarity with EVs. Trehalose can also reduce protein aggregation. The OH side of the sugar binds with the phospholipid layer instead of water molecules, hence protecting the layer from the ice crystals. Trehalose concentration as low as 2mM in PBS is regarded sufficient. Another technique used for preservation of biological materials such as liposomes is lyophilization [73]. Here, water around the biological entity is removed by vacuum sublimation and desorption. A combination of CPA and lyophilization is considered ideal since lyophilization alone can lead to protein aggregation [38].

Although extensive research is not done for storage of lemon EVs or plant derived EVs in general, Q Wang et. al. [38] found that grapefruit EVs had higher stability than liposomes at room temperature and they were very stable and maintained their biological activity even when stored at 4°C with a loaded cargo.

CHAPTER 3

MATERIALS AND METHODS

3.1. MATERIALS

The raw material for this process is lemon juice which is extracted using a kitchen juicer. The lemons were always bought from several local markets and processed together to reduce disparity in results. This juice is diluted with phosphate buffered saline.

Membranes used for filtration

- Sartobind Q average pore size of 3 μm
- Sartorius Regenerated Cellulose, average pore size of 0.45 μm
- Polyether sulfone from Sartorius Stedim Biotech, MWCO of 100kDa
- Polyvinylidene fluoride from Alfa Laval, MWCO of 100kDa, 250kDa
- Minitan Regenerated Cellulose, MWCO of 300kDa

Materials for SEC-FPLC

- BioRad Econo column - column (75x1.5 cm)
- Sepharose ™ CL-2B resin
- 0.1 M Phosphate buffered saline, pH 7.4

Materials for SEC-HPLC

- Sigma Aldrich Water HPLC Plus
- 0.1 M phosphate buffered saline, pH 6.7
- Yarra SEC-2000 chromatographic column (150X7.8) (Phenomenex®)
- 2 mL HPLC vials

Materials for BCA

- Pierce™ BCA reagent A, reagent B from Thermo Scientific™
- Albumin standard
- Ethanol

Materials for DLS

- Disposable cuvettes
- Gold electrode cuvettes

3.2. INSTRUMENTS

Table 2: Instruments used

Instrument	Purpose
Thermo Scientific™ SL16R centrifuge	Pre-treatment
Millipore AMICON™ 8200	Pre-treatment Stage diafiltration
Millipore MINITAN S™.	Diafiltration in tangential flow mode
Waters Alliance separation module 2695	SEC-HPLC analytical mode
Akta purifier 100	SEC-FPLC analytical mode
Beckman Coulter optima L-90K	Ultracentrifugation comparisons
Axiolab-5	Microscopy of membrane gel layer
Zetasizer Nano ZS	Size measurement Zeta potential measurement
Shimadzu UV Visible spectrophotometer	BCA assay

3.2.1. CENTRIFUGATION

Once lemons are peeled and the juice is extracted with a kitchen juicer, it is centrifuged at a low speed 5000 rpm (4700 x g) using a Thermo Scientific™ SL16R. For this, a TX-400, swinging bucket rotor is used. Centrifugation is carried out in 15 ml falcon tubes. Before doing analyses in SEC-HPLC or SEC-FPLC, another centrifugation at a higher speed is carried out to remove particles that can clog the columns employed. To achieve a speed of 10000rpm (9000 x g), Thermofisher 30 x 2mL microliter fixed angle rotor from Thermo Scientific™ is used is used and the lemon juice is loaded in 2 ml eppendorfs. The centrifuge has a control panel where speed can be provided in rpm or rcf, centrifugation time, acceleration, deceleration, and the temperature of operation. All centrifugation is carried out at 4°C to protect the vesicular fraction.

Figure 26: Thermofisher SL16 centrifuge

Figure 27: Thermofisher TX-400

Figure 28: Thermofisher 30x2 microliter rotor

3.2.2. STAGE FILTRATION CELL

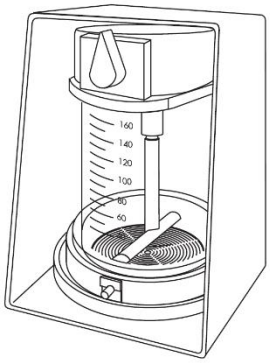

Figure 29: AMICON cell

After the centrifugation at 5000 rpm, the pellet is discarded and the supernatant is diluted with 0.1M PBS and subjected to a dead-end filtration in Millipore AMICON™ series 8200 stirred cell. The cell contains a poly sulfone body with a stirrer that can be operated magnetically. The stirrer rotates once placed on a magnetic table and reduces concentration polarization as well as creates high turbulence. This helps in reduction of cake formation. The speed is kept at 200 rpm. The cell can process 200 ml and offers 28.7 cm^2 of effective membrane area. A pressure line can be attached behind the cell to provide a pressure up to 5.3 bars. The cell is kept safe using a pressure relief valve at the front. Membranes are cut to a circle of diameter 63.5 mm and is placed, shiny side up at the bottom using a silicon O-ring which prevents leakage. The permeate is collected by connecting a silicon tube at the outlet to a graduated cylinder. All membranes are initially washed with water and equilibrated with PBS at least 3 times prior to use. The driving force is provided by connecting the pressure line to compressed air. A pressure of 1.5 bars is set for all the operations using an in-line pressure gauge. The pressure is maintained using a casing that encloses the cell.

As the initial membrane process is a dead-end filtration, fluid is approaching perpendicular to the membrane surface. A Sartobind Q membrane of 3 µm pore size is employed here to remove larger cell debris and the permeate is collected for vesicle purification using diafiltration. The pre-treatment steps are now complete and depicted in figure 30.

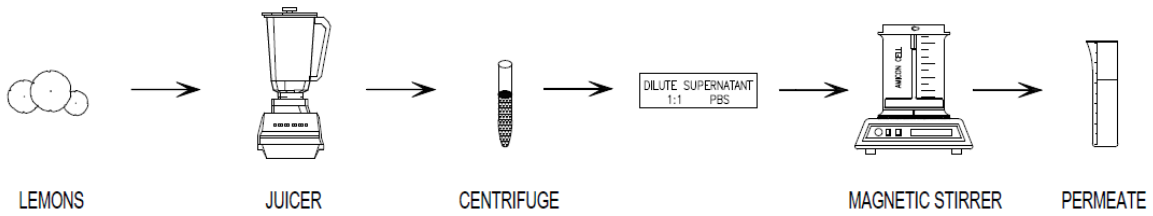

Figure 30: Pre-treatment method

In diafiltration using AMICON™ cell, an initial starting volume of 90 ml is collected from the permeate of the previous step and 90 ml PBS is added. Since the membrane pores are much smaller, smaller impurities and proteins are taken out and the exosome like fraction is concentrated in the retentate. Once the volume of 90 ml is removed as permeate, it is replaced by the addition of 90 ml buffer and this is considered as the first stage. This is repeated for 4 more stages and the final product is collected in the fifth retentate. After use, all membranes are scraped off to remove the gel layer and cleaned with water and finally stored in a 25% solution of ethanol and water at 4°C.

3.2.3. TANGENTIAL FLOW FILTRATION

The stage diafiltration in the previous step is limited by low process volume and the tedious process of adding buffer with each stage and most importantly, immediate fouling due to the dead-end flow. Diafiltration in tangential flow filtration mode offers continuous operation with the use of a pump which constantly flows the feed to the cell. The feed flow is directed across the membrane and is swept tangentially over it. This reduces the formation of gel layer or fouling which is common and rapid for dead-end filtration and hence increases the membrane life. Additionally, larger volumes can be processed and the process can be carried out for longer time. The retentate which contains the exosome like fraction is recycled back to the feed and the permeate containing buffer and smaller impurities are collected as permeate in a graduated cylinder. While a certain quantity of permeate is removed, an equal amount of buffer (PBS) is added to the feed tank. A pressure controller is usually kept at the inlet to control the driving force. Usually, TFF involves at least 1-2 diavolumes where one diavolume is defined as the number of times the starting volume of feed has been replaced by buffer. A typical TFF setup is shown below.

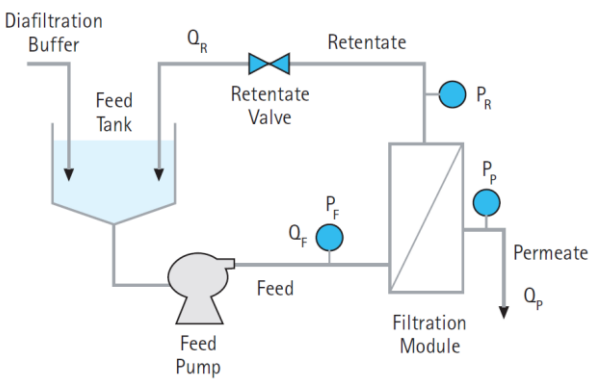

Figure 31: Typical TFF scheme

The process is carried out with a tangential flow filtration cell, Millipore MINITAN S™. The cell consists of a stainless-steel frame with acrylic manifolds which houses the membrane and the inlets and outlets for the process. A single membrane is cut into a rectangle of dimensions 14 x 10 cm. MINITAN S™ offers 30 cm^2 of membrane area. The membranes are kept between the manifolds along with an open flow separator made of silicone to provide space for the feed to flow between the membrane surfaces. These separators are highly recommended for feed with large amounts of cells and suspended solids. A volume of 100-500 ml of feed at maximum pressure of 2.1 bars can be processed in this system.

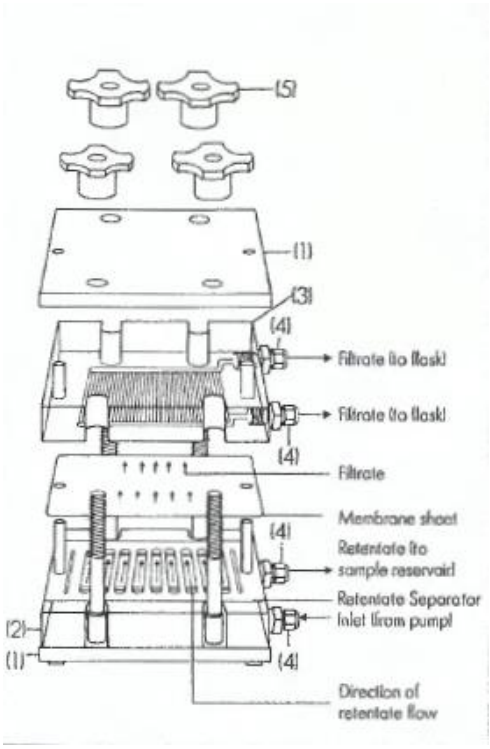

Figure 32: Millipore MINITAN S cell

The typical TFF system is slightly modified for better monitoring and control of the system. A pump (P-900) which is the auxiliary of AKTApurifier FPLC system from GE Healthcare is employed for this purpose. There are two pumps namely pump A and B with 2 inlet lines each. The pump offers a maximum flowrate of 100 ml/min. The pump is chemically resistant to aqueous solutions and organic solvents and works across a wide range of pH. The pump should be washed prior to use with the use of the UNICORN software by giving the command 'pump wash purifier'. It also requires a rinsing solution of 20% ethanol/water mixture that should be changed monthly.

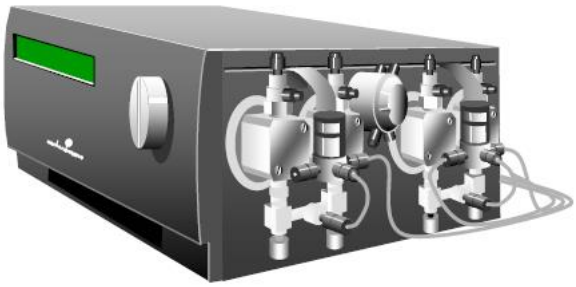
Figure 33: AKTA FPLC PUMP P-900

The pump is connected to a pressure indicator which displays the pressure on the computer. The system is controlled by the UNICORN software. The pump draws liquid from the feed tank which is kept in an ice bath with a temperature maintained at 6°C, controlled using a probe. The tank is kept on a magnetic stirrer to maintain mixing of the feed and the retentate. The feed flows though the MINITAN S™ cell and the permeate is collected in a graduated

cylinder. The retentate is sent to the AKTA FPLC system which consists of a series of detectors for UV, conductivity, and pH and finally is sent back to the feed tank as recycle. The presence of these detectors can be used as for in-line detection and live control of the process. The UV detector can also be used for specific targeting. Once an impurity which absorbs a particular wavelength is identified, its concentration can be compared against the concentration of EVs which typically absorb at 260 and 280 nm. The distinction in the absorption spectrum of proteins in EVs and the proteins in the juice has not yet been devised. So, this could be a future perspective since the software can visually depict the extent of purification using UV signal against time or volume processed.

The P&ID of the TFF is given below.

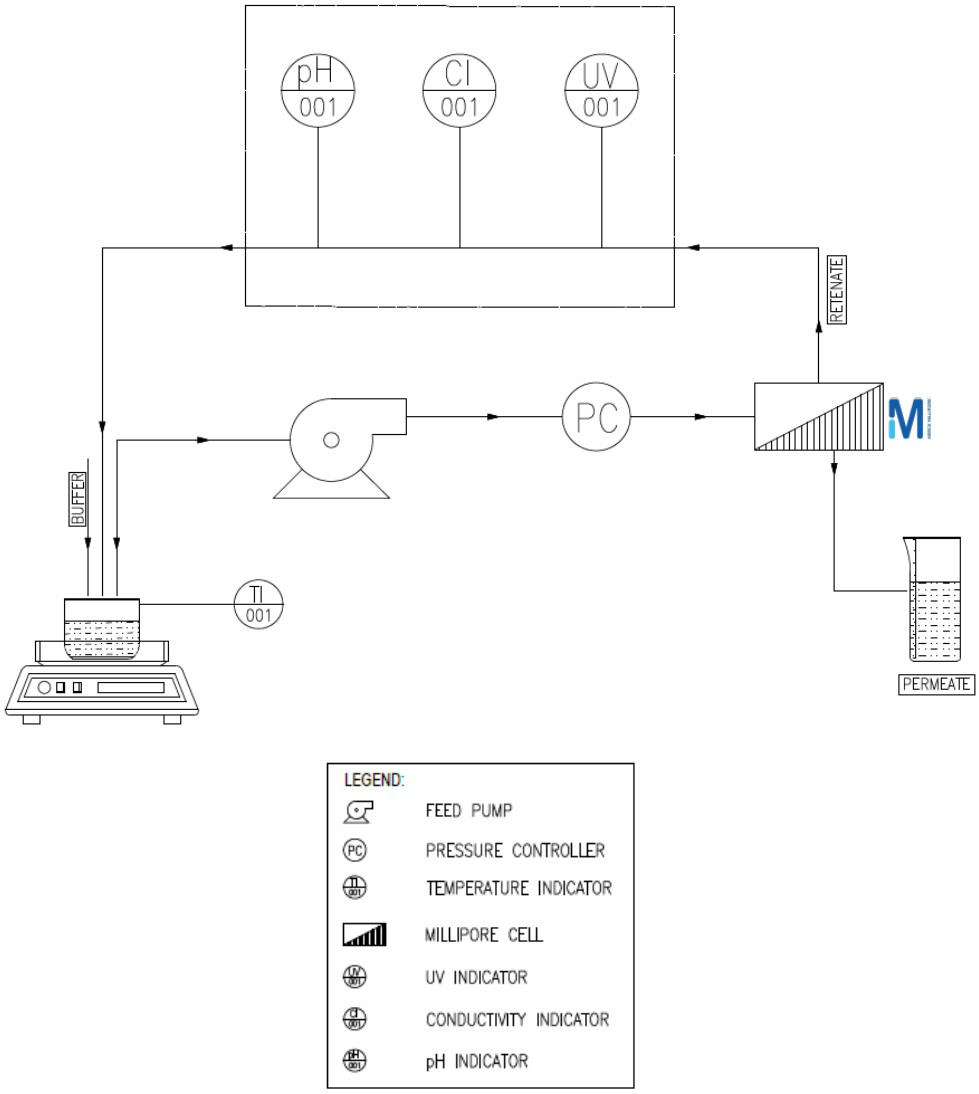

Figure 34: P&ID of TFF protocol

Once the connections are made with the required tubes, the UNICORN software allows to define a particular flow path and the required flowrate. On the computer screen, the pressure, flowrate, pH, conductivity, and 3 different UV signals can be plotted live with respect to time or volume. In this way constant flowrate operation can be carried out. Even though FPLC pumps usually run at constant flowrate, using the feature of the software called 'Press flow control', constant pressure operation can be carried wherein the pump automatically adjusts its flowrate to maintain the set point pressure. Both are common practises for TFF and constant pressure operation is chosen here. First, water is flushed through the system as a cleaning procedure followed by membrane equilibration of with PBS. The pH and conductivity meter gives an idea about what is exiting from the retentate of the system. For every 5 ml removed through permeate, 5 ml of PBS is added to the feed to carry out the TFF. Since the membrane system deals with larger tubes and the FPLC system contains tubes of smaller diameter, significant pressure drops are expected in the system. To further increase the pressure drop, the feed is sent through an additional 2 ml sample loop which is a tube of 0.5 mm diameter. This is done by choosing the 'inject' valve in the software.

After each use, 0.5 M NaOH is sent to the system to clean the MINITAN cell as well as the detectors in the AKTA FPLC system. This prevents accumulation of impurities in the tubing. Filtered water is fluxed to remove the NaOH and the cell is disassembled and cleaned.

3.2.4. HIGH PERFORMANCE LIQUID CHROMATOGRAPHY

Size exclusion chromatography is a popular technique in a preparative mode for the purification of EVs and HPLC is commonly used for quantitative and qualitative evaluation of liquid samples. Here, it is employed as an analytical technique to determine the concentration of vesicles and the impurities in the filtration process. The stationary phase comprising of gels or resins of a particular size range is packed inside a column. The inlet mixture will have particles of different size ranges. Molecules of large molecular weights do not pass through the pores of the packed resin/gel and are eluted first. The smaller molecules on the other hand gets travel longer paths inside the pores of the resin/gel and exit out later. This is detected using an UV detector and using a computer program, the result of the analysis is obtained as a peak of absorbance unit v/s time or volume of retention. The height of the peak is proportional to the concentration and the area under the peak is the volume eluted.

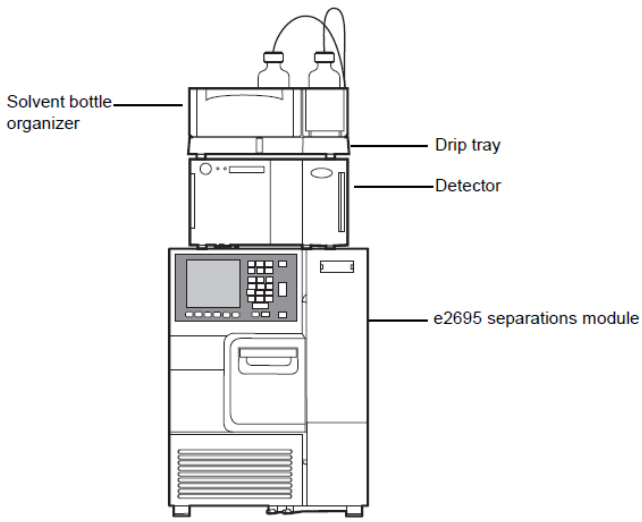

Figure 35: Waters Alliance separation module 2695

The SEC-HPLC was carried out with Waters Alliance separation module 2695 (figure 35) with a Waters 2487 Dual λ Absorbance UV detector. The display on the separation module shows the flowrates, solvent lines used and the back pressure. It can also be used for manually controlling the flowrates and carrying out activities such as pump wash, needle wash, temperature control, cleaning, and degassing. There are 4 valves that controls the flow path during these operations, all housed below the sample compartment. In the sample compartment, there is a carousel where 99 different samples can be loaded at a specified temperature for injection. The machine consists of 2 pumps which can draw liquids from 4 different solvent lines for the purpose of supplying HPLC water, mobile phase, or cleaning agent such as methanol into the system. These lines can be blended and used simultaneously. The 250 µl syringe draws sample from the carousel which holds the sample in 2 ml HPLC vials and sends it to the sample loop and eventually to the column. From the column the elution is recorded. The machine, needle and the sample loop are cleaned monthly with monosodium phosphate solution of pH 3.2. In case of erratic chromatograms, chemical cleaning is also carried out with a reverse flow at 0.05 ml/min.

The HPLC machine was controlled using a computer software, EMPOWER. The time of analysis and the amount of sample to withdraw can be specified in the 'run samples' tab. Usually a blank (PBS) is inserted in the first vial to establish a baseline and all injections are done with a duplicate, each 25 µl. Sample run time is specified as 30 minutes. An isocratic flow of of 1 ml/min flowrate is used. At this flowrate, the back pressure is found to be about

1200 psi which is within the limits provided by the column manufacturer. Since the column needs a continuous flow of buffer even after analysis, the column is continuously conditioned at low flowrate after injections are complete. All these can be programmed as set of instructions in the 'browse project' tab. After the analysis, the resulting chromatograms can be viewed and exported using the 'review data' tab.

The column employed was Yarra® SEC-2000 by Phenomenex® with a dimension of 150 x 7.8 mm. Column consists of silica resins packed with a pore size of 145 Å and particle size of 3 µm. pH range is provided from 2.5 to 7.5 and MW range is between 1kDa and 300kDa. An additional pre-column is added before the column inlet for trapping large particles that can clog the column. A Phenomenex® Security Guard is used for this purpose. The column when not in use is stored with 25% mixture of methanol and HPLC grade water. The mobile phase consists of PBS with pH of 6.8 (Appendix I) made with HPLC grade water. HPLC calibration curve is obtained with molecules such as IgG, BSA, Tyrosine and Myoglobin whose molecular weights are known.

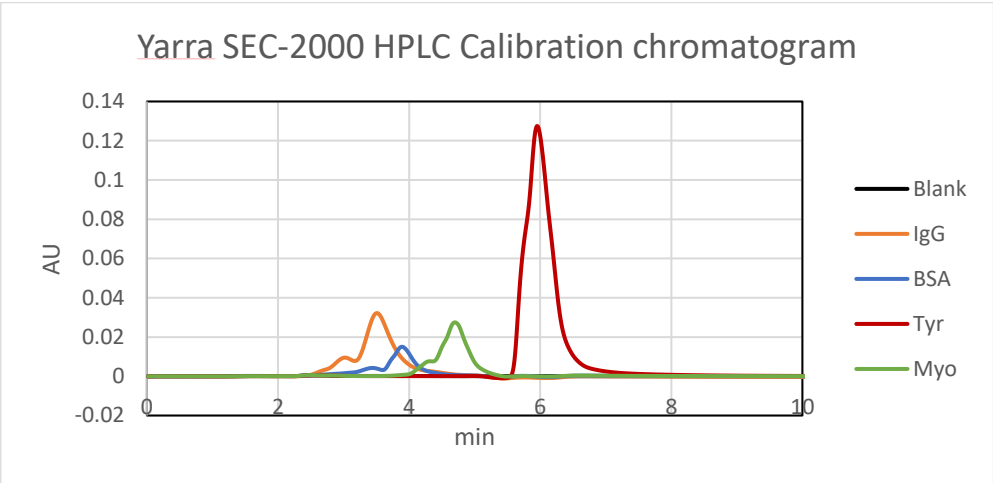

Figure 36: Yarra SEC chromatogram with IgG, BSA, Tyrosine and Myoglobin

Table 3: HPLC Calibration curve data

Compound	**Molecular weight**	**$\log_{10}$(MW)**	**Retention time**
	Da	Da	min
IgG	150000	5.176	3.5
BSA	66000	4.819	3.88
Myo	16700	4.222	4.7
Tyr	181	2.257	5.95

Using the retention time and the known molecular weights, it is possible to develop a calibration line by plotting them with linear regression as shown in figure 37. The plot of lemon juice that underwent filtration, when sent to the HPLC column had 3 peaks. First peak associated with EVs, that elutes around 2.4 minutes and the two peaks corresponding to impurities which elutes later, around 6 and 8 minutes. Once the plot of log MW vs retention time is repeated using the equation of the line y = -1.1823x + 9.4482, it is possible to determine the range around which the column operates as well as approximate the molecular weights of EVs and impurities.

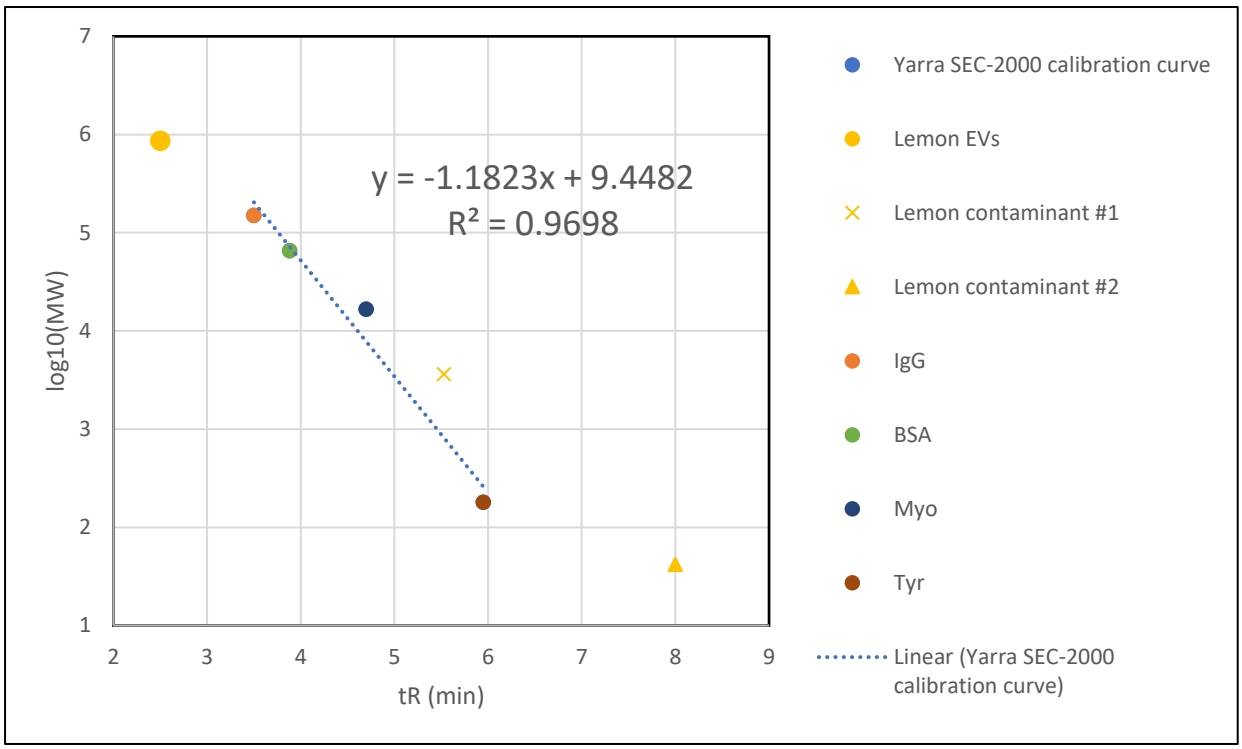

Figure 37: Yarra SEC calibration curve

From plugging in the value of retention time of EVs as 2.6, the molecular weight of EVs is found to be approximately 862 kDa. It is interesting to note that the column operates in a molecular weight range that is much higher than the maximum limit of 300kDa. Yarra-SEC 2000 being a short column, the process times are shorter and the possibility of programming multiple injections simultaneously, makes it an interesting option for comparison of different results, especially in the case of stage filtration which contains 5 retentates and 5 permeates to be analysed. This SEC will also be performed for storage tests.

3.2.5. FAST PROTEIN LIQUID CHROMATOGRAPHY

Fast Protein Liquid Chromatography is a common technique for separation of protein mixtures in preparative mode. Here, however it is used to analyse the filtered lemon juice through size exclusion or gel filtration principle. The FPLC used is AKTApurifier 100 which is generally used for laboratory scale purification of proteins. The system consists of pump P-900 which is a combination of reciprocating pumps A and B with 4 heads each, for the flow of mobile phase or water for cleaning. All solvents are filtered using Whatman 0.22 µm filter papers prior to use to protect the column and the system. The pump offers up to 100ml/min in flowrate and maximum 100 bars in pressure. Pump is lubricated with a 0.4% mixture of acetone and filtered water. Pump also requires a rinsing solution of 25% solution of ethanol and water. A mixer allows mixing of eluents if needed for the applications such as ion exchange.

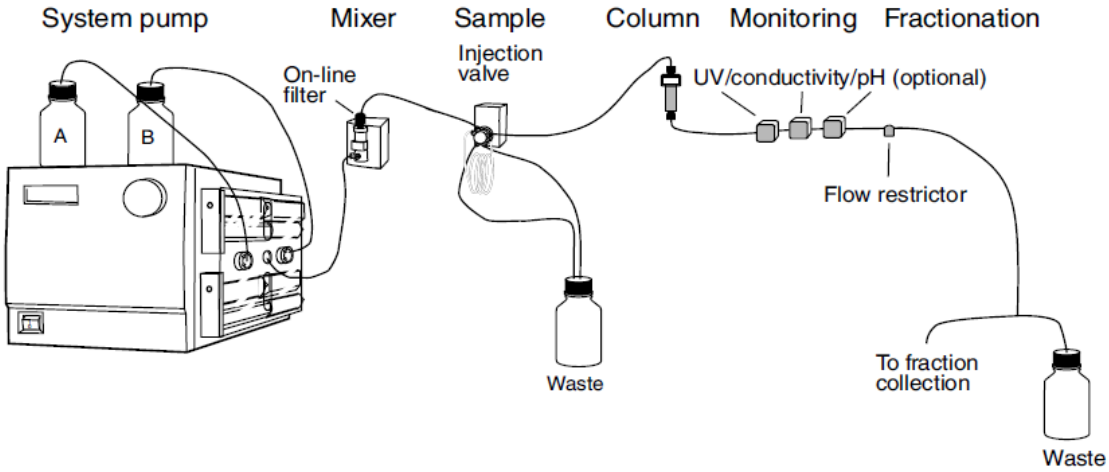

Figure 38: AKTA FPLC system

A syringe is used to inject the sample manually to the sample injection valve. The sample flows to the column along with the mobile phase. The sample injection valve contains sample loop, a tube of known volume which is determined as 2-5% of the volume of the column bed. The injection valve has 3 main positions to offer flexibility of operation.

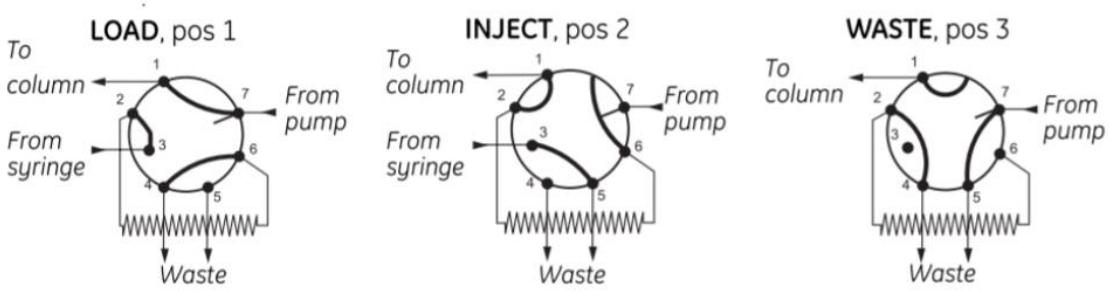

Figure 39: AKTA FPLC injection valve

In the load position, the buffer (PBS, pH 7.4) enters the valve and is sent to the column to carry out column equilibration. The sample is injected while the valve is in the load position and remains in the sample loop. In the inject mode, the sample is sent to the column along with the buffer entering. Finally, in the waste position, the column is excluded and the inlet solution is sent to waste.

The outlet of the column is connected to a series of detectors for UV, conductivity, and pH. The range of the UV detector is 190-700 nm. These detectors analyse the sample that is finally sent to another valve which is directed to waste.

The system is controlled using UNICORN software. The software comprises of a system control window where the flowrates and other instructions such as valve position, pump selection, mixing ratio etc. can be provided. At the same time, the system control can monitor the process with respect to the absorbance, pH, temperature, pressure, and flow with time. It is possible to complete the entire operation in automatic mode by using a predefined method. The method is a series of instructions given to the system using 'method editor' window. The entire process can be elucidated step by step here. Once the analysis is over, the results are saved and can be viewed in the 'evaluation' window. Here there are different tools to view and integrate the curves obtained from analysis. This chromatogram and data can be directly exported to a software such as Microsoft Excel.

The column employed here was an Econo-Column® glass column of dimensions 75 x 1.5 cm from Bio-Rad. The resin used, Sepharose™ CL-2B, 2% cross linked Agarose gel which is commonly employed for EV separation. A 75% mixture of Sepharose™ gel in 0.1 M PBS is used and packed in the column up to a volume of 120 ml. The recommended packing flowrate is 30 cm/h. The recommended sample volume is 2-5% of the column volume. The gel is chemically and physically resistant across several biological fluids. Column cleaning is carried out monthly using 0.5 M NaOH. The molecular weight range of the column is between 70 and 4000 kDa. The bead size ranges from 60 to 200 µm. The resin is stable between a pH of 2 and 14 which falls in the range of lemon juice. The performance testing of packing was carried out using 2% solution of acetone and water at a wavelength of 260 and 280.

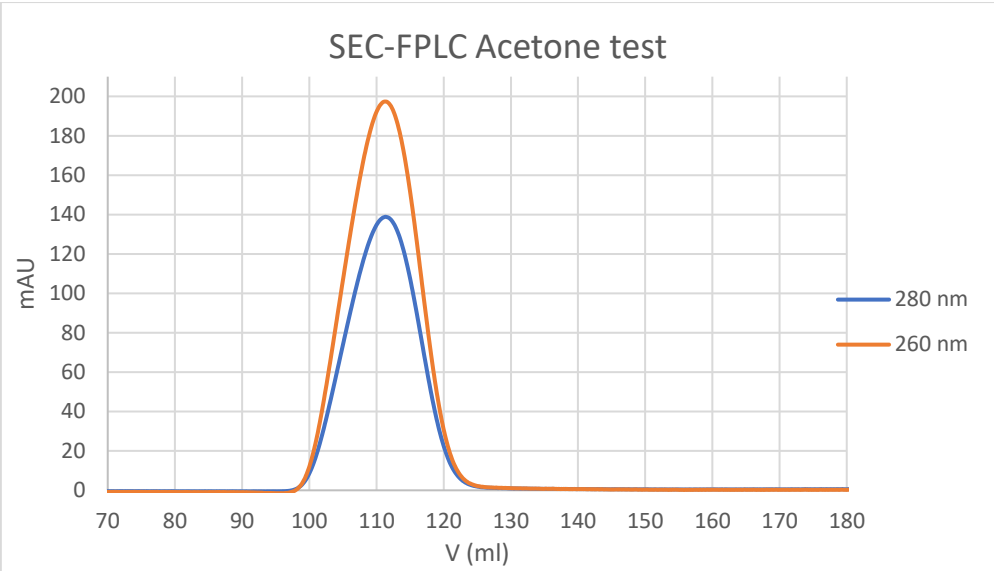

Figure 40: SEC FPLC Acetone chromatogram

The asymmetric factor and the number of plates is found using the instructions given in the manual of the resin for acetone tests.

$$Number\ of\ plates, \qquad \frac{N}{m} = 5.54\,(\frac{V_R}{W_H})^2 * \frac{1000}{L}$$

Where V_R = maximum retention volume

W_H = width of the peak at 50% peak height

$$Asymmetry\ factor, A_S = \frac{a}{b}$$

Where a and b are the left and right sided width of the peak from the centre at 10% peak height.

Table 4: Asymmetry factor and No of plates of Sepharose CL-2B column

PROPERTIES	280 nm	260nm	UNITS
L (bed height)	0.67	0.67	*m*
V_R (Retention time)	111.4	111.36	*ml*
Peak height	138.521	197.21	*mAu*
Peak width	34.01	29.7	*ml*
W_h (width at half height)	12.32	12.36	*ml*
Area	1739.14	2474.96	*mAu*ml*
a	100.65	100.61	-
	120.92	120.83	-
A_s (asymmetry factor)	0.88	0.88	-
N/m (plate number)	676058	671207	-

The values above were directly extracted using UNICORN software and the number of plates is found to be above the minimum of 3000 and the asymmetry factor was 0.88 which is between the limits of 0.7 and 1.3.

As the column is about 67 cm long and the recommended flowrate is as low as 0.4 ml/min for the resin the process time is 7.5 hours, which is much higher than the time required by HPLC analysis. Moreover, there is no possibility to make multiple injections in one go. However, the length of the column assures that the resolution and elution will be much better and more precise results can be obtained with FPLC.

3.2.6. ULTRACENTRIFUGATION

Ultracentrifugation (UC) is considered as gold standard for EV isolation from any sample. So, it is imperative to compare the results obtained using diafiltration with that of UC. The protocol employed was analogous to Thery et. al [12] and Pocsfalvi et. al [70]. A series of low-speed centrifugations are carried at 400 x g for 20 minutes and 1000 x g for 20 minutes followed by high-speed centrifugation at 25700 x g for 20 minutes using Thermo Scientific™ SL16R. The pellets in these steps are discarded and the supernatant is collected for carrying out UC. Ultracentrifugation was done using a Beckman Coulter Optima L-90K Ultracentrifuge in FABIT department, University of Bologna. The rotor used is a fixed angle, 50.2 Titanium rotor from Beckman which needs to be lubricated with Spinkote™ lubricant. The maximum permissible speed is 302000 x g and the capacity is 468 ml. 20 ml Beckman Coulter polycarbonate UC tubes are used to process a total of 80 ml juice.

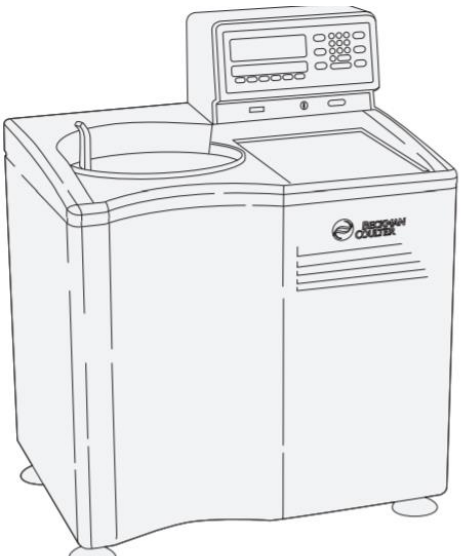

Figure 41: Beckman Coulter Optima L-90K

Figure 42: Beckman 50.2 Titanium rotor

2 protocols of ultracentrifugation were attempted at a temperature of 4°C

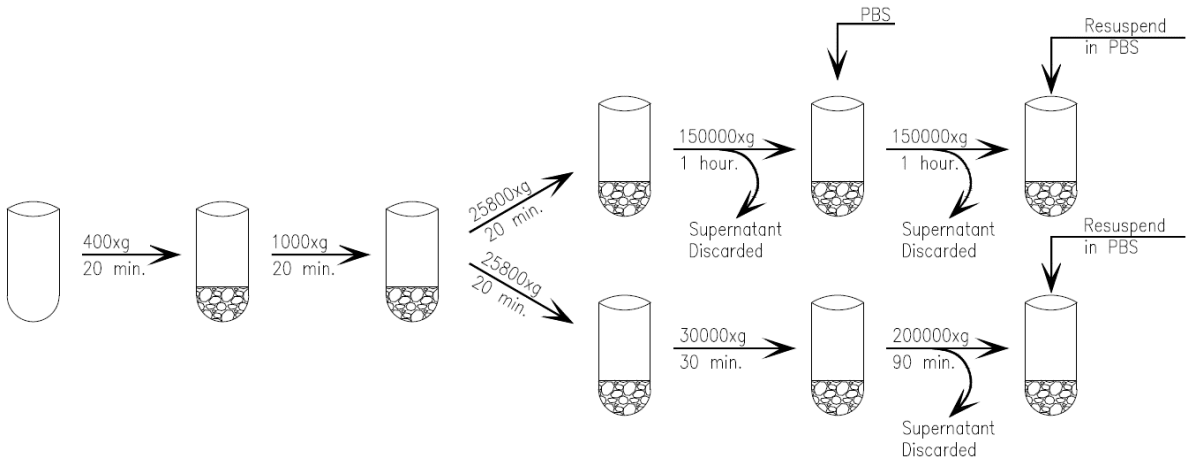

Figure 43: Ultracentrifugation protocols

1. An ultracentrifugation is done at 150000 x g for 1 hour, supernatant is discarded, pellet is resuspended in PBS with a glass Potter pestle and a micropipette. The resuspended pellet is sent to UC at the same speed for the same time. Final pellet is resuspended in PBS as done before.
2. A preliminary step of 30000 x g for 30 minutes is done, pellet is discarded and the supernatant is centrifuged at 200000 x g for 90 minutes in the ultracentrifuge. The pellet is resuspended in PBS using a Potter pestle and micropipette.

3.2.7. MICROSCOPIC ANALYSIS

To visualize the suspended gel layer on the membrane which evidently contained a large portion of vesicles after diafiltration, a lab microscope, Zeiss Axiolab 5 was employed. This microscope combined with Axiocam can provide with colorized snapshots of the specimen viewed. The scaling information for the colouring is automatic and needs no additional software.

Figure 44: Zeiss Axiolab 5

3.2.8. BICICHRONIC ACID ASSAY

A bicinchronic acid assay was carried out using Pierce™ BCA protein assay kit from Thermo Fisher Scientific. It is a technique for colorimetric detection and quantification of proteins in a sample. The range of total protein content is from 0.5 µg/mL to 1.5 mg/ml. This method utilizes the biuret reaction (reduction of Cu^{2+} to $Cu^{1+}$by proteins in an alkaline medium) with the colorimetric detection of the cuprous cation Cu^{1+} with the use of a working reagent containing bicinchoninic acid. The kit contains reagents A and B and BSA standards in 2 ml ampules.

There are 2 prescribed protocols, a standard protocol with a range of 20–2000 µg/ml and an enhanced protocol with 5–250 µg/ml. The standard protocol is used here due to the uncertainty in the total protein content. The procedure starts with the preparation of BCA working reagent. The two reagents, A and B are mixed in a 50:1 ratio to prepare the working reagent. The amount of working reagent required is calculated as,

$$Volume\ required = (No\ of\ standard + samples) \times 2 \times (vol\ of\ WR\ per\ sample\ )$$

The multiplication of 2 indicates the duplicates taken. The working reagent should be mixed well. Next, standards are prepared using bovine serum albumin at different concentrations. As prescribed, a range of concentration from 0 to 2000 µg/ml in 9 different standards and their

duplicates are taken by diluting with PBS. Now, in a 5ml test tube, 2 ml of the working sample and 0.1 ml of the standard is introduced. This test tube is sealed and incubated in a water bath at 37°C for 30 minutes. The test tubes are labelled A to I in the order of decreasing concentration where I only contains PBS. Afterwards, the standards needs to be cooled down to room temperature before measuring absorbance.

A Shimadzu UV Visible spectrophotometer UV-1601 with a wavelength range of 190-1100 nm is considered for absorbance measurements. The machine was zeroed by using deionized water. The wavelength is set to 562 nm as per protocol. The samples from A to I are analysed with the UV spectrophotometer. The cuvettes are washed with ethanol and then water between each standard. Measurements must be taken within 10 minutes of each other since the colours can change with time. The absorbance readings are averaged between the replicates and the readings of A to H are subtracted with the value of I which is the blank. The absorbance is plotted against the protein concentration in each standard. Hence a standard curve can be generated. Now, 0.1 ml of the samples to be analysed are taken in a test tube with 2 ml working reagent and incubated as before. The absorbance readings are noted and the standard curve is referred to find the total protein content representing the absorbance value. The protocol is shown in figure 45.

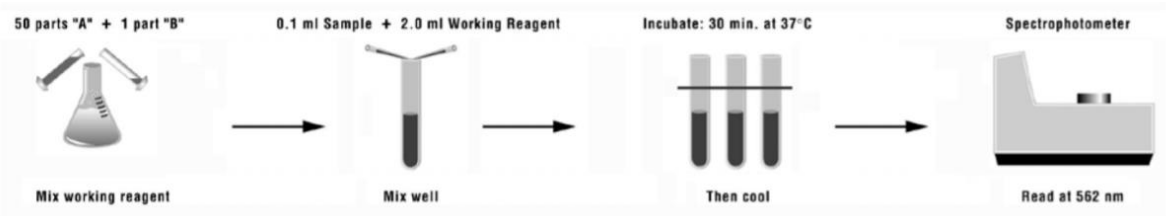

Figure 45: BCA protocol

3.2.9. DYNAMIC LIGHT SCATTERING

Dynamic light scattering (DLS) is a rapid and non-invasive analytical technique that determines the hydrodynamic sizes of molecules and nanoparticles by measuring the Brownian motion. Brownian motion is the random movement of particles resulting in collision with the solvent molecules in a solution.

In DLS, particles are illuminated by laser and the particles will scatter the incoming light. The light scattering intensity changes with time due to the random diffusion of particles. Small particles diffuse quickly leading to large variation in intensity meanwhile larger ones moves slowly creating lower variation. This changing intensity signal is measured on a detector over time. The light scattering signals are taken as rapid snapshots. These snapshots are continuously correlated with the previous ones.

The rate of Brownian motion can be expressed as Translational Diffusion Coefficient. This coefficient can be used in the Stokes Einstein equation to determine the hydrodynamic size as follows.

$$Hydrodynamic\ size, d_H = \frac{kT}{3\pi\eta D}$$

The size of all the particles in a sample can be shown as an intensity distribution. This can be converted to volume or number size distribution.

The temperature and viscosity of the sample will alter the Brownian movement and hence these values should be known.

Another parameter that can be evaluated is the surface charge of the particles through zeta potential. Zeta potential is the surface charge density of dispersions and it is correlated to the stability of dispersions. Since the zeta potential is an indication of the extent of repulsion between nearby, similarly charged particles high zeta potential, either negative or positive means that the nanoparticles are far apart and stable. Zeta potential can be useful for measuring isoelectric points of proteins as well.

For this analysis, Malvern Zetasizer Nano ZS is used, at the Industrial Chemistry department (Toso Montanari) at the University of Bologna. The analyser offers a size range from 0.3 nm to 10 μm and a molecular weight range of 342 Da to $2x10^7$ Da. Temperature range is from 0 to 90°C. This instrument can measure a zeta potential upto +-500 mV

Figure 46: Zetasizer Nano ZS

A Helium Neon laser of 4 mW, 633 nm is used to illuminate the particles. Solution to be tested is loaded on to a 1.5 ml polystyrene cuvette. For the analysis of size, disposable polystyrene cuvettes are used. On the other hand, zeta potential measurements were made using special cuvettes equipped with gold electrodes.

Figure 48: Disposable polystyrene cuvettes

Figure 47: Malvern Gold electrode cuvette

The system is controlled by using a software supplied by the manufacturer called Malvern Zetasizer. Through specific algorithm, the software correlates the intensity signals from the detector to particle diameter or potential. Multiple measurements are usually made. The software needs the values of the buffer used to predict the viscosity of the sample. The size distribution can be obtained in terms of volume and number distribution in addition to intensity distribution. The intensity is displayed in terms of peaks which can be averaged to find average particle diameter. The feed and the retentates were tested through DLS. As a pre-treatment and for accurate measurements, sample were vortexed and centrifuged before analysis.

CHAPTER 4

RESULTS AND DISCUSSION

This research focusses on 4 main steps

1. Concentration of the juice and removal of pulp and large cell debris
2. Diafiltration to remove smaller impurities and purify EV fraction
3. Analysis of retentates and permeates using SEC (HPLC and FPLC) for evaluating the concentrations of EVs and impurities
4. Analysis of size and protein concentrations in the samples through analytical techniques

Table 5: Tested parameters

Variables	Tests carried out
Isolation method	• Diafiltration • Ultracentrifugation
Filtration mode	• Stage diafiltration • Tangential flow filtration
Membrane material	• Regenerated cellulose • Polyvinylidene fluoride (PVDF) • Polyether sulfone (PES)
Membrane cut off	• 0.45 µm • 100 kDa • 250 kDa • 300 kDa
Pre-treatment step	• Centrifugation at 4700 x g + 3 µm filtration • Centrifugation at 4700 x g + centrifugation at 25800 x g
Buffer	• PBS • Tris buffer
AnalysesCVB	• SEC-HPLC • SEC-FPLC • BCA assay • DLS • Storage tests

4.1. PRE-TREATMENT

The juice is centrifuged at 5000 rpm (4700 x g) in Thermo Fischer SL16 centrifuge for 40 minutes and the pellet containing larger cell debris and larger impurities are discarded. Usually, there is a floating fibrous material in suspension which is also discarded before sending it for the next step. The juice is diluted 1:1 with 0.1 M PBS. Two different concentration steps have been tried, one with a high-speed centrifugation (25000 x g for 30 minutes) and other using a Sartobind Q 3µm membrane in an AMICON filtration cell. After the centrifugation, pellet is discarded and the supernatant is collected as feed to the diafiltration. For the membrane process, the pressure applied is 1.5 bars since larger pressures can damage the membrane. A stirring speed of 200 rpm is applied using a magnetic stirrer to aid in the reduction of concentration polarization. The chromatogram at this stage given in figure 49 can be considered as the concentrated feed leading to the diafiltration step. 2 ml of the final feed is collected and SEC-FPLC analysis is performed on the two different steps. The wavelength selected is 260 and 280 nm since a variety of proteins absorb at this wavelength.

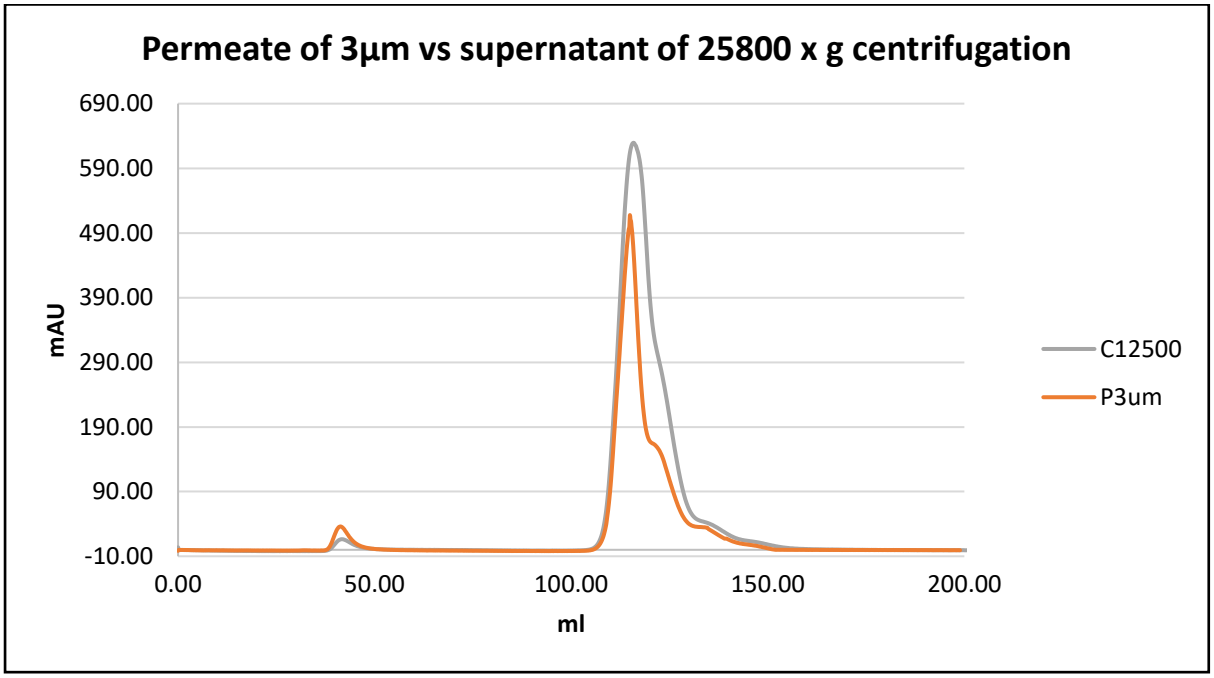

Figure 49: FPLC chromatogram of pre-treatment step

In general, the chromatogram involves the small EV peak which exits the column between 30 and 50 ml retention volume and a large peak between 100 and 150 ml representing small protein impurities. It is clear from the chromatogram that both concentration steps are efficient in removal of impurities, but the additional centrifugation has higher area of EV peak which represents higher amount.

The integrated areas of the 2 peaks are given in table 6.

Table 6: Integrated peaks of pre-treatment step

Analysis	EVs	Impurities
P3µm	201.1	12329.65
C12500	127,30	7726.91

4.2. STAGE WISE DIAFILTRATION

The next step is to reduce the impurities in the sample and for this diafiltration step, several parameters are to be optimized. This step is first carried out in a stagewise manner in a Millipore AMICON cell. This cell maintains the previously mentioned 1.5 bar pressure. 80 ml of the permeate of 3µm filtration is collected and is diluted again with 80ml PBS adding up to a starting volume of 160 ml in the 200 ml cell and hence initiating the first stage. The permeate collected is measured across time for all the membranes tested.

1. 0.45 µm regenerated cellulose
2. 100 kDa PVDF
3. 250 kDa PVDF
4. 100 kDA PES
5. 300 kDa regenerated cellulose

The 0.45 µm membrane is used to compare microfiltration and ultrafiltration. Most of literature recommends PVDF and PES membranes since they do not interact or attach to the various protein-based impurities that are subjected to removal here. PVDF is also considered, since it was previously used for urinary exosomes isolation and urine has an acidic pH, like lemon juice [27]. Finally, PES is an interesting option since several commercial centrifugal concentrators such as Vivaspin from Sartorius employ PES as the membrane material [29].

The permeate flux of 0.45 µm membrane is shown in figure 50.

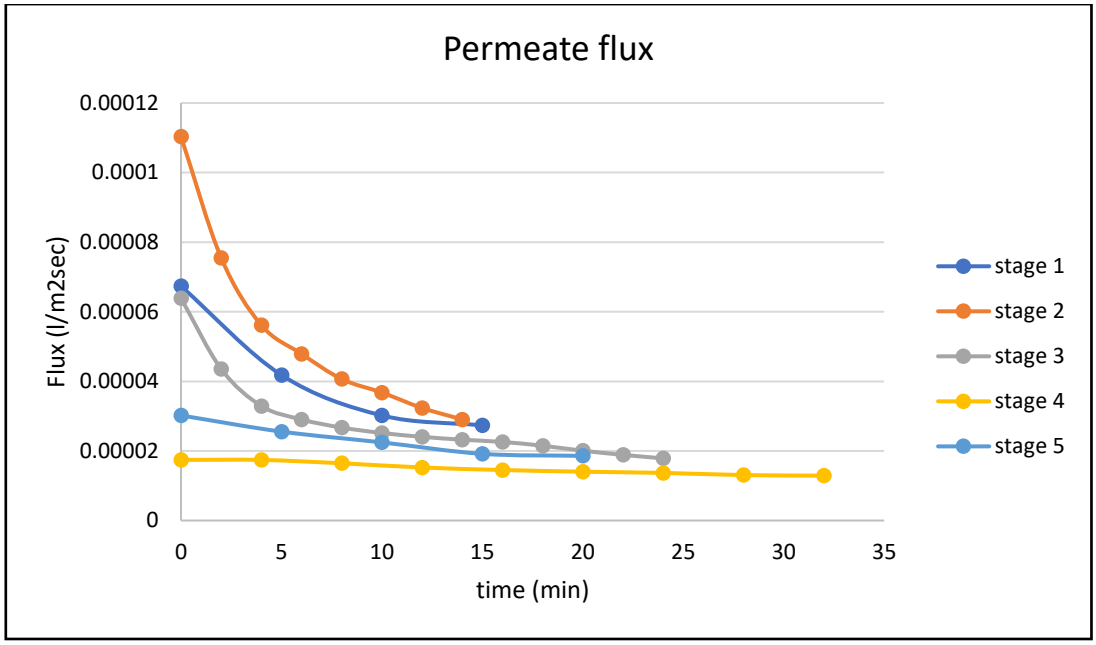

Figure 50: Flux of 0.45 µm RC membrane

For the 5-stage filtration, starting volume of 80 ml of juice and 80 ml PBS is taken. Once 80 ml of permeate is collected, 80 ml more of PBS is added to dilute the retentate and to start the second stage as per diafiltration protocol. This is repeated 5 times and the permeate and retentate in each stage is collected in a 2 ml Eppendorf for analysis. As stage diafiltration involves a total of 5 retentates and 5 permeates to be analysed, HPLC-SEC is preferred since it is a faster way to analyse multiple samples. The chromatograms are shown in figure 51 and 52.

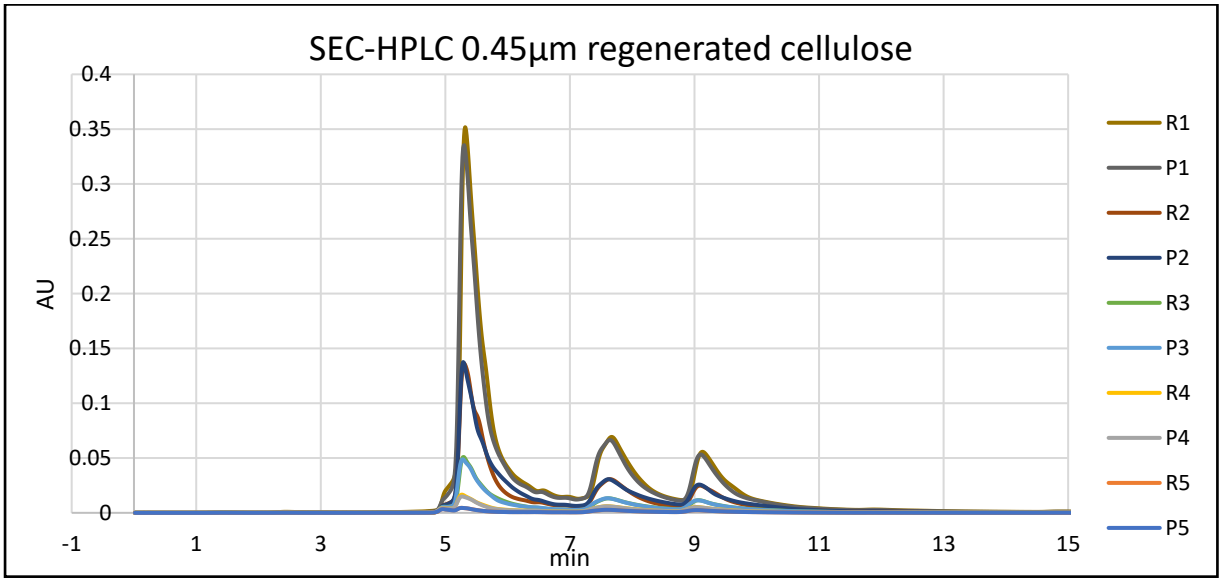

Figure 51: HPLC chromatograms of 0.45µm RC stage filtration

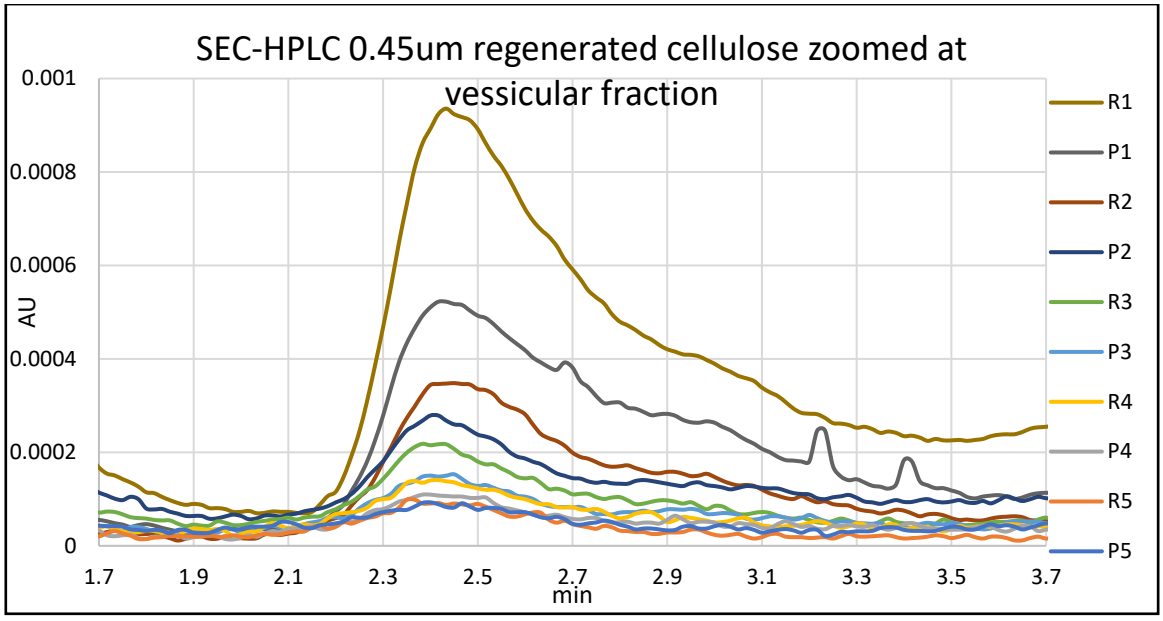

Figure 52: Zoomed HPLC chromatograms of 0.45µm RC stage filtration

The 5 stage chromatograms of the other membranes are reported in Appendix II.

4.3. MEMBRANE GEL LAYER

Across all membranes, impurities are removed with each stage which ensures the proper functioning of the diafiltration step. However, the peak related to vesicles is also decreasing. In the smaller membranes, some vesicles are passing through the membrane to be detected in the permeate sample. However, it was evident from examining the membrane that the loss of vesicles is attributed to the formation of a gel layer on each of the membranes used. To confirm this, the gel was carefully scraped off the membrane and diluted in PBS. To resuspend the cake, a micropipette with PBS was used and it is sent to a horizontal shaker for 30 minutes to enable proper mixing. The resuspended cake is sent to SEC-HPLC and the chromatogram obtained is reported in figures 53 and 54.

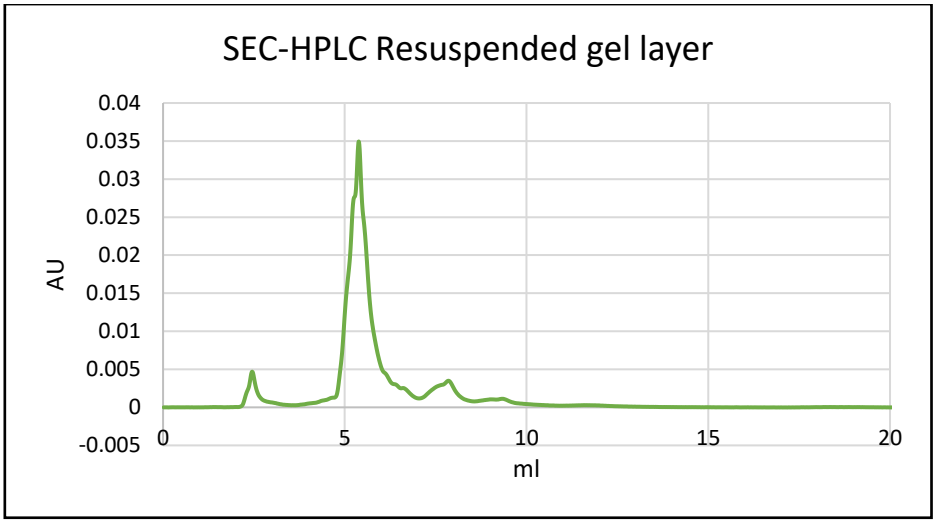

Figure 53: HPLC chromatogram of resuspended cake

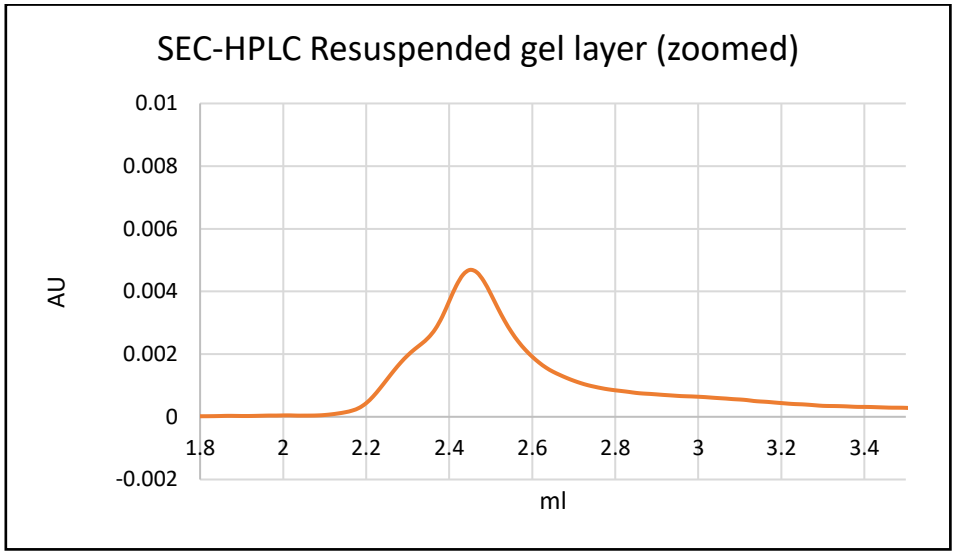

Figure 54: Zoomed HPLC chromatogram of resuspended cake

A large amount of vesicular fraction is seen to be lost on the membrane gel layer. Hence, a way to resuspend the cake and reintroduce this to the diafiltration should be considered.

4.4. MEMBRANE SELECTION

To carry out a comparison among the membranes, every membrane was tested with the same juice with a single stage to determine the comparative data between the retentate and permeate of the first stage. The areas of the peaks are integrated to quantify the EVs and impurities fractions in the retentate and permeate of each membrane. A comparison of the different membranes is shown in in figure 55.

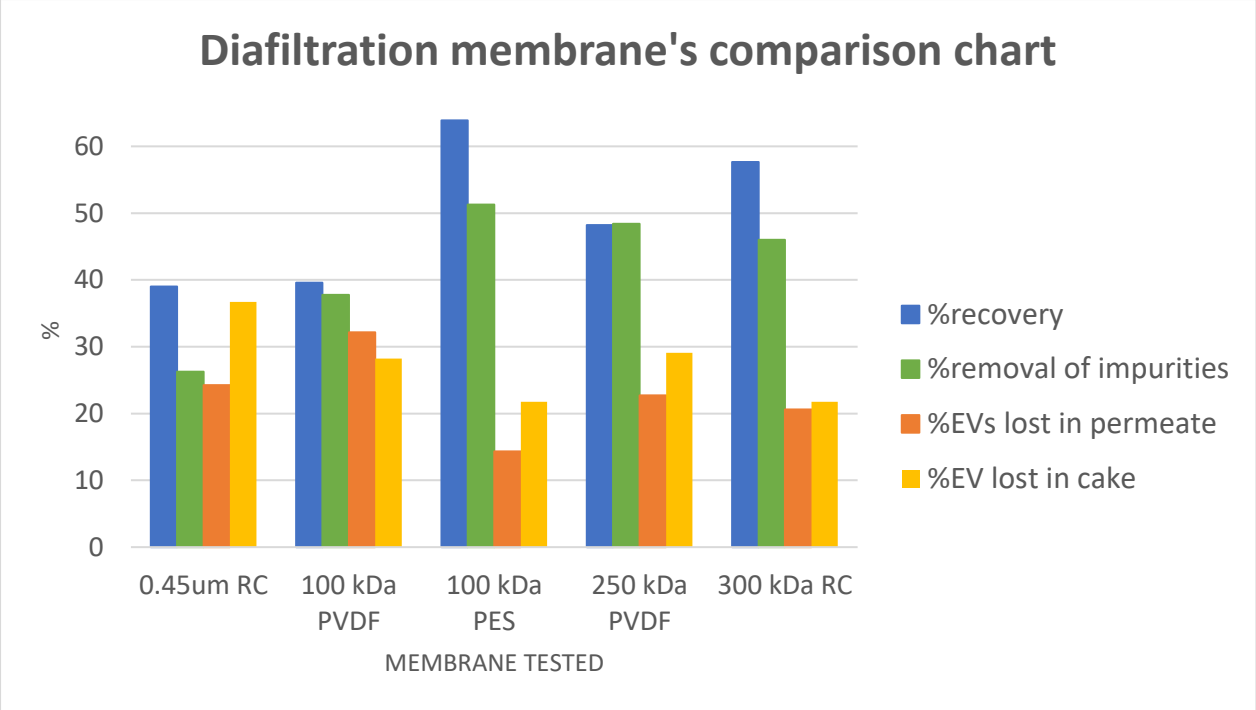

Figure 55: % recovery, removal of impurities, and EV losses of tested membranes

From the HPLC chromatograms of the 0.45 µm it is seen that the membrane is efficiently removing impurities. However, in comparison to the other membranes, the quantity of impurities removed with each stage is regarded as insufficient. More importantly, a large portion of vesicular fraction is lost in the permeate. Therefore, microfiltration should be neglected and the other membranes needs to be compared.

Both the PVDF membranes (100 kDa and 250 kDa) have the same issue of high vesicular fraction in the permeate as shown in the chromatogram in figure 56.

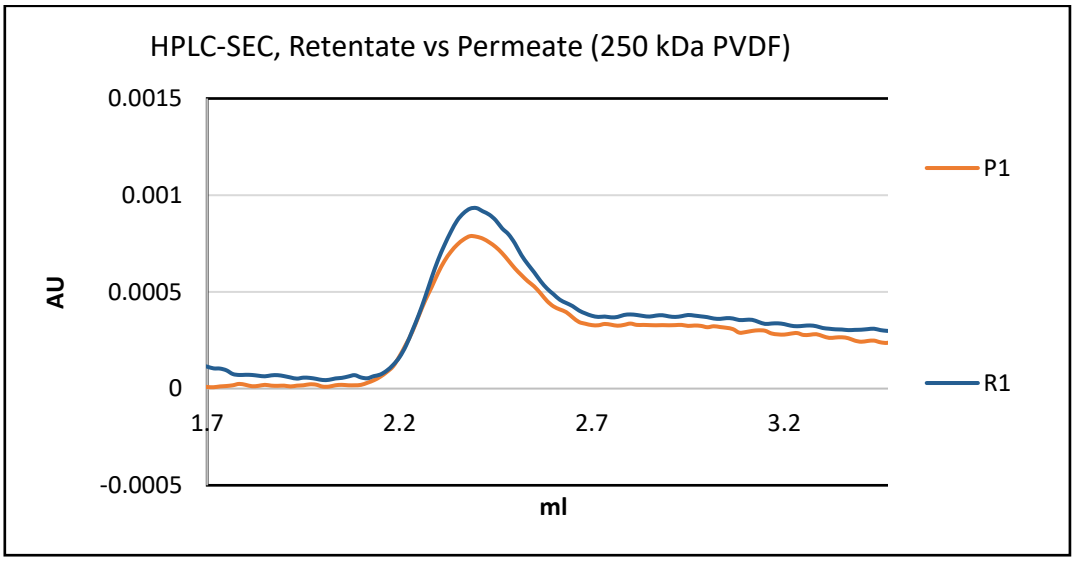

Figure 56: HPLC chromatogram of 250 kDa PVDF

To further understand the extent of vesicle loss in the permeate, a 5-stage filtration was carried out and the SEC-FPLC analysis is reported in fig 57. The blue line represents the feed to the stage diafiltration (permeate of 3 µm filtration) and this line is compared with the different stages. The integrated areas of the peaks are reported in table 7.

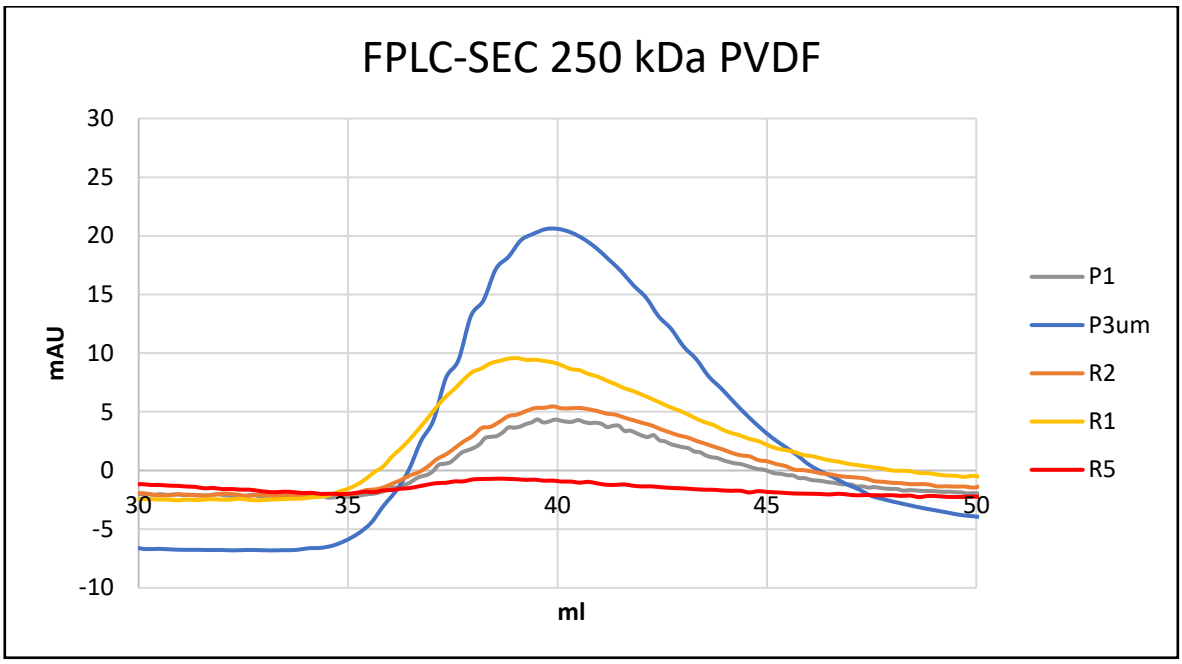

Figure 57: Zoomed FPLC chromatogram of 250 kDa PVDF

Table 7: Integrated peaks, 250 kDa PVDF

Analysis	EVs (mAU*ml)	Impurities (mAU*ml)
FEED	172.30	9007.54
R1	60.80	4561.92
R2	22.65	1893.19
R5	10.15	161.47

% Recovery of EVs = 5.8%

% Removal of impurities = 98.2%

The loss of vesicles in the cake and possibly the permeate is very significant and there is hardly any vesicle in the retentate of the fifth stage. Due to these reasons, PVDF membranes have not been considered for applying in tangential flow filtration.

Even though the 300 kDa regenerated cellulose membrane is efficient in purifying the feed while trapping only a small fraction of cake, 100 kDa PES offered higher recovery and the lowest percentage of EVs lost. Since PES offers significant improvement from PVDF membrane having the same cut off, PES 100 kDa membrane has been considered for applying in tangential flow filtration. The 5-stage chromatogram of the 100 kDa PES is shown in fig 58. As seen in the zoomed chromatogram in fig 59, permeate fractions contain very little quantities of vesicles.

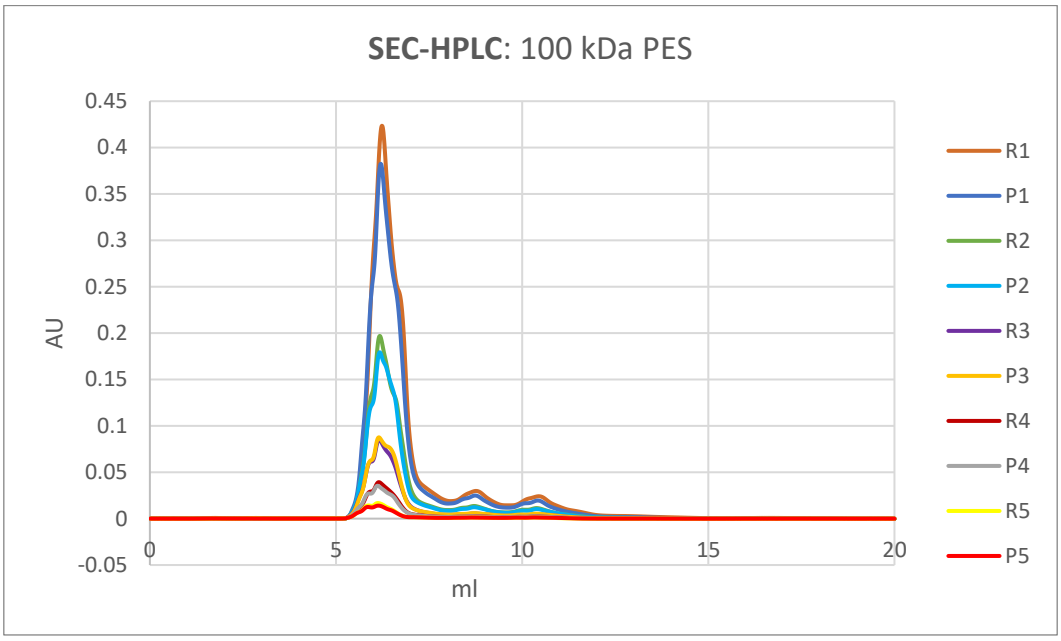

Figure 58: HPLC chromatogram of 100 kDa PES

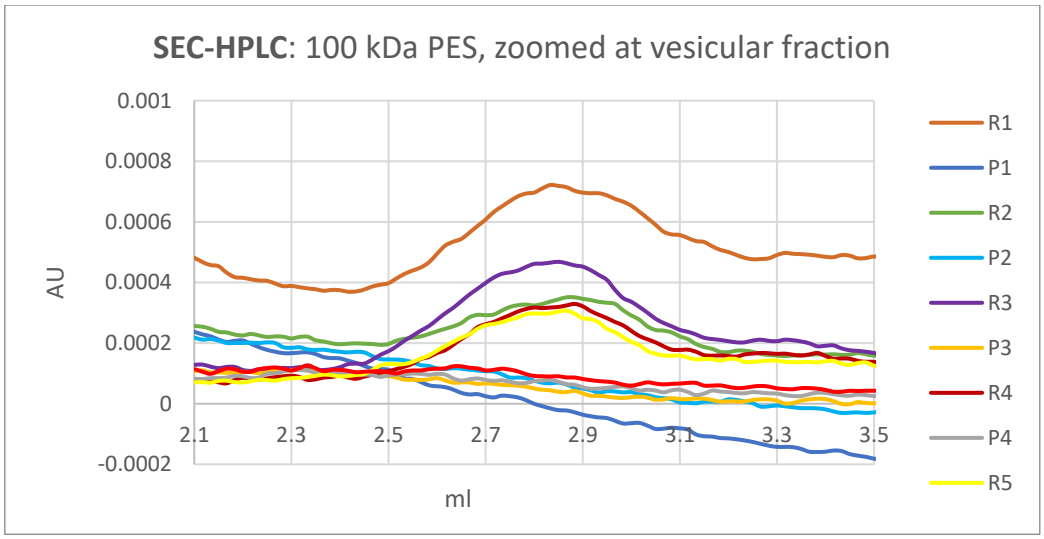

Figure 59: Zoomed HPLC chromatogram of 100 kDa PES

The feed and the retentates of first and final stages with this membrane was also analysed using SEC-FPLC and the chromatogram is reported in figure 60 and 61. Integrated peaks are reported in table 8.

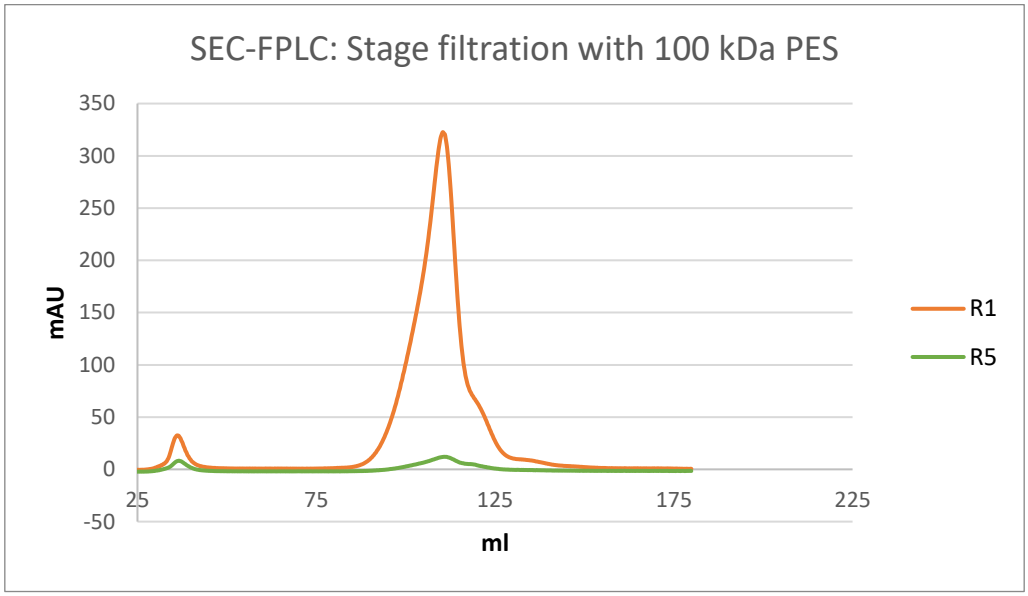

Figure 60: FPLC chromatogram of 100 kDa PES

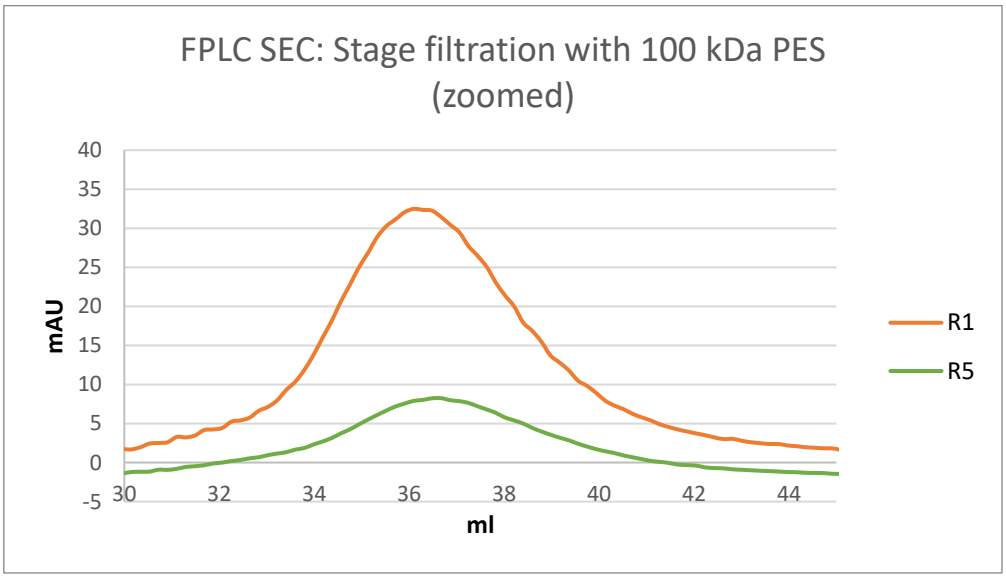

Figure 61: Zoomed FPLC chromatogram of 100 kDa PES

Table 8: Integrated peaks of stage filtration with 100 kDa PES

Analysis	EVs (mAU*ml)	Impurities (mAU*ml)
R1	183.41	4629.92
R5	55.71	194.41

4.5. MODEL FOR STAGE DIAFILTRATION

A mathematical model for diafiltration is considered to evaluate the distinction between theoretical and experimental values. The model for stage diafiltration is described below,

$$D^{-n} = \frac{C_{P_imp}}{C_{0_imp}} = \frac{C_{R_imp}}{C_{0_imp}} \qquad (1)$$

Where D = Dilution factor

n = Number of stages

C_0 = Concentration of impurities in the feed (EV peak in the permeate of 3µm)

C_R = Concentration of impurities in the retentate

C_P = Concentration of impurities in the permeate

The model assumes that no impurities are deposited on the membrane which is not the case in the present scenario. Therefore, variations can be expected. To develop the theoretical data, the dilution factor is 2 (1:1 dilution with PBS) and the number of stages is 5.

The experimental data for concentration of impurities in the feed and the retentate and permeate of each stage can be obtained by integrating the curves of the HPLC chromatograms corresponding to impurities. The comparison between experimental and theoretical data is plotted in figure 62.

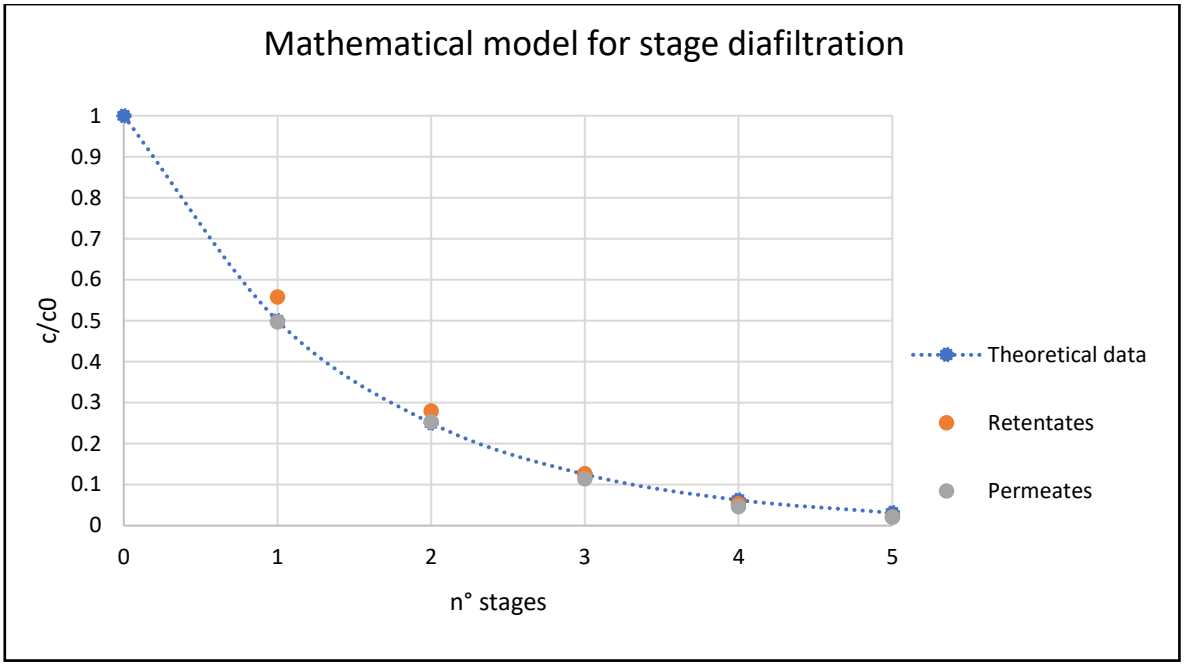

Figure 62: Stage diafiltration model

Initially, the experimental data somewhat follows the theoretical ones since the permeate lines are directly coinciding with the theoretical one. However, after the fourth stage, the concentration of contaminant is slightly lower than what should be expected which indicates that the membrane is performing better than theoretically predicted. Regarding the retentates, the data is deviated highly in the first 2 stages since the points are well above the trend. As mentioned before, the assumptions for this model could be too crude to represent the data. The membrane clearly rejects impurities since they are present in both samples. Also, there is deposition on the membrane surface. Hence the deviation could be caused by that.

4.6. THE EFFECT OF BUFFER USED

In a previous study on isolating mammalian exosomes through diafiltration, the buffer employed was Trizma buffer and it was shown to aid the filtration process and reduce aggregation and deposition on membrane surface over time [31]. To evaluate the effect of buffer, the results of diafiltration using tris buffer and PBS are compared through SEC-HPLC analysis. The results are shown in figures 63 and 64 and the data for areas and their % differences are reported in table 9.

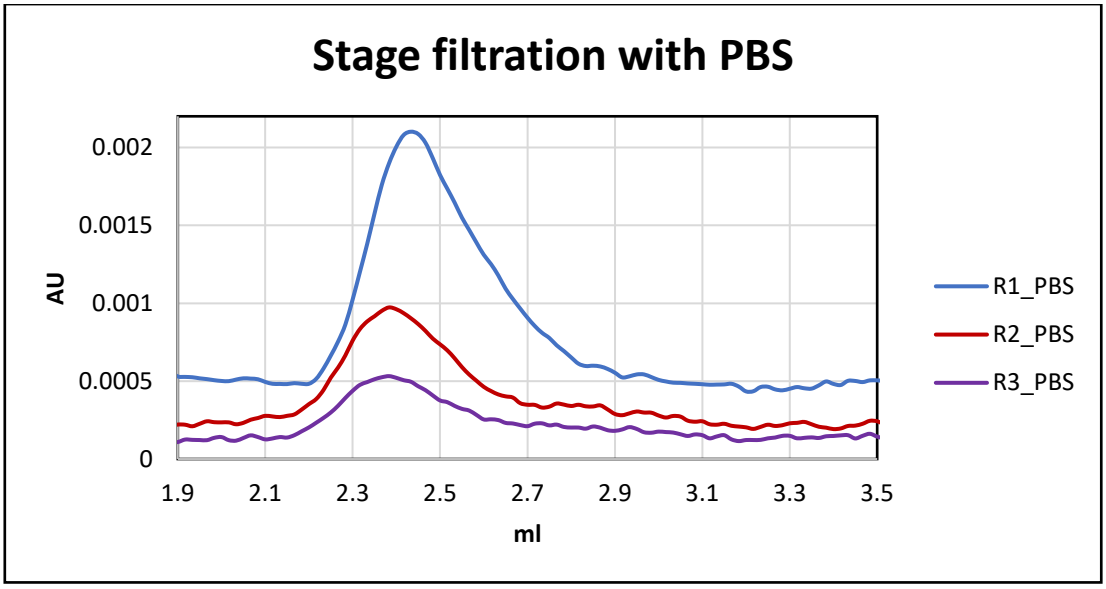

Figure 63: HPLC chromatogram with PBS

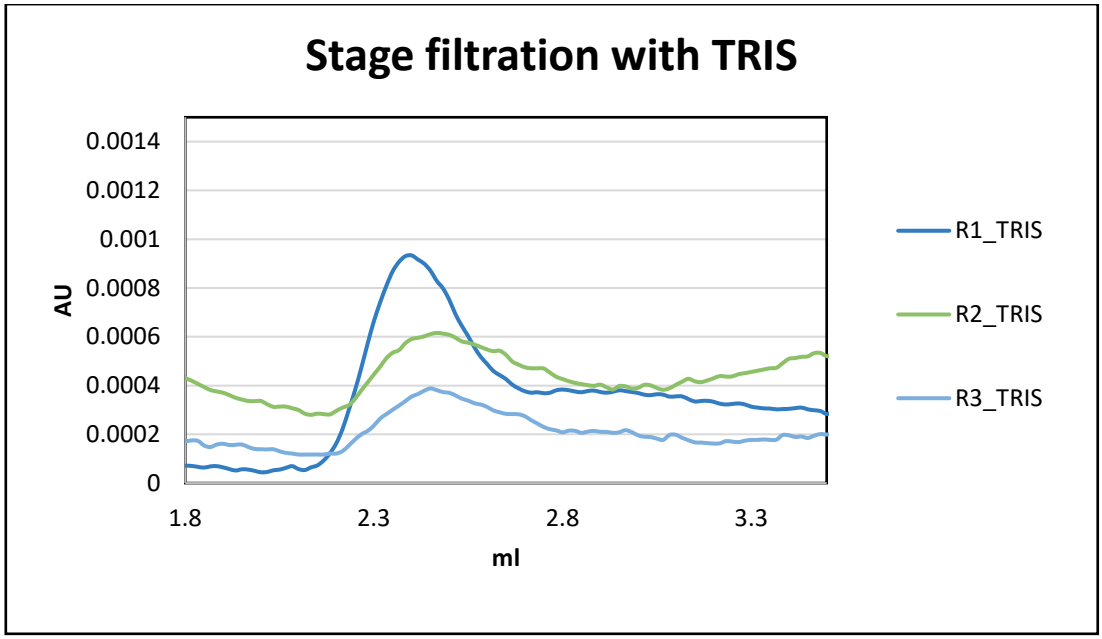

Figure 64: HPLC chromatogram with TRIS buffer

Table 9: Integrated peaks of 2 different buffers on same juice

BUFFER USED	Chromatogram area EV fraction (mVsec)		
	Stage 1	Stage 2	Stage 3
PBS	21352	9072	5476
TRIS	20429	8078	5626
% difference	0.04	0.1	0.02

The same test repeated on FPLC resulted in chromatograms that are basically indistinguishable. Since the two different buffers lead to similar recovery of vesicular fraction. The areas are very similar as well. Hence, it is concluded that changing the buffer has not led to the same effects seen in mammalian vesicles. The chromatogram is shown in figure 65.

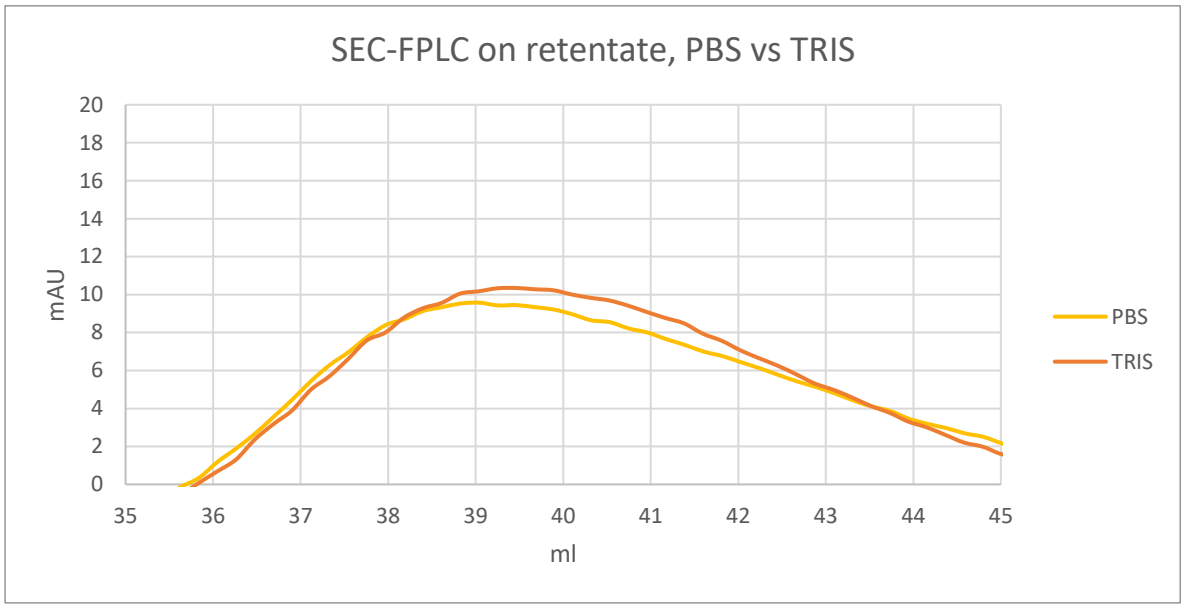

Figure 65: FPLC chromatograms with different buffers

4.7. TANGENTIAL FLOW FILTRATION

It was clear that even though stage diafiltration works to remove impurities, large amount of vesicular fraction is lost in the membrane cake. With tangential flow filtration, it was hypothesized that the fouling can be reduced to some extent. Moreover, a continuous protocol can be developed in this way.

The membrane is first cleaned with water and the permeate volume vs time is plotted in figure 66. The experiment is performed at 1.5 bars.

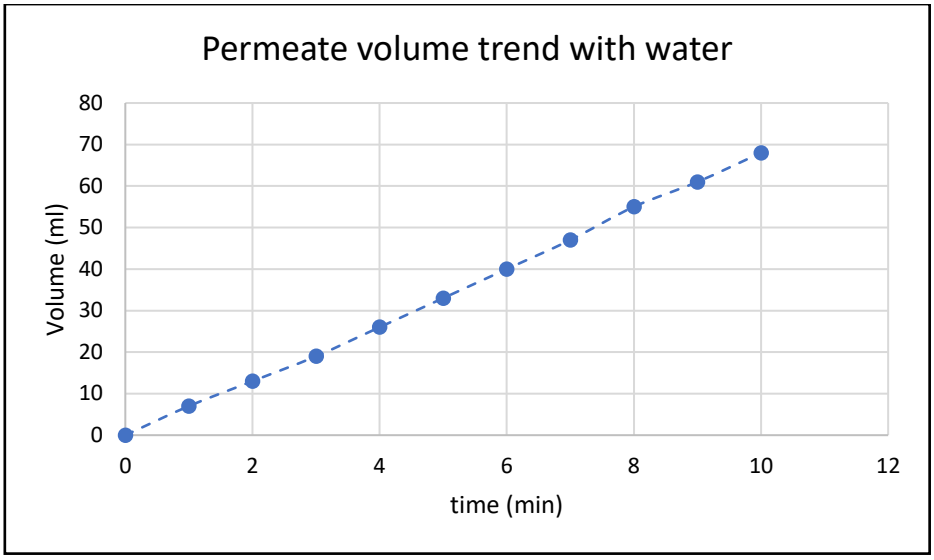

Figure 66: Water permeability with time

The hydraulic permeability of the membrane can be determined by plotting Flux vs TMP and evaluating the slope. For this, water is sent to the system at different pressures and they are plotted in figure 67.

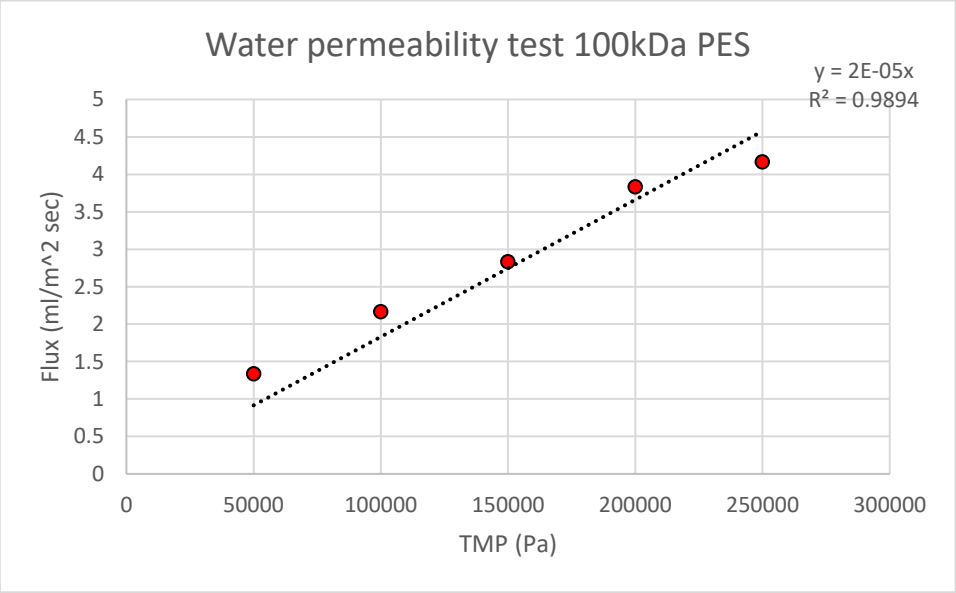

Figure 67: Flux vs TMP of 100 kDa PES

Hydraulic permeability = slope = 2×10^{-5} L m^{-2} sec^{-1} Pa^{-1}

4.7.1. TFF WITH 0.5 DIAVOLUMES

First, tangential flow filtration was tried with half of a diavolumes to analyse the process and the retentate and permeate obtained in the end. First, the feed, permeate of 3µm filtration is analysed for carrying out the level of purification and recovery. The starting volume is 200 ml of pre-treated lemon juice and the TMP is 1.5 bars. The constant volume diafiltration lasted for 515 minutes and the permeate flow and flux of the membrane is plotted in fig 68. The area of the membrane is 30 cm^2

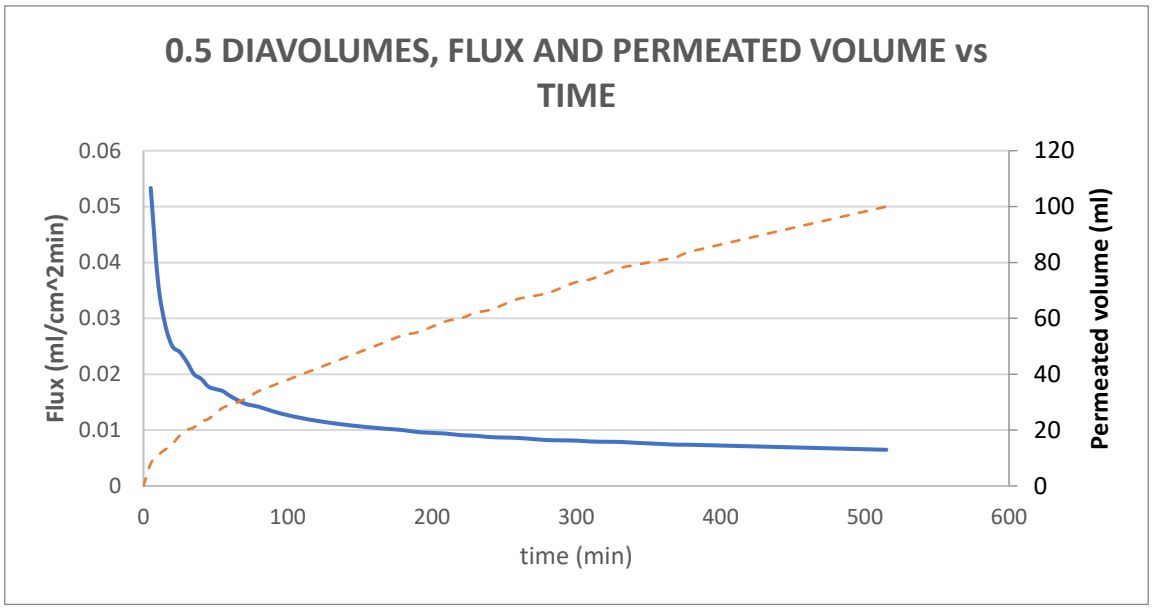

Figure 68: Flux at 0.5 diavolumes

The chromatograms of the feed, permeate, and retentate are given in figure 69 and 70 whilst the results of peak integration in table 10.

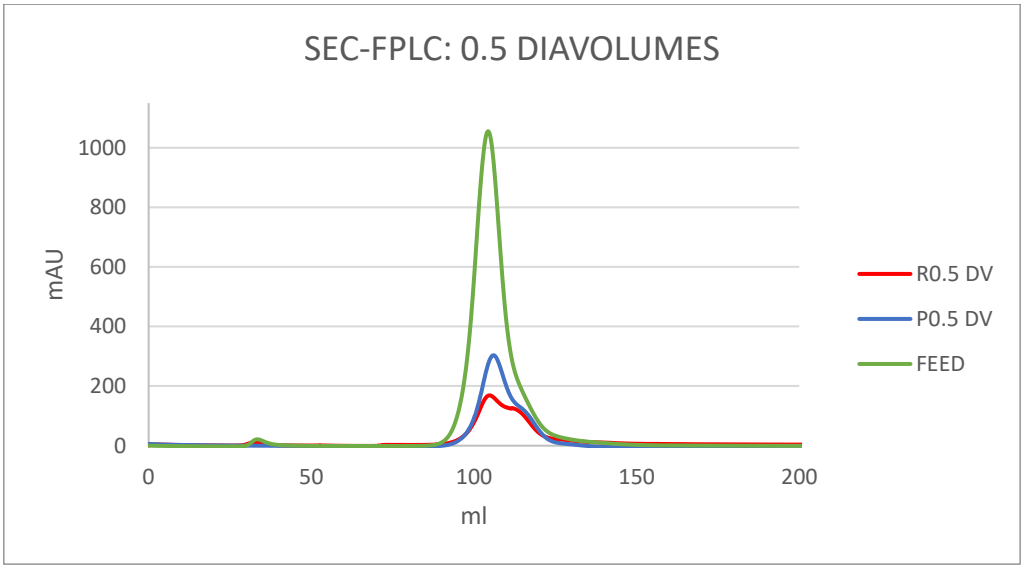

Figure 69: FPLC chromatograms at 0.5 diavolumes

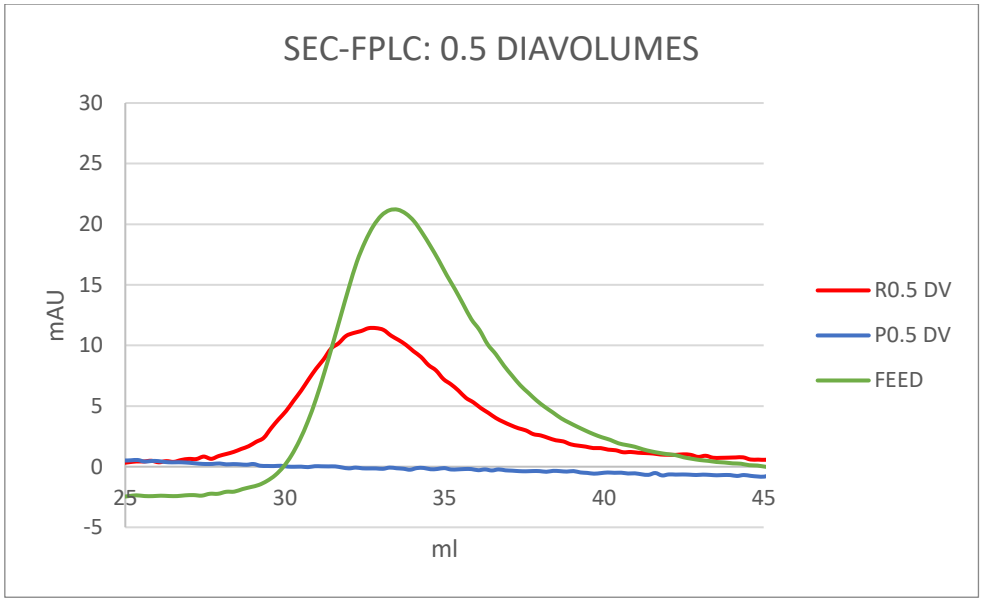

Figure 70: Zoomed FPLC chromatograms at 0.5 diavolumes

Upon integrating the areas of the chromatograms, the following are quantified.

Table 10: Integrated peaks of 0.5 diavolumes

ANALYSIS	EV (mAU*ml)	IMPURITIES (mAU*ml)
FEED	118.15	12390.16
R0.5	22.54	2279.93
P0.5	0	4220.35

% Recovery of EVs = 19.07%

% Removal of impurities = 65.93%

Even though an impurity removal of 66% is achieved with a short process time, a large portion (about 80%) of the EVs are lost during this time interval as well. The material balance does not account for this loss in permeate as there is no detected peak in the permeate. Even though this permeate value is not instantaneous, but at the end of the process, such large loss could be described due to the gel layer formation on the surface of the membrane. The lost EVs must be recovered and to do this, a modified protocol is tried.

4.7.2. TFF WITH 1.5 DIAVOLUMES

To investigate if the loss of vesicles can be attributed to the cake formation, a tangential flow filtration was carried out with the same feed as before, but for a longer duration. A starting volume of 75 ml juice and 75 ml PBS is taken since undiluted juice seems to rapidly foul the

membrane. Once the process reached one diavolumes, the process is stopped, the membrane is removed and the gel layer is scraped off. This layer is resuspended in 4-6 ml PBS and the resuspended cake is extracted in a falcon tube. The falcon tube is subjected to mixing by using a horizontal shaker for 30 minutes. After this, the cake is added to the feed tank and the diafiltration is continued for another 0.5 diavolumes. The membrane is washed with PBS and connected back to the Millipore cell. The flux and permeate volume are plotted in figure 71.

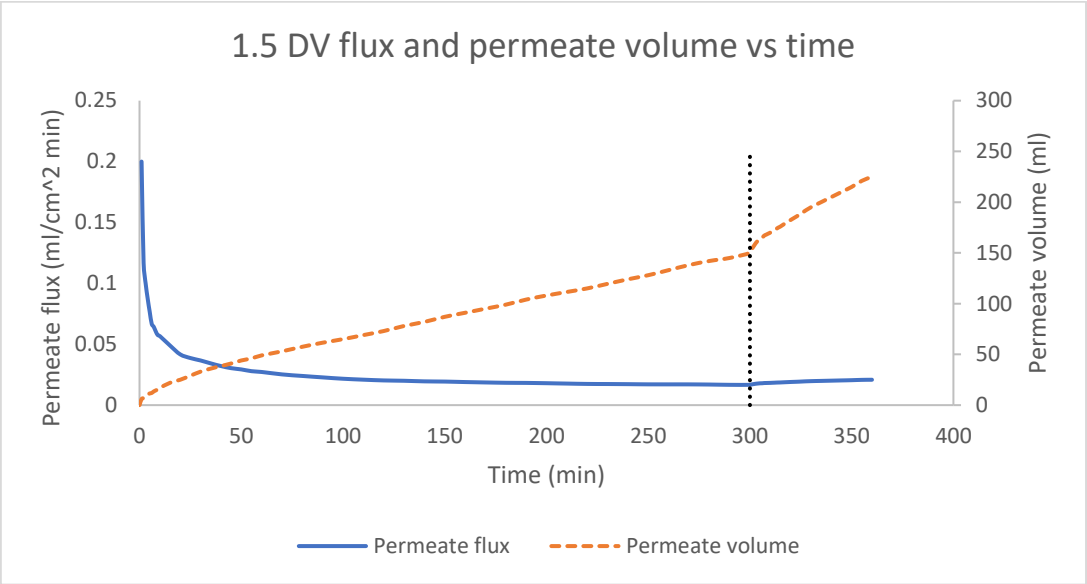

Figure 71: Flux at 1.5 diavolumes

A slight improvement in the flux is seen after the membrane cleaning. The chromatograms of this run are reported in figures 72 and 73 along with the integrated areas in table 11.

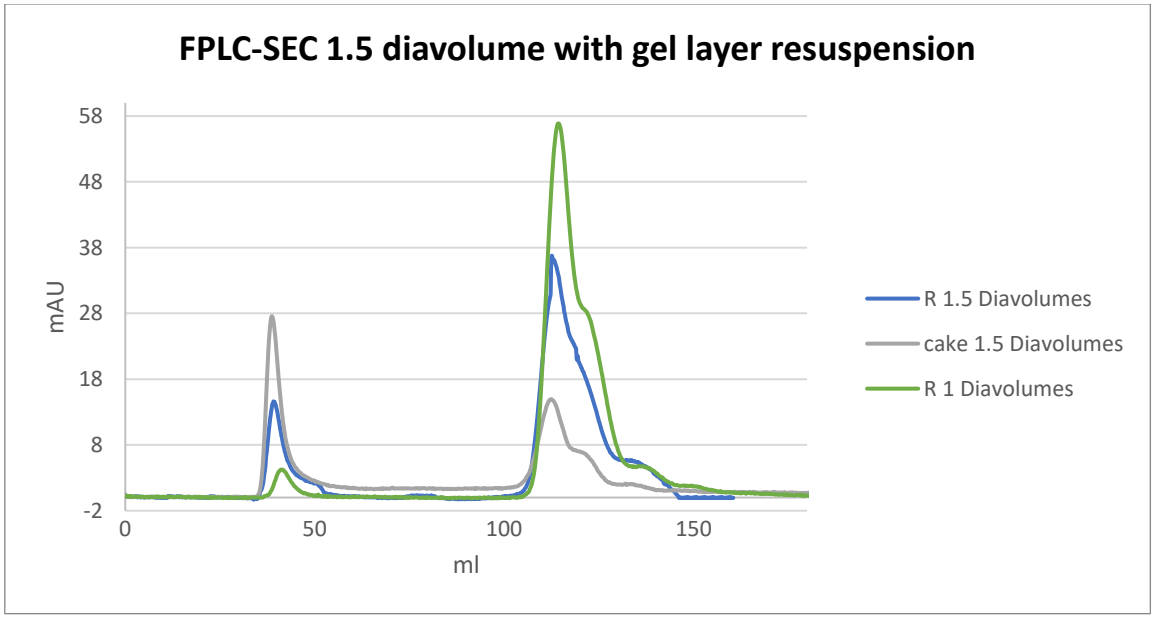

Figure 72: FPLC chromatograms at 1.5 diavolumes

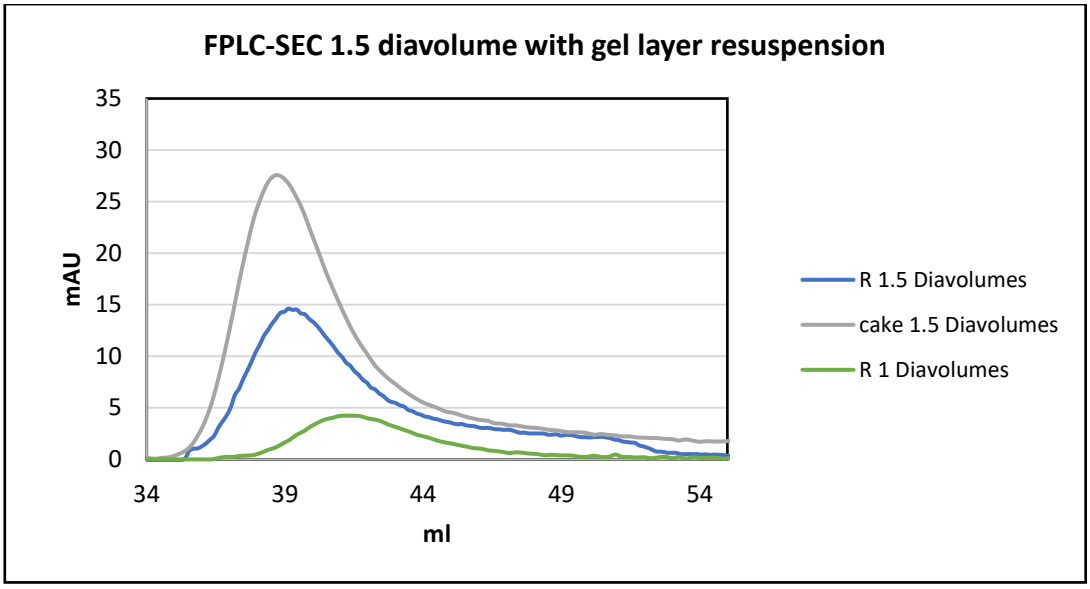

Figure 73: Zoomed FPLC chromatograms at 1.5 diavolumes

Table 11: Integrated peaks of 1.5 diavolume

Analysis	EVs (mAU*ml)	Impurities (mAU*ml)
Feed	223.88	4079.50
R1	17.84	690.69
R1.5	92.85	489.01
CAKE1.5	154.33	193.49

% Recovery of EVs after 1 diavolume = 5.8%

% Recovery of EVs after 1.5 diavolumes = 41.47%

% Increase due to resuspension of gel layer = 80.78%

% Removal of impurities = 88.01

By carrying out a 1.5 diavolume of TFF, 96% of the impurities were removed, a value that increased from the 94% obtained with 1 diavolume. To understand the extent of EVs that could be recovered by resuspending the cake back into the feed tank, the percentage increase from the retentate of 1 diavolume to 1.5 is calculated. A substantial percentage increase of 80% was obtained suggesting that this protocol can be acceptable in terms of yield.

4.7.3. FINAL PROTOCOL WITH RESUSPENSION OF CAKE WITH EVERY DIA VOLUME

To effectively introduce the resuspended cake back to the final product a protocol was developed with a smaller starting volume of 100 ml. 50 ml juice and 50 ml PBS is sent to the

TFF system in the same protocol as before. When the process approaches each diavolume, the process is paused. The membrane is removed from the cell and the gel layer is scraped off, resuspended in PBS, subjected to horizontal shaking for 30 minutes and introduced back to the feed or retentate tank. This is repeated for a total of 3 diavolumes and the resulting flux data and the chromatograms are presented in figures 74-76 and the integrated areas are given in table 12.

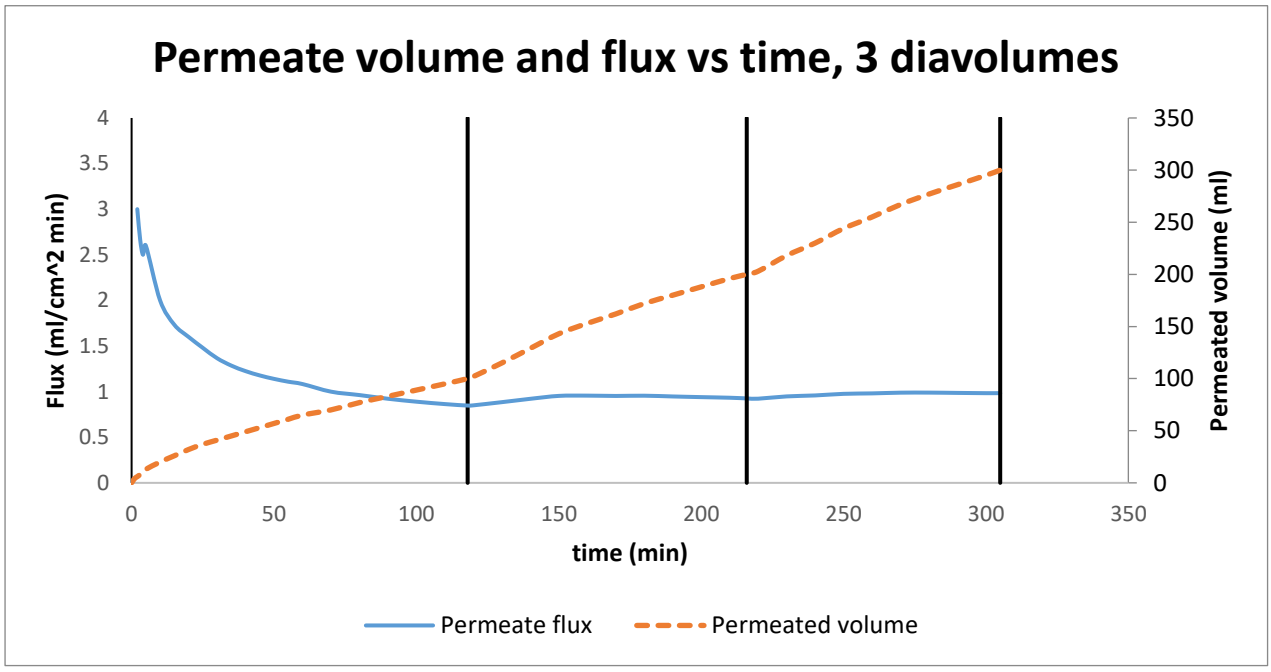

Figure 74: Flux at 3 diavolumes

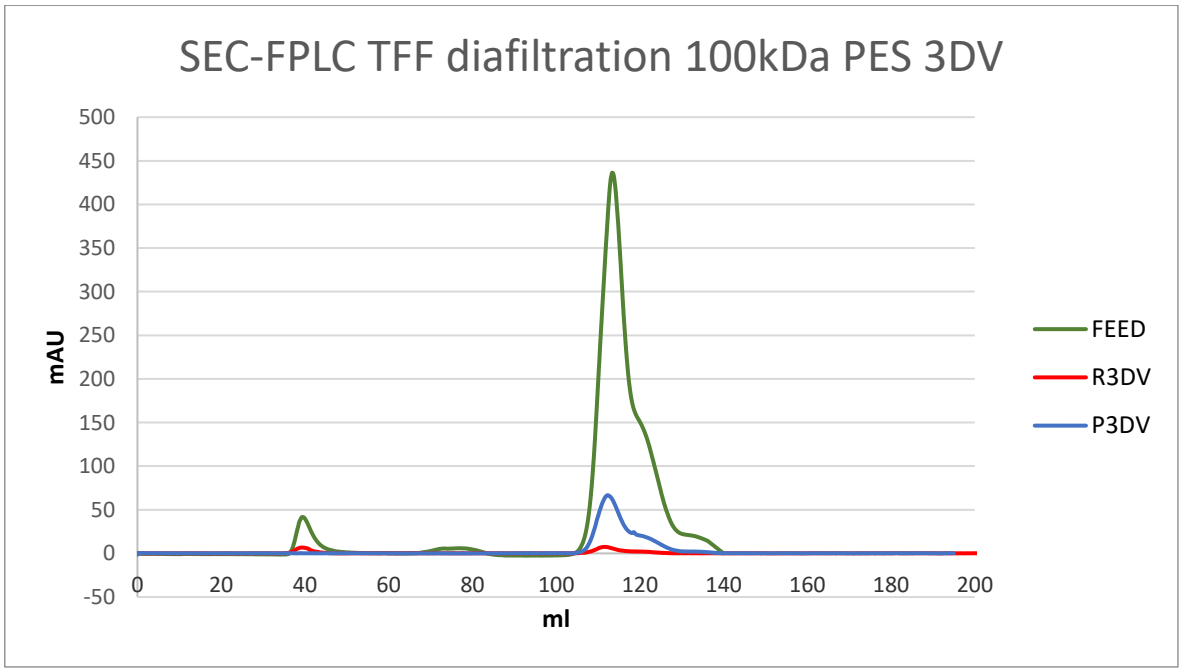

Figure 75: FPLC chromatograms at 3 diavolumes

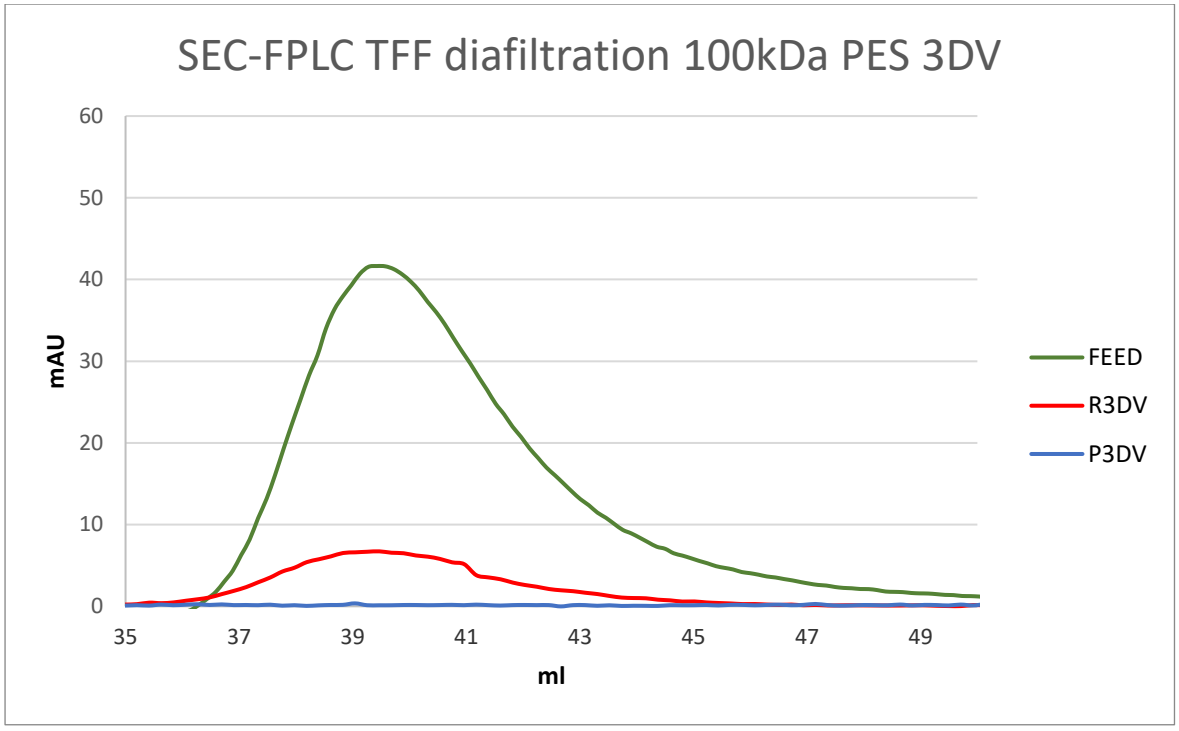

Figure 76: Zoomed FPLC chromatograms at 3 diavolumes

The areas of the chromatograms for the fractions are reported below.

Table 12: Integrated peaks of 3 diavolume

Analysis	**EVs (mAU*ml)**	**Impurities (mAU*ml)**
Feed	223.88	4079.50
R 3DV	34.66	62.8
P 3DV	0	615.45

% Recovery of EVs = 15.48%

% Removal of impurities = 98.46%

Although it is recommended to do up to 2 or 3 diavolumes to attain an appreciable extent of purification, the deposition of the gel layer on the membrane is the primary issue with the protocol. The recovery rate after 3 diavolumes of filtration is merely 15.5% even after the introduction of 2 resuspended cakes back into the feed tank.

4.8. MICROSCOPIC ANALYSIS OF MEMBRANE GEL LAYER.

The membrane gel layer is very visible even after running the system for processing a short period of time. A picture of gel layer after 1.5 diavolumes of TFF is given in fig 77.

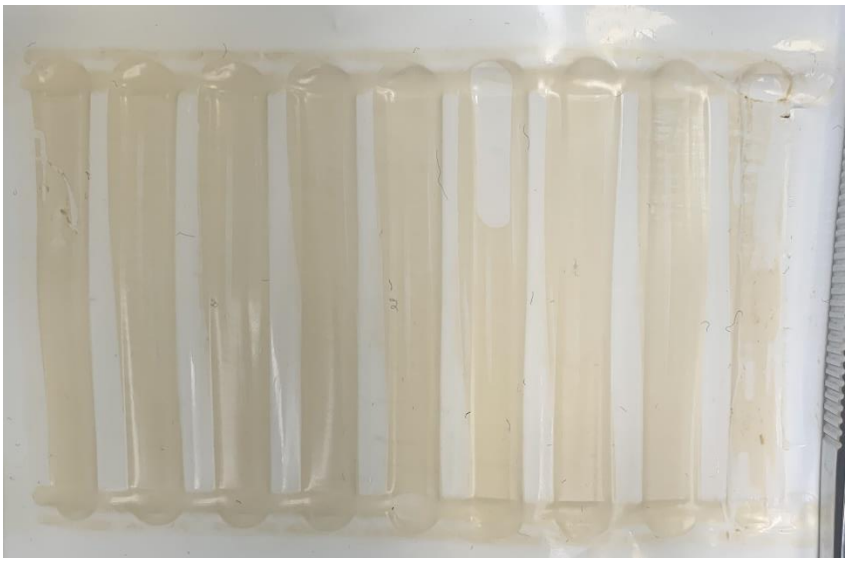

Figure 77: Membrane gel layer

This membrane is viewed under a Zeiss Axiolab 5 microscope to obtain the following snapshots in fig 78.

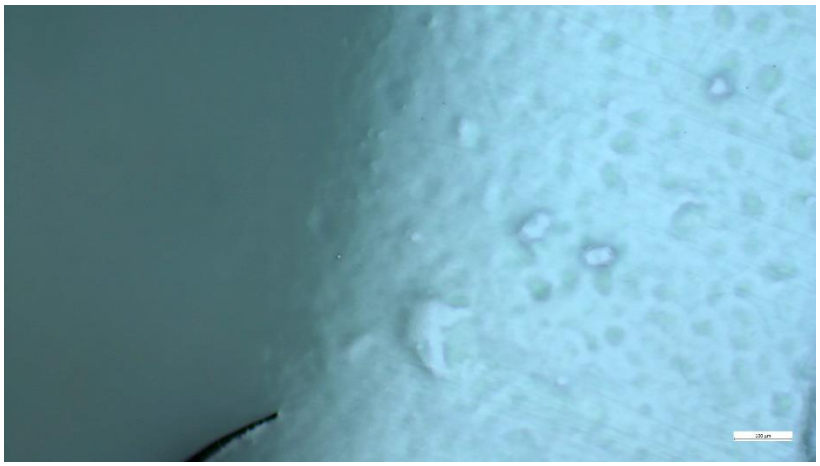

Figure 78: Membrane gel layer: 100µm scale

Even though a remarkable quantity of vesicles were detected in the membrane gel layer through chromatography, it seems that the gel layer contains large aggregates of diameters ranging from a few micrometres to a few hundred micrometres. More microscopic analyses can determine whether there are vesicles free of aggregation in the gel layer. However, the aggregation in this

layer will be a problem to tackle if this layer is to be reintroduced back into the filtration system. The presence of large aggregates could also cause concentration polarisation and will lead to fouling of the membrane.

4.9. MODEL OF TANGENTIAL FLOW FILTRATION

Mathematical modelling of tangential flow filtration was considered analogous to the stage diafiltration where concentrations of contaminants are plotted against time.

A material balance on the concentration of impurities can be written as

$$V\frac{C_{imp}}{dt} = -Q\ C_0\ (1 - R) \qquad (2)$$

Where, R = rejection of impurities by the membrane

Q = Permeate flowrate

C_{IMP} = Instantaneous concentration of impurities

C_0 = Impurity concentration in feed

V = Volume of feed

Assuming rejection is 0 and rearranging,

$$\frac{d\ C_{imp}}{C_0} = -\frac{Q * t}{V} \rightarrow \ln\left(\frac{C_{imp}}{C_0}\right) = -\frac{V_P}{V} \qquad (3)$$

The permeate volumes are noted down with time during filtration and the curve corresponding to the theoretical model can be plotted. Samples of retentates and permeates were collected at intervals of 0.5 diavolumes. From the chromatograms of these samples, the integrated area of impurity fraction can be used as a representation of impurity concentration. This can be divided with the integrated area of impurities of the feed to get the left-hand side of equation (3). The volume of feed is kept constant at 100 ml.

The comparison of experimental and the theoretical data is shown in fig 79.

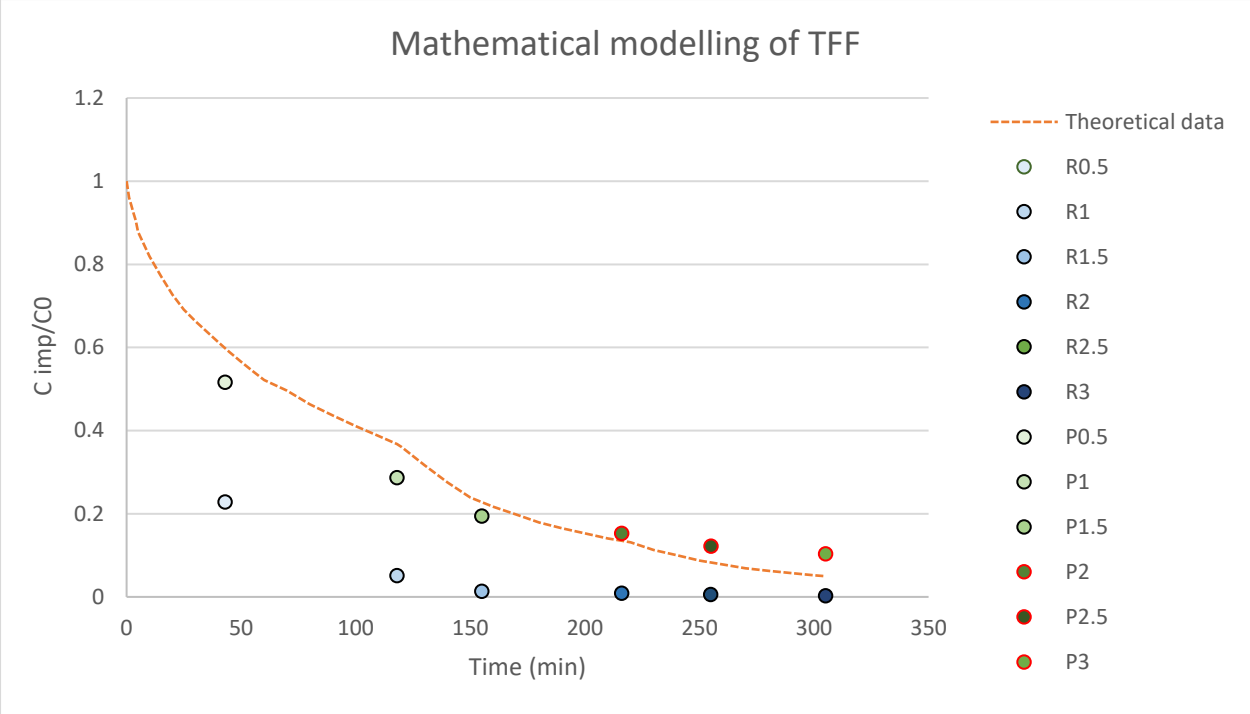

Figure 79: Constant volume TFF model

Parallel to the model of stage diafiltration, all the experimental points are below the theoretical line. This means that the removal of impurities is higher than expected. Only the points of permeates with red border (P2, P2.5, P3) shows appreciably similar behaviour as that of theoretical plot. There can be two reasons attributed to this. First, analogous to the stage diafiltration model, the assumption of no rejection and no deposition on the membrane could be considered as crude. Moreover, the fact that the membrane cake layer is continuously scraped off and resuspended and reintroduced back into the feed tank will influence the material balance and can give such erratic values. Exactly like stage diafiltration, the model does not completely fit experimental and theoretical data although it gives a good indication.

4.10. ULTRACENTRIFUGATION

Two protocols have been considered for ultracentrifugation, starting from 80 ml of the same feed. Preliminary slow centrifugation sequence of 400 x g, 1000 x g and 25700 x g have been carried out to remove cell debris and fibrous materials.

Protocol 1:

- UC at 150000 x g for 1 hour, supernatant is discarded, pellet is resuspended in PBS
- Resuspended pellet subjected to UC at 150000 x g for 1 hr. Final pellet resuspended in PBS

Protocol 2:

- Centrifugation at 30000 x g for 30 minutes, pellet discarded
- Supernatant centrifuged at 200000 x g for 90 minutes. Final pellet resuspended in PBS

The SEC-FPLC chromatograms of both samples are reported in figure 80.

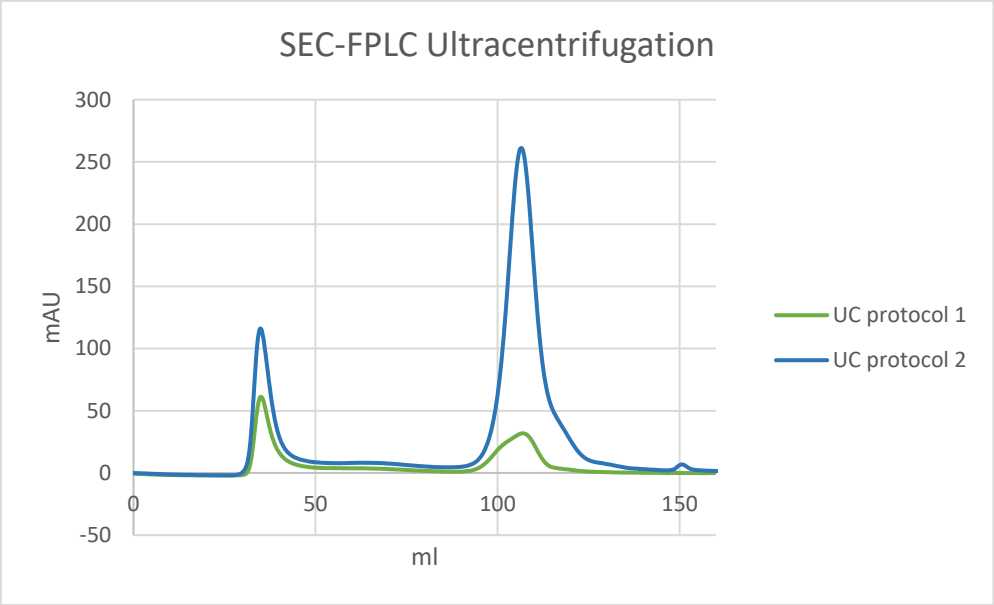

Figure 80: FPLC chromatogram for comparison of UC protocols

The chromatogram is a further proof of why UC is considered as the gold standard for EV isolation. The concentration of EV fraction is higher than that is usually obtained through diafiltration. However, it is important to note that from 80 ml of starting sample, 2-4 ml of final product could be recovered. Additionally, the total process time was close to 4 hours and through protocol 1, a large percentage of the impurities were removed and co-contamination is low.

Protocol 2 has higher EV content than protocol 1, but the impurity content is much higher as well. This could be further removed with an additional resuspension and carrying out an extra ultracentrifugation step with the final pellet.

Due to the shear forces present in high-speed centrifugation, the EVs are expected to be highly aggregated and fused together. For clinical applications, these are unsatisfactory results.

The two methods are compared with diafiltration with 3 diavolumes in figure 81.

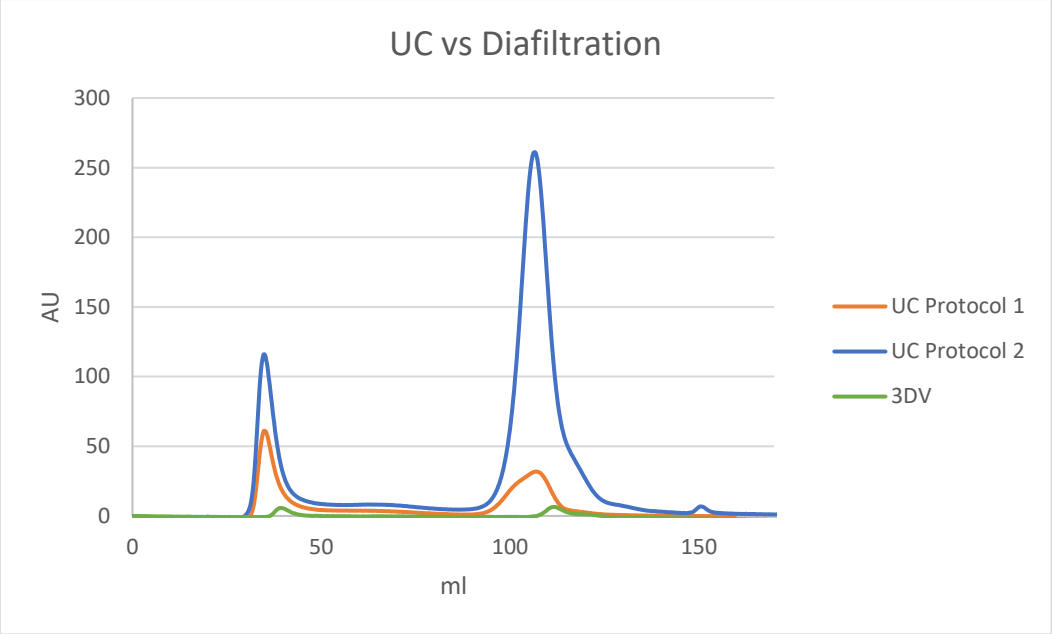

Figure 81: FPLC chromatograms of UC and diafiltration 3 DV

The peaks have been integrated and the data is given in table 13.

Table 13: Integrated peaks of 3 diavolumes and UC protocols

Method	**EV peak area (mAu*ml)**	**Impurity peak area (mAu*ml)**
UC protocol 1	395.33	469.73
UC protocol 2	1032.52	3002.66
TFF	34.66	62.8

Even though diafiltration purifies the EV fraction by removing a large amount of EVs, the final product contains less EVs. However, diafiltration has apparent advantages such as

- Ability to process large volumes
- Removal of impurities at much higher rates than UC
- Fast and simple procedure
- Continuous process
- Scalable

4.11. DYNAMIC LIGHT SCATTERING

Using a Zetasizer Nano ZS, the size characterisation was carried out on the permeate of 3 µm and the purified retentates of diafiltrations at different diavolumes. 5 duplicate measurements

are carried out on each sample tested. The deviation in the duplicate can indicate several issues with the samples such as turbidity, high or low concentration or aggregation. Zetasizer software aids in correlating the laser scattered signals to the particle diameter using specific algorithms. The software also specifies the quality of the results based on certain criteria placed on the duplicate measurements. The software can display the size distribution with respect to intensity of signal detected, the volume as well as the number distribution. These distributions are displayed in the form of peaks each of which has a specific mean diameter. The values of these are averaged and displayed by the software.

The DLS results on p3µm is given in figure 82. The result quality was considered good by the software due to minimum deviation in measurements.

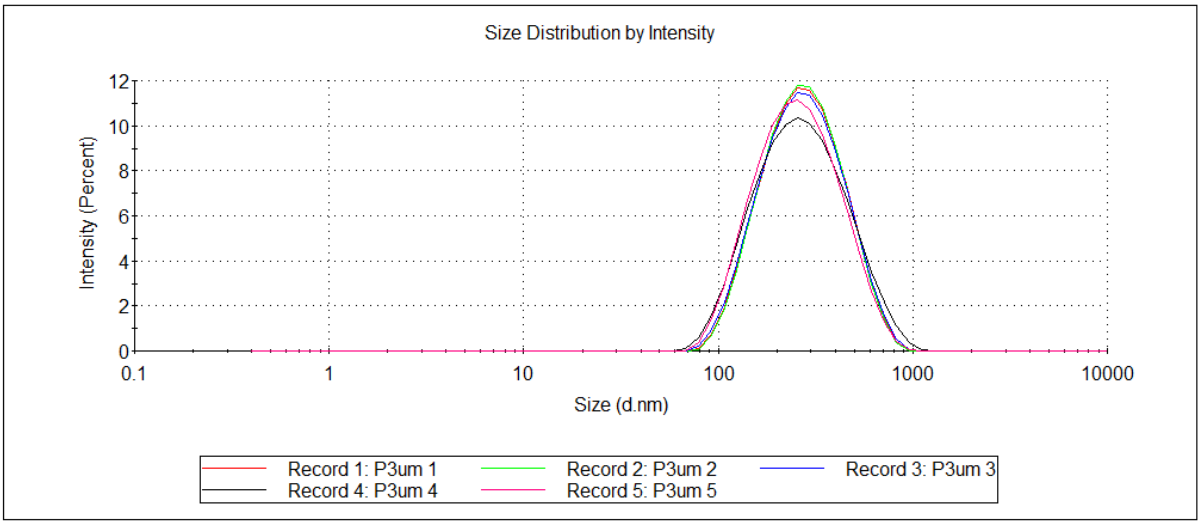

Figure 82: Size distribution by intensity, Permeate 3µm

As seen from the size distribution, particles are ranging from 70 nm to 1000 nm in the feed.

The wide size distribution suggests that the EV particles are largely aggregated in the sample. For example, in the results of retentate after 1.5 diavolumes in figure 83, there are particles as large as in the range of a few thousand nanometres which could suggest that the large cells or debris was not removed adequately. Similar characteristics were observed in the retentate after 0.8 diavolumes and as expected, in the membrane gel layer.

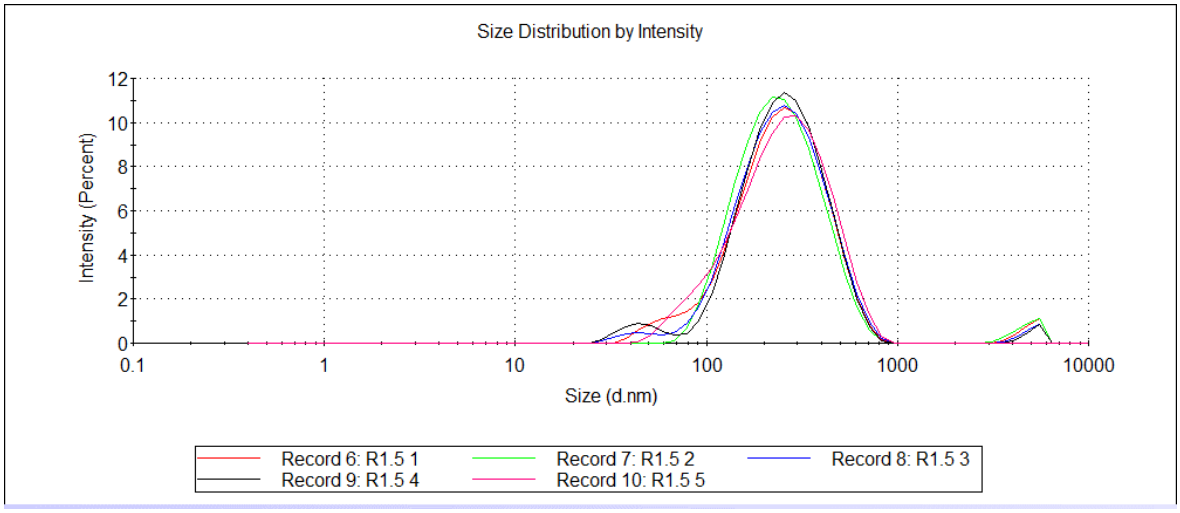

Figure 83:: Size distribution by intensity, Retentate 1.5

However, the % intensity which represents the quantity of the samples corresponding to these largely sized particles are low as reported in table 14.

Table 14: Detection of large size distributions

Sample Name	Size (nm)	%intensity
R_0.5DV	5036	1.7%
R_0.8DV	4367	2.1%
Gel layer_0.8DV	3673	7.3%

However, the results related to retentate after 3 diavolume diafiltration has few size distributions in the range of 70 to 100 nm suggesting that there could be vesicles or particularly exosomes free of aggregation present in the sample. This is also slightly seen in Retentate after 1.5 diavolumes shown in fig 84.

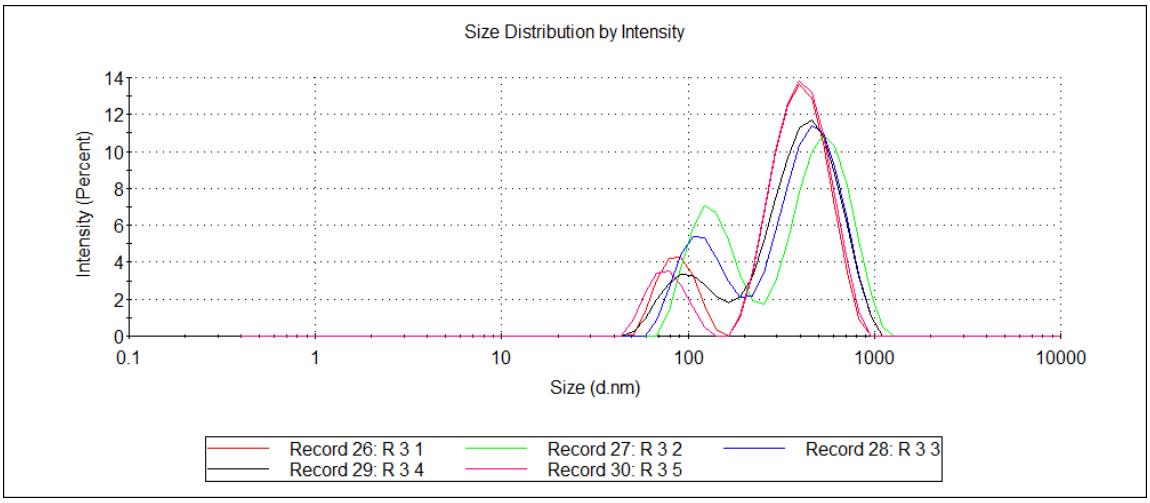

Figure 84: Size distribution by intensity, Retentate 3 DV

The percentage distribution of the sizes can also be obtained from the software. For 3 diavolumes, it is reported in table 15.

Table 15: Samples with exosomal size range

Sample name	Size (nm)	%intensity
R_1.5 DV	46.31	4
R_3 DV	78.95	15.1

In comparison to the feed, permeate 3µm where a single peak of 228.8 nm average diameter s obtained, here 15% of the total material detected is free of aggregation and is in the preferred size range.

The remaining size distribution charts are provided in Appendix III

The software averages the value of size obtained through 5 runs and they are reported in table 16.

Table 16: Average particle diameter from DLS

Sample Name	Average particle diameter (nm)
Permeate of 3µm filtration	228.8
R0.5 Diavolumes	253
R0.8 Diavolumes	218
Resuspended gel layer 0.8 Diavolumes	210.6
R1.5 Diavolumes	217.5
R3 1 Diavolumes	298

Zeta potential can be directly related to the stability of particles in the solution. Higher zeta potential, either negative or positive means that the particles are wide apart and repelled from each other. Hence, the tendency of aggregation is lower. The zeta potential of stable vesicles ranges from -10 to -50 mV. As expected, the feed had much lower negative value of -3.75 mV suggesting high instability. However, the zeta potential of retentates after 1.5 and 3 diavolumes

show promising results since the zeta potential is in the range for stable EVs. As obtained in the size distribution, small number of vesicles are free of aggregation in these samples. The zeta potential values of the samples are reported in table 17.

Table 17: Zeta potential through DLS

Sample Name	Zeta potential (mV)	Conductivity (ms/cm)
Permeate of 3µm filtration	-3.75	7.23
R0.5 Diavolumes	-3.83	7.9
R0.8 Diavolumes	-6.26	10.7
Gel layer 0.8 Diavolumes	-9.21	10.8
R1.5 Diavolumes	-10.3	11.1
R3 1 Diavolumes	-9.4	12.5

4.12. BCA ASSAY

The total protein content of the feed, retentate and permeate of the final tangential flow filtration has been evaluated using BCA. To develop the standard curve, 0.1 ml of the standards from A to I are added to 2 ml of the BCA working reagent and the absorbance is measured after incubating at 37°C for 30 minutes. The BSA standards analysis is given in table 18.

Table 18: BCA standard curve data

STANDARD	BSA concentration (ug/ml)	Absorbance	Absorbance – absorbance of blank
A	2000	2.46	2.16
B	1500	1.89	1.59
C	1000	1.39	1.09
D	750	1.22	0.92
E	500	0.87	0.57
F	250	0.61	0.31
G	125	0.53	0.23
H	25	0.38	0.08
I	0	0.29	0

The absorbances are subtracted to the absorbance of blank (I) and is plotted with concentration of BSA to develop the standard curve (green) shown in figure 85 along with the points of samples collected.

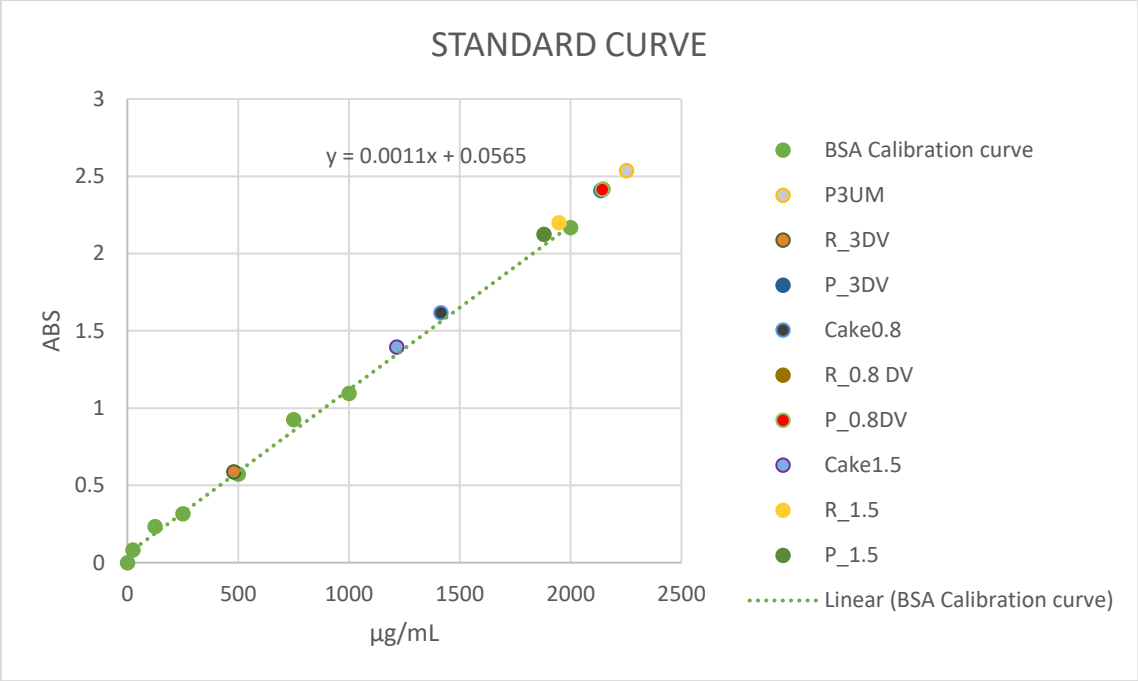

Figure 85: BCA standard curve

The values of the protein content are estimated from the standard curve and the equation of the curve, y = 0.0011x + 0.0565

The total protein contents of the samples are reported in table 19.

Table 19: Total protein concentrations using BCA

Sample	**Concentration (ug/ml)**
Feed to TFF (Permeate of 3µm)	2252.63
Retentate after 3 DV	480.63
Permeate after 3 DV	2136.18
Retentate after 0.8 DV	2144.72
Permeate after 0.8 DV	2142.31
Cake after 0.8 DV	1415.40
Retentate after 1.5 DV	1946.73
Permeate after 1.5 DV	1878.81
Cake after 1.5 DV	1214.68

4.13. STORAGE TEST

To evaluate the effect of storage on the vesicle and its degradation with time, the retentate of the tangential flow filtration was stored at different temperature conditions. The most common method of storing mammalian EVs for therapeutic application is freezing at -80°C. Despite being an economic disadvantage, even at this temperature, EVs can lose its structure and its biological activity. The protective phospho-lipid bilayer can be broken up during freeze thaw. Freezing also promotes aggregation of EVs which is a major disadvantage for therapeutical applications. It has been suggested that EVs degrade due to proteolytic activities in the biological fluids and protease inhibitor cocktails were previously used to prevent this. To reduce aggregation and decrease the effect of freeze-thaw, sugars such as trehalose are used as a cryo-protectant. The disaccharide trehalose acts as a protective cover outside the EV surface and reduce formation of ice crystals that can break the membranous bilayer.

To evaluate these effects, retentate of the tangential flow filtration is sampled in 2 ml Eppendorf tubes and diluted 1:1 with PBS and stored at 3 different temperatures.

- 4°C in the fridge
- -20°C freezer
- -80°C freezer

To understand the effects of sugar as a cryoprotectant and to understand its ability to prevent degradation of EVs, additional samples are taken and diluted 1:1 with a solution of 25 mM Trehalose in PBS.

Samples were taken out after 5 days of storage and sent to HPLC for analysis. The chromatogram thus obtained is compared with the chromatogram of the retentate and the peaks are integrated to compare the areas. The EV chromatogram area after 5 days of storage is reported in fig 86 and the data of the peak elaboration in table 20. The % degradation reported in table 21 was calculated as $\frac{Integrated\ area\ day\ 5 - Integrated\ area\ day\ 0}{Integrated\ area\ day\ 0}$

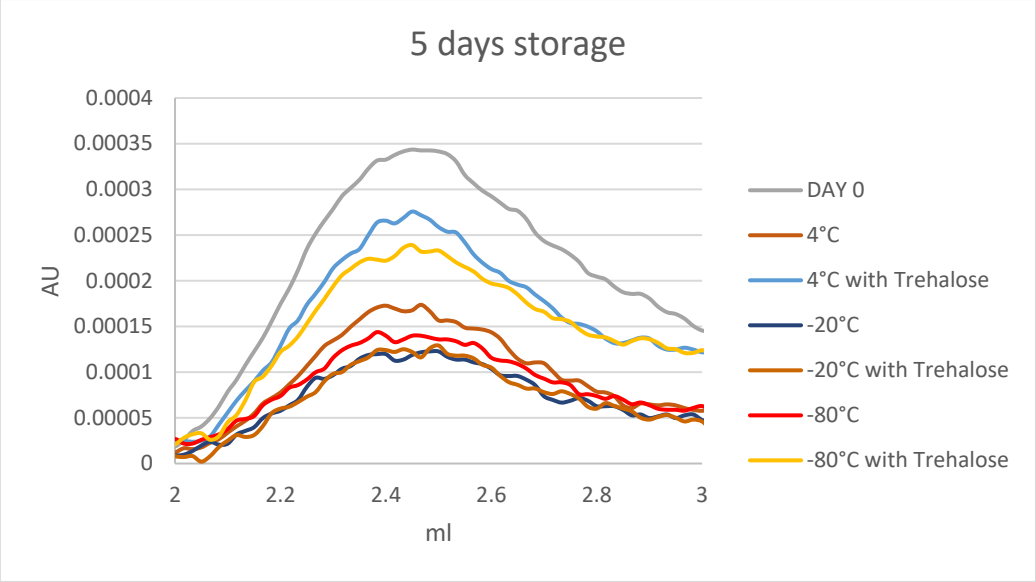

Figure 86: Zoomed HPLC chromatograms after 5 days of storage

Table 20: Integrated area after 5 days

Temperature	**Chromatogram area (mVsec)**	
	With PBS	With Trehalose
DAY 0	10.825	
4°C	5.129	5.367
-20°C	2.589	3.898
-80°C	4.126	5.317

Table 21:% Degradation after 5 days

% DEGRADED		
Temperature	**With PBS**	**With Trehalose**
4°C	52.62	50.42
-20°C	76.08	63.99
-80°C	61.88	50.88

After 5 days the chromatogram areas have been considerably decreased in comparison with the day 0 and even the shape of the peak has been altered. However, there is no striking difference between the peaks of the samples stored at 4°C and -80°C with trehalose. This shows that lemon derived EVs can be stored in the fridge (4°C) for at least 5 days without major degradation.

It is interesting to note that all the peaks involving trehalose are higher than that of its corresponding peak with PBS which shows the effect of trehalose in storage. Since the time considered is much smaller, it is evident that the freeze thaw has resulted in significant loss of vesicles and therefore the peaks related to lower temperatures are lower. The -20°C freezer seems to be very ineffective in preventing the degradation of vesicles, even with addition of trehalose.

The rest of the samples were collected after 10 days and the HPLC analysis as above is carried out. EV chromatogram area after 10 days of storage. The most notable feature is that the resolution and the shape of the peak is different compared to that of day 0 as shown in figure 87. The integrated peak areas are given in table 22 and the % deviation, calculated as before is given in table 23.

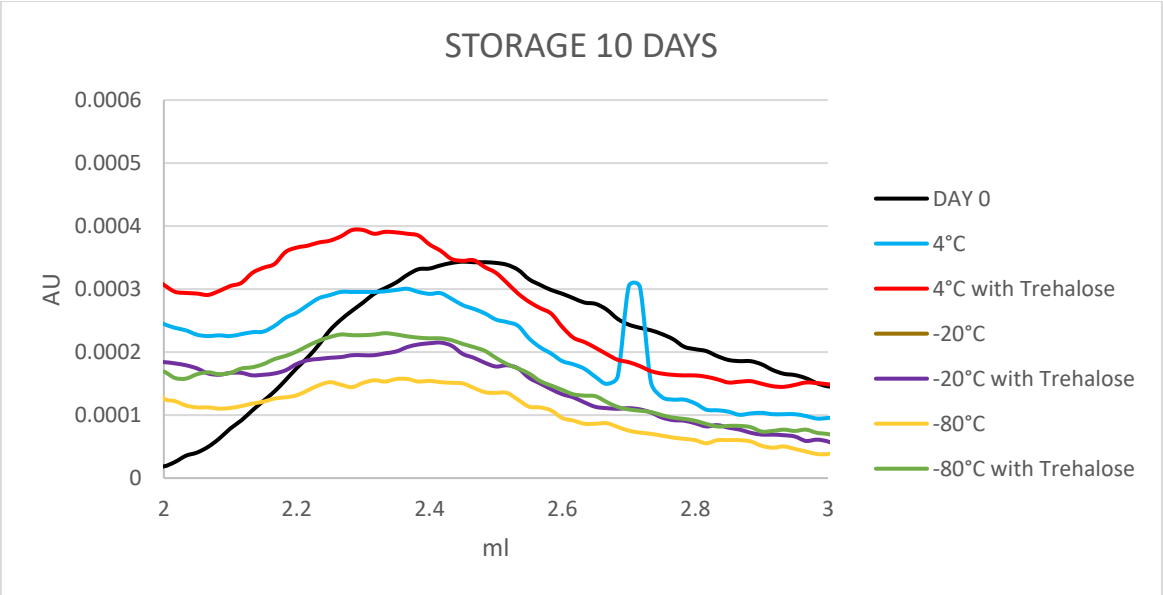

Figure 87: Zoomed HPLC chromatograms after 10 days of storage

Table 22: Integrated area after 10 days

Temperature	Chromatogram area (mVsec)	
	With PBS	**With Trehalose**
DAY 0	10.825	
4°C	4.129	4.826
-20°C	2.975	5.167
-80°C	3.273	4.883

Table 23: %Degradation after 10 days

% DEGRADED		
TEMPERATURE	**With PBS**	**With Trehalose**
4°C	61.86	55.42
-20°C	72.52	52.27
-80°C	69.76	54.89

The shape and the resolution of the peaks have been altered even more than 5 days ago. By visual inspection, a large amount of deposited matter was observed. Once again, freeze thaw at -20°C seems to degrade about 80% of the vesicles present. Due to the short time frame, there is not much difference in degradation at room temperature and -80°C. The effect of Trehalose is very evident across all samples since the % degradation is lower. trehalose is efficient in avoiding the freeze thaw effect as explained previously. However, the extent of degradation is alarmingly high in only 10 days. The aggregation or partial lysis of EVs could be attributed to any of the wide constituents in lemon juice. Along with trehalose, a protein inhibitor cocktail must be tried to prevent aggregation. Ideally, a protease inhibitor could lower protein lysis and hence the degradation.

4.14. QUANTIFICATION OF EVs

A method of approximating the concentration of vesicles in the lemon juice is by using Beer's law which states that absorbance is directly proportional to the concentration. To determine this, a standard curve is developed by sending solutions serially diluted with known values of

concentration to the HPLC column used. Here, Bovine Serum Albumin has been chosen as the known solute. The concentration and the peak heights of the corresponding standard is reported in table 24.

Table 24: BSA concentrations and peak heights

CONCENTRATION (mg/ml)	PEAK HEIGHT (AU)
0.1	0.0013
0.037	0.00041
0.014	0.00021
0.0005	0.00008

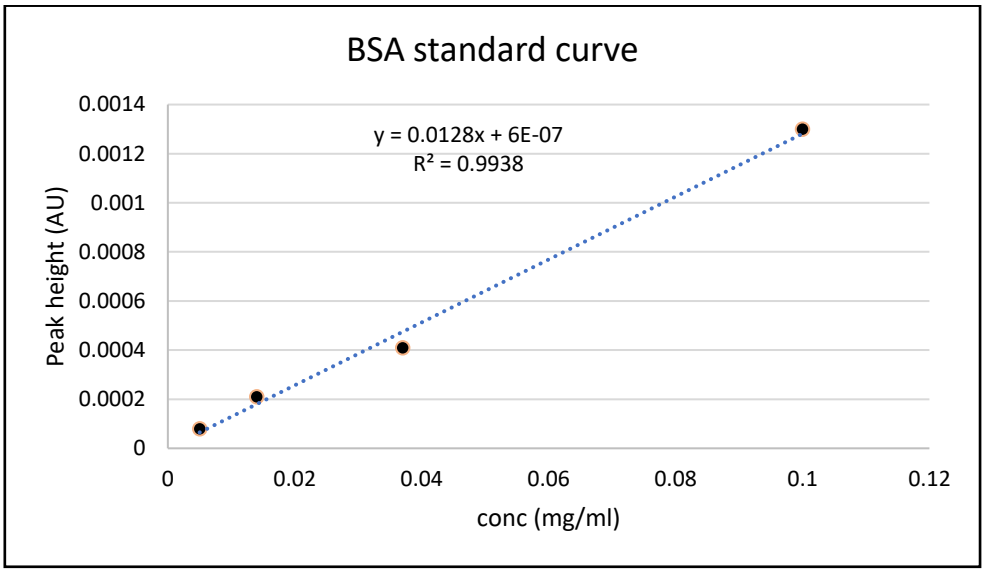

Figure 88: BSA standard curve from HPLC peak heights

From the equation of the standard curve, the peak heights of the EV fraction of the feed (P3µm), retentates and permeates are estimated in table 25.

Table 25: EV concentrations from HPLC peak heights

Analysis	Peak height (AU)	Concentration (mg/ml)
P3 µm	0.0018	0.141
Stage filtration 1st stage	0.00045	0.035
Stage filtration 5th stage	0.00024	0.019
R0.5 Diavolumes	0.00051	0.039
R1 Diavolumes	0.0014	0.108
R1.5 Diavolumes	0.00115	0.089
Cake 1.5 Diavolumes	0.00168	0.131
R2 Diavolumes	0.00109	0.085
Cake 3 Diavolumes	0.00109	0.085
R 3 Diavolumes	0.00107	0.084
Cake 3 Diavolumes	0.00108	0.085

With a starting volume of 50 ml lemon juice, final purified product containing 0.0847 mg/ml of extracellular vesicles fraction is obtained. On an average, 45 ml of juice can be extracted from a single lemon. So, approximating the quantity of vesicles, 3.76 mg of vesicles can be obtained from a single lemon through this TFF protocols with 3 diavolumes.

CHAPTER 5

CONCLUSION AND FUTURE PROSPECTS

The innate capability of extracellular vesicles to carry out intercellular communication and to maintain pathophysiological processes has enabled their applications in the therapeutic field. Due to their distinctive bio cargo and their ability to transport this cargo, EVs can influence target cells and hence carry huge potential towards drug delivery and as disease markers. Mammalian vesicles are limited by availability and ethical concerns. Plant vesicles offer a feasible alternative. They are proven to have similar bio cargo and functions as that of mammalian EVs. Since plants are introduced to human cells through diet, they would offer no toxicity and immunogenicity in therapeutic applications.

Although several techniques exist for isolation of plant and mammalian EVs, the common methods such as ultracentrifugation are limited by process time, process volume, reproducibility, and co-contamination. Due to the shear force, EVs could get damaged or aggregated. Other novel methods such as affinity interaction and microfluidics are limited by the lack of standardisation. The isolation method can influence the morphology and biological properties of the extract. For therapeutic and pharmaceutical applications, exosomes, subtype of EVs should be free from aggregation with the size below 300 nm. In the current study, a diafiltration was proposed to extract extracellular vesicles from citrus lemon juice. Before diafiltration, a centrifugation and dead-end filtration was carried out as a pre-treatment step to remove large impurities and to lighten downstream process load. Diafiltration offers high amount of purification of larger volumes in shorter process time. The process is economic and can be scaled up with ease.

In this study, a one stage diafiltration is investigated to screen the several membranes tested and to develop a diafiltration protocol in continuous, tangential flow mode with the selected membrane. All retentates and permeates were analysed using size exclusion chromatography in analytical mode with both HPLC and FPLC to quantify and analyse the final product using the integrated area of the peak. Even though tangential flow filtration was effective in removing large quantity of impurities in short time, the quantity of vesicles lost in the membrane gel layer was not inconsequential. A protocol was implemented to resuspend and reintroduce this gel layer into the feed tank manually. However, if industrially applied, a reverse flow or backwashing would be ideal. The reintroduction of the gel layer affected the recovery rate

positively. After 3 filtration diavolumes, 15.5% of the EV fraction was recovered while 98.5% of impurities were removed. A mathematical modelling was done on stage and continuous diafiltration but both models showed appreciable fit of data where the deviation is possibly due to the large deposition on the membrane gel layer.

Despite the shortcomings, ultracentrifugation is still considered a benchmark for EV isolation. The results from this study have been compared with 2 different ultracentrifugation protocols. Even though the quantity of vesicles recovered does not match up to UC standards, co contamination has been largely reduced. However, the final product quantity obtained from UC is significantly low (4ml) considering the same starting volume.

To characterise the dimensions and zeta potential of the extract, DLS measurements were taken on the feed and the retentates after tangential flow filtration. The study showed that the size ranges from 100 to 1000 nm and the average size for most samples range from 200-300 nm. This shows that the vesicles are present in aggregated form since the size range from literature is much lower. In the retentate after 3 diavolumes of filtration, there were 15% particles with the size range of 74 nm which is the exosomal size range. This suggests that the vesicles in the final product could be less aggregated. Zeta potential is a measure of stability and the zeta potential of stable EVs range from -10 mV to -50 mV. The feed had a zeta potential of -3.75 mV which suggests high tendency for aggregation. However, the final product retentates had zeta potential close to -10 mV suggesting that the tendency is lower and the nano particles are stable.

A BCA assay was carried out to find total concentration of proteins in the feed and the retentates and permeates at different diavolumes. The feed had high total concentration (2252.63 µg/ml) while the retentate after 3 diavolumes had lower concentration (1214.68 µg/ml) of protein content. All the permeates also had high protein concentration suggesting the quantified protein could be mostly attributed to impurities as opposed to vesicles. Another approximation was done with a BSA standard curve in HPLC column to quantify the yield from lemon to be 3.76 mg EVs/lemon.

Due to the high tendency of the vesicles to form aggregates which deem them unusable in clinical applications, storage tests were done at different temperature to study the degradation with respect to storage duration and temperature. Trehalose has been used as a cryoprotectant and to reduce protein aggregation. The results showed that even with trehalose, large amounts of vesicles were degraded after only 10 days. The freeze thaw effect was lower in samples

containing trehalose. Along with trehalose, a protease inhibitor cocktail could be evaluated for long term storage.

As a future prospective, it would be ideal to have standardisation in isolation and characterisation techniques of vesicles from plants. The lack of information is a limiting factor for this budding field of study. To have a better understanding of aggregation, microscopic techniques or monitoring of nanoparticles through nanoparticle tracking analysis (NTA) could be carried out consistently at each step of diafiltration. This could help in optimising the protocol better. For efficiently applying the present system of TFF coupled with UV detector, it would be ideal to have lemon EV specific protein markers where the UV signals could be used to analyse the extent of purification and the removal of impurities. Another prospect could be the use of Tangential flow for analyte capture (TFAC) for recovering the large quantity of EV fraction lost in the membrane cake. Nevertheless, process should be constantly monitored to analyse whether the captured vesicles are in the aggregated form or freely available.

REFERENCES

[1] E. CHARGAFF and R. WEST, “The biological significance of the thromboplastic protein of blood.,” *The Journal of biological chemistry*, vol. 166, no. 1, 1946, doi: 10.1016/S0021-9258(17)34997-9.

[2] M. Yànez-Mo *et al.*, “Biological properties of extracellular vesicles and their physiological functions,” *Journal of extracellular vesicles*, vol. 4, 2015.

[3] S. Gandham *et al.*, “Technologies and Standardization in Research on Extracellular Vesicles,” *Trends in Biotechnology*, vol. 38, no. 10. 2020, doi: 10.1016/j.tibtech.2020.05.012.

[4] S. Walker *et al.*, “Extracellular vesicle-based drug delivery systems for cancer treatment,” *Theranostics*, vol. 9, no. 26, 2019, doi: 10.7150/thno.37097.

[5] S. A. Muhammad, “Are extracellular vesicles new hope in clinical drug delivery for neurological disorders?,” *Neurochemistry International*, vol. 144. Elsevier Ltd, p. 104955, Mar. 01, 2021, doi: 10.1016/j.neuint.2021.104955.

[6] M. Romano *et al.*, “Extracellular vesicles in regenerative medicine,” in *Nanomaterials for Theranostics and Tissue Engineering*, Elsevier, 2020, pp. 29–58.

[7] P. Pérez-Bermúdez, J. Blesa, J. M. Soriano, and A. Marcilla, “Extracellular vesicles in food: Experimental evidence of their secretion in grape fruits,” *European Journal of Pharmaceutical Sciences*, vol. 98, 2017, doi: 10.1016/j.ejps.2016.09.022.

[8] J. Mu *et al.*, “Interspecies communication between plant and mouse gut host cells through edible plant derived exosome-like nanoparticles,” *Molecular Nutrition and Food Research*, vol. 58, no. 7, 2014, doi: 10.1002/mnfr.201300729.

[9] S. Raimondo *et al.*, “Citrus limon-derived nanovesicles inhibit cancer cell proliferation and suppress CML xenograft growth by inducing TRAIL-mediated cell death,” *Oncotarget*, vol. 6, no. 23, 2015, doi: 10.18632/oncotarget.4004.

[10] M. P. Zaborowski, L. Balaj, X. O. Breakefield, and C. P. Lai, “Extracellular Vesicles: Composition, Biological Relevance, and Methods of Study,” *BioScience*, vol. 65, no. 8. 2015, doi: 10.1093/biosci/biv084.

[11] H. Zhou *et al.*, “Exosomal Fetuin-A identified by proteomics: A novel urinary biomarker for detecting acute kidney injury,” *Kidney International*, vol. 70, no. 10, 2006, doi: 10.1038/sj.ki.5001874.

[12] C. Théry *et al.*, “Proteomic Analysis of Dendritic Cell-Derived Exosomes: A Secreted Subcellular Compartment Distinct from Apoptotic Vesicles,” *The Journal of Immunology*, vol. 166, no. 12, 2001, doi: 10.4049/jimmunol.166.12.7309.

[13] Y. Xing, Z. Cheng, R. Wang, C. Lv, T. D. James, and F. Yu, “Analysis of extracellular vesicles as emerging theranostic nanoplatforms,” *Coordination Chemistry Reviews*, vol. 424. 2020, doi: 10.1016/j.ccr.2020.213506.

[14] M. C. Cufaro *et al.*, “Extracellular vesicles and their potential use in monitoring cancer progression and therapy: The contribution of proteomics,” *Journal of Oncology*, vol. 2019. 2019, doi: 10.1155/2019/1639854.

[15] R. van der Meel, M. H. A. M. Fens, P. Vader, W. W. van Solinge, O. Eniola-Adefeso, and R. M. Schiffelers, “Extracellular vesicles as drug delivery systems: Lessons from the liposome field,” *Journal of Controlled Release*, vol. 195. 2014, doi: 10.1016/j.jconrel.2014.07.049.

[16] N. Jasiewicz, C. Drabenstott, and J. Nguyen, “Harnessing the Full Potential of Extracellular Vesicles as Drug Carriers,” *Current Opinion in Colloid & Interface Science*, 2020, doi: 10.1016/j.cocis.2020.101412.

[17] D. Yang *et al.*, “Progress, opportunity, and perspective on exosome isolation - Efforts for efficient exosome-based theranostics,” *Theranostics*, vol. 10, no. 8. 2020, doi: 10.7150/thno.41580.

[18] M. Y. Konoshenko, E. A. Lekchnov, A. v Vlassov, and P. P. Laktionov, “Isolation of Extracellular Vesicles: General Methodologies and Latest Trends,” *BioMed Research International*, vol. 2018. 2018, doi: 10.1155/2018/8545347.

[19] F. Momen-Heravi *et al.*, “Current methods for the isolation of extracellular vesicles,” *Biological Chemistry*, vol. 394, no. 10. 2013, doi: 10.1515/hsz-2013-0141.

[20] M. A. Livshts *et al.*, “Isolation of exosomes by differential centrifugation: Theoretical analysis of a commonly used protocol,” *Scientific Reports*, vol. 5, 2015, doi: 10.1038/srep17319.

[21] C. Paganini, U. C. Palmiero, G. Pocsfalvi, N. Touzet, A. Bongiovanni, and P. Arosio, “Scalable Production and Isolation of Extracellular Vesicles: Available Sources and Lessons from Current Industrial Bioprocesses,” *Biotechnology Journal*, vol. 14, no. 10. 2019, doi: 10.1002/biot.201800528.

[22] M. Popovic and A. de Marco, “Canonical and selective approaches in exosome purification and their implications for diagnostic accuracy,” *Translational Cancer Research*, vol. 7. 2018, doi: 10.21037/tcr.2017.08.44.

[23] T. Liangsupree, E. Multia, and M. L. Riekkola, “Modern isolation and separation techniques for extracellular vesicles,” *Journal of Chromatography A*, vol. 1636, 2021, doi: 10.1016/j.chroma.2020.461773.

[24] O. J. Arntz, B. C. H. Pieters, P. L. E. M. van Lent, M. I. Koenders, P. M. van der Kraan, and F. A. J. van de Loo, “An optimized method for plasma extracellular vesicles isolation to exclude the copresence of biological drugs and plasma proteins which impairs their biological characterization,” *PLoS ONE*, vol. 15, no. 7 July, 2020, doi: 10.1371/journal.pone.0236508.

[25] Y. Yuana, J. Levels, A. Grootemaat, A. Sturk, and R. Nieuwland, “Co-isolation of extracellular vesicles and high-density lipoproteins using density gradient ultracentrifugation,” *Journal of Extracellular Vesicles*, vol. 3, no. 1, 2014, doi: 10.3402/jev.v3.23262.

[26] R. D. Worsham, V. Thomas, and S. S. Farid, “Potential of Continuous Manufacturing for Liposomal Drug Products,” *Biotechnology Journal*, vol. 14, no. 2. 2019, doi: 10.1002/biot.201700740.

[27] M. L. Merchant *et al.*, “Microfiltration isolation of human urinary exosomes for characterization by MS,” *Proteomics - Clinical Applications*, vol. 4, no. 1, 2010, doi: 10.1002/prca.200800093.

[28] M. L. Heinemann *et al.*, “Benchtop isolation and characterization of functional exosomes by sequential filtration,” *Journal of Chromatography A*, vol. 1371, 2014, doi: 10.1016/j.chroma.2014.10.026.

[29] A. Cheruvanky *et al.*, “Rapid isolation of urinary exosomal biomarkers using a nanomembrane ultrafiltration concentrator,” *American Journal of Physiology - Renal Physiology*, vol. 292, no. 5, 2007, doi: 10.1152/ajprenal.00434.2006.

[30] R. J. Lobb *et al.*, “Optimized exosome isolation protocol for cell culture supernatant and human plasma,” *Journal of Extracellular Vesicles*, vol. 4, no. 1, 2015, doi: 10.3402/jev.v4.27031.

[31] S. Busatto *et al.*, “Tangential Flow Filtration for Highly Efficient Concentration of Extracellular Vesicles from Large Volumes of Fluid,” *Cells*, vol. 7, no. 12, 2018, doi: 10.3390/cells7120273.

[32] N. Heath *et al.*, “Rapid isolation and enrichment of extracellular vesicle preparations using anion exchange chromatography,” *Scientific Reports*, vol. 8, no. 1, 2018, doi: 10.1038/s41598-018-24163-y.

[33] N. Dimov, E. Kastner, M. Hussain, Y. Perrie, and N. Szita, “Formation and purification of tailored liposomes for drug delivery using a module-based micro continuous-flow system,” *Scientific Reports*, vol. 7, no. 1, 2017, doi: 10.1038/s41598-017-11533-1.

[34] B. Wu *et al.*, “Separation and characterization of extracellular vesicles from human plasma by asymmetrical flow field-flow fractionation,” *Analytica Chimica Acta*, vol. 1127, 2020, doi: 10.1016/j.aca.2020.06.071.

[35] S. Sitar *et al.*, “Size Characterization and Quantification of Exosomes by Asymmetrical-Flow Field-Flow Fractionation,” *Analytical Chemistry*, vol. 87, no. 18, 2015, doi: 10.1021/acs.analchem.5b01636.

[36] H. Zhang *et al.*, “Identification of distinct nanoparticles and subsets of extracellular vesicles by asymmetric flow field-flow fractionation,” *Nature Cell Biology*, vol. 20, no. 3, 2018, doi: 10.1038/s41556-018-0040-4.

[37] K. Yakimchuk, “Exosomes: isolation methods and specific markers,” *Materials and Methods*, vol. 5, 2015, doi: 10.13070/mm.en.5.1450.

[38] M. A. Rider, S. N. Hurwitz, and D. G. Meckes, “ExtraPEG: A polyethylene glycol-based method for enrichment of extracellular vesicles,” *Scientific Reports*, vol. 6, 2016, doi: 10.1038/srep23978.

[39] D. D. Taylor, W. Zacharias, and C. Gercel-Taylor, “Exosome isolation for proteomic analyses and RNA profiling,” *Methods in Molecular Biology*, vol. 728, 2011, doi: 10.1007/978-1-61779-068-3_15.

[40] J. Caradec, G. Kharmate, E. Hosseini-Beheshti, H. Adomat, M. Gleave, and E. Guns, “Reproducibility and efficiency of serum-derived exosome extraction methods,” *Clinical Biochemistry*, vol. 47, no. 13–14, 2014, doi: 10.1016/j.clinbiochem.2014.06.011.

[41] M. Dash, K. Palaniyandi, S. Ramalingam, S. Sahabudeen, and N. S. Raja, “Exosomes isolated from two different cell lines using three different isolation techniques show variation in physical and molecular characteristics,” *Biochimica et Biophysica Acta - Biomembranes*, vol. 1863, no. 2, 2021, doi: 10.1016/j.bbamem.2020.183490.

[42] S. N. Neerukonda *et al.*, “Comparison of exosomes purified via ultracentrifugation (UC) and Total Exosome Isolation (TEI) reagent from the serum of Marek’s disease virus (MDV)-vaccinated and tumor-bearing chickens,” *Journal of Virological Methods*, vol. 263, 2019, doi: 10.1016/j.jviromet.2018.10.004.

[43] T. S. Martins, J. Catita, I. M. Rosa, O. A. B. D. C. e Silva, and A. G. Henriques, “Exosome isolation from distinct biofluids using precipitation and column-based approaches,” *PLoS ONE*, vol. 13, no. 6, 2018, doi: 10.1371/journal.pone.0198820.

[44] Y. Zhang *et al.*, “High-Efficiency Separation of Extracellular Vesicles from Lipoproteins in Plasma by Agarose Gel Electrophoresis,” *Analytical Chemistry*, vol. 92, no. 11, 2020, doi: 10.1021/acs.analchem.9b05675.

[45] M. Yang, X. Liu, Q. Luo, L. Xu, and F. Chen, “An efficient method to isolate lemon derived extracellular vesicles for gastric cancer therapy,” *Journal of Nanobiotechnology*, vol. 18, no. 1, 2020, doi: 10.1186/s12951-020-00656-9.

[46] S. Marczak *et al.*, “Simultaneous isolation and preconcentration of exosomes by ion concentration polarization,” *Electrophoresis*, vol. 39, no. 15, 2018, doi: 10.1002/elps.201700491.

[47] M. Kosanović, B. Milutinović, S. Goč, N. Mitić, and M. Janković, “Ion-exchange chromatography purification of extracellular vesicles,” *BioTechniques*, vol. 63, no. 2, 2017, doi: 10.2144/000114575.

[48] C. Théry, L. Zitvogel, and S. Amigorena, “Exosomes: Composition, biogenesis and function,” *Nature Reviews Immunology*, vol. 2, no. 8. 2002, doi: 10.1038/nri855.

[49] Z. Zhao, Y. Yang, Y. Zeng, and M. He, “A microfluidic ExoSearch chip for multiplexed exosome detection towards blood-based ovarian cancer diagnosis,” *Lab on a Chip*, vol. 16, no. 3, 2016, doi: 10.1039/c5lc01117e.

[50] A. Ghosh *et al.*, “Rapid isolation of extracellular vesicles from cell culture and biological fluids using a synthetic peptide with specific affinity for heat shock proteins,” *PLoS ONE*, vol. 9, no. 10, 2014, doi: 10.1371/journal.pone.0110443.

[51] Y. G. Zhou *et al.*, “Interrogating Circulating Microsomes and Exosomes Using Metal Nanoparticles,” *Small*, vol. 12, no. 6, 2016, doi: 10.1002/smll.201502365.

[52] A. K. Rupp *et al.*, “Loss of EpCAM expression in breast cancer derived serum exosomes: Role of proteolytic cleavage,” *Gynecologic Oncology*, vol. 122, no. 2, 2011, doi: 10.1016/j.ygyno.2011.04.035.

[53] E. Multia, C. J. Y. Tear, M. Palviainen, P. Siljander, and M. L. Riekkola, “Fast isolation of highly specific population of platelet-derived extracellular vesicles from blood plasma by affinity monolithic column, immobilized with anti-human CD61 antibody,” *Analytica Chimica Acta*, vol. 1091, 2019, doi: 10.1016/j.aca.2019.09.022.

[54] K. Zhang, Y. Yue, S. Wu, W. Liu, J. Shi, and Z. Zhang, “Rapid Capture and Nondestructive Release of Extracellular Vesicles Using Aptamer-Based Magnetic Isolation,” *ACS Sensors*, vol. 4, no. 5, 2019, doi: 10.1021/acssensors.9b00060.

[55] S. C. Guo, S. C. Tao, and H. Dawn, “Microfluidics-based on-a-chip systems for isolating and analysing extracellular vesicles,” *Journal of Extracellular Vesicles*, vol. 7, no. 1. 2018, doi: 10.1080/20013078.2018.1508271.

[56] C. Chen *et al.*, “Microfluidic isolation and transcriptome analysis of serum microvesicles,” *Lab on a Chip*, vol. 10, no. 4, 2010, doi: 10.1039/b916199f.

[57] Y. Meng *et al.*, “Microfluidics for extracellular vesicle separation and mimetic synthesis: Recent advances and future perspectives,” *Chemical Engineering Journal*, vol. 404. 2021, doi: 10.1016/j.cej.2020.126110.

[58] C. Liu *et al.*, “Field-Free Isolation of Exosomes from Extracellular Vesicles by Microfluidic Viscoelastic Flows,” *ACS Nano*, vol. 11, no. 7, 2017, doi: 10.1021/acsnano.7b02277.

[59] M. Wu *et al.*, “Isolation of exosomes from whole blood by integrating acoustics and microfluidics,” *Proceedings of the National Academy of Sciences of the United States of America*, vol. 114, no. 40, 2017, doi: 10.1073/pnas.1709210114.

[60] S. Rome, “Biological properties of plant-derived extracellular vesicles,” *Food and Function*, vol. 10, no. 2, 2019, doi: 10.1039/c8fo02295j.

[61] S. Iravani and R. S. Varma, “Plant-Derived Edible Nanoparticles and miRNAs: Emerging Frontier for Therapeutics and Targeted Drug-Delivery,” *ACS Sustainable Chemistry and Engineering*, vol. 7, no. 9, 2019, doi: 10.1021/acssuschemeng.9b00954.

[62] C. Yang, M. Zhang, and D. Merlin, “Advances in plant-derived edible nanoparticle-based lipid nano-drug delivery systems as therapeutic nanomedicines,” *Journal of Materials Chemistry B*, vol. 6, no. 9. 2018, doi: 10.1039/c7tb03207b.

[63] J. Munir, M. Lee, and S. Ryu, “Exosomes in Food: Health Benefits and Clinical Relevance in Diseases,” *Advances in Nutrition*, vol. 11, no. 3. 2020, doi: 10.1093/advances/nmz123.

[64] M. Pucci and S. Raimondo, “Plant extracellular vesicles: the safe for bioactive compounds,” *Advances in Biomembranes and Lipid Self-Assembly*, 2020, doi: 10.1016/bs.abl.2020.04.002.

[65] X. Zhuang *et al.*, “Grapefruit-derived nanovectors delivering therapeutic miR17 through an intranasal route inhibit brain tumor progression,” *Molecular Therapy*, vol. 24, no. 1, 2016, doi: 10.1038/mt.2015.188.

[66] M. Klimek-szczykutowicz, A. Szopa, and H. Ekiert, “Citrus limon (Lemon) phenomenon—a review of the chemistry, pharmacological properties, applications in the modern pharmaceutical, food, and cosmetics industries, and biotechnological studies,” *Plants*, vol. 9, no. 1. 2020, doi: 10.3390/plants9010119.

[67] N. Baldini, E. Torreggiani, L. Roncuzzi, F. Perut, N. Zini, and S. Avnet, “Exosome-like Nanovesicles Isolated from Citrus limon L. Exert Antioxidative Effect,” *Current Pharmaceutical Biotechnology*, vol. 19, no. 11, 2018, doi: 10.2174/1389201019666181017115755.

[68] T. Zhou *et al.*, “Protective effects of lemon juice on alcohol-induced liver injury in mice,” *BioMed Research International*, vol. 2017, 2017, doi: 10.1155/2017/7463571.

[69] X. Lv *et al.*, “Citrus fruits as a treasure trove of active natural metabolites that potentially provide benefits for human health,” *Chemistry Central Journal*, vol. 9, no. 1. 2015, doi: 10.1186/s13065-015-0145-9.

[70] G. Pocsfalvi *et al.*, “Protein biocargo of citrus fruit-derived vesicles reveals heterogeneous transport and extracellular vesicle populations,” *Journal of Plant Physiology*, vol. 229, 2018, doi: 10.1016/j.jplph.2018.07.006.

[71] B. Qin *et al.*, “How does temperature play a role in the storage of extracellular vesicles?,” *Journal of Cellular Physiology*, vol. 235, no. 11. 2020, doi: 10.1002/jcp.29700.

[72] A. Jeyaram and S. M. Jay, “Preservation and Storage Stability of Extracellular Vesicles for Therapeutic Applications,” *AAPS Journal*, vol. 20, no. 1. 2018, doi: 10.1208/s12248-017-0160-y.

[73] Q. Wang *et al.*, “Delivery of therapeutic agents by nanoparticles made of grapefruit-derived lipids,” *Nature Communications*, vol. 4, 2013, doi: 10.1038/ncomms2886.

LIST OF FIGURES

Figure 1: Classification of EVs and their release [10] EE: early endosome; MVB: multi-vesicular body; N: Nucleus; 7
Figure 2: Figure 2: Formation of EVs subtypes [10]. 8
Figure 3: Cells recieving EVs [10] 9
Figure 4: EV composition SM: Sphingomyelin; PE: phosphatidylethanolamine; PC: phosphatidylcholine; PE-O: alkyl-ether substituted phosphatidylethanolamine PS: phosphatidylserine; CHOL: cholesterol [3] 10
Figure 5: No of publications based on cancer and EVs research in the past decade (PubMed) 16
Figure 6: Number of publications of EV isolation methods in the last 2 decades 17
Figure 7: UC protocol [20] 18
Figure 8: Figure 3: (a) “swinging bucket” and (b) “fixed angle” rotors of a centrifuge [17] 19
Figure 9: A.Isopycnic density-gradient UC and B.Moving-zone gradient UC [17] 19
Figure 10: EV isolation using SEC [17] 20
Figure 11: Coupled MF-UF protocol developed by Heinemann et. al [30] 22
Figure 12: Dead end filtration vs crossflow filtration 23
Figure 13: Proteins from ExtraPEG method [38] 26
Figure 14: Exoquick protocol [System Biosciences] 27
Figure 15: Comparison of different methods with Exoquick in terms of proteins recovered [24] 27
Figure 16: Comparison of commercial precipitation reagents (TEI, Exoquick) with column-based methods (ExoS) in terms of exosome purity [44] 28
Figure 17: A) The size and B) zeta potential comparison of common lipoproteins with EVs. C) The migration of the lipoproteins and EVs under electric field on an agarose gel [46] 29
Figure 18: Microfluidic cell with electrophoresis and an ion selective membrane [47] 30
Figure 19: immunoaffinity-based exosome isolation by Yang et al. [48] 31
Figure 20: Immunoaffinity monolithic disk column for EV isolation from plasma developed by Multia et al. [53] 32
Figure 21: Microfluidic devices with surface coating and functionalized beads (red are vesicles while blue is impurities) [58] 34
Figure 22: Viscoelastic separation [59] 34
Figure 23: Separation using acoustofluidics. A) Protocol of 2 seperate units for cell removal and exosome separation. B) Setup. C) Pressure nodes separate larger and smaller particles [60] 35
Figure 24: Extracellular vesicles in plants and lower organisms [61] 39
Figure 25: Structural comparison of A) Mammalian and B) Plant derived EVs [63] 39
Figure 26: Thermofisher SL16 centrifuge 49
Figure 27: Thermofisher TX-400 49
Figure 28: Thermofisher 30x2 microliter rotor 49
Figure 29: AMICON cell 50
Figure 30: Pre-treatment method 50
Figure 31: Typical TFF scheme 51
Figure 32: Millipore MINITAN S cell 52
Figure 33: AKTA FPLC PUMP P-900 52
Figure 34: P&ID of TFF protocol 53
Figure 35: Waters Alliance separation module 2695 55
Figure 36: Yarra SEC chromatogram with IgG, BSA, Tyrosine and Myoglobin 56
Figure 37: Yarra SEC calibration curve 57

Figure 38: AKTA FPLC system 58
Figure 39: AKTA FPLC injection valve 58
Figure 40: SEC FPLC Acetone chromatogram 60
Figure 41: Beckman Coulter Optima L-90K 61
Figure 42: Beckman 50.2 Titanium rotor 61
Figure 43: Ultracentrifugation protocols 62
Figure 44: Zeiss Axiolab 5 63
Figure 45: BCA protocol 64
Figure 46: Zetasizer Nano ZS 66
Figure 47: Malvern Gold electrode cuvette 66
Figure 48: Disposable polystyrene cuvettes 66
Figure 49: FPLC chromatogram of pre-treatment step 68
Figure 50: Flux of 0.45 µm RC membrane 70
Figure 51: HPLC chromatograms of 0.45µm RC stage filtration 70
Figure 52: Zoomed HPLC chromatograms of 0.45µm RC stage filtration 71
Figure 53: HPLC chromatogram of resuspended cake 72
Figure 54: Zoomed HPLC chromatogram of resuspended cake 72
Figure 55: % recovery, removal of impurities, and EV losses of tested membranes 73
Figure 56: HPLC chromatogram of 250 kDa PVDF 73
Figure 57: Zoomed FPLC chromatogram of 250 kDa PVDF 74
Figure 58: HPLC chromatogram of 100 kDa PES 75
Figure 59: Zoomed HPLC chromatogram of 100 kDa PES 75
Figure 60: FPLC chromatogram of 100 kDa PES 76
Figure 61: Zoomed FPLC chromatogram of 100 kDa PES 76
Figure 62: Stage diafiltration model 78
Figure 63: HPLC chromatogram with PBS 79
Figure 64: HPLC chromatogram with TRIS buffer 79
Figure 65: FPLC chromatograms with different buffers 80
Figure 66: Water permeability with time 81
Figure 67: Flux vs TMP of 100 kDa PES 81
Figure 68: Flux at 0.5 diavolumes 82
Figure 69: FPLC chromatograms at 0.5 diavolumes 82
Figure 70: Zoomed FPLC chromatograms at 0.5 diavolumes 83
Figure 71: Flux at 1.5 diavolumes 84
Figure 72: FPLC chromatograms at 1.5 diavolumes 84
Figure 73: Zoomed FPLC chromatograms at 1.5 diavolumes 85
Figure 74: Flux at 3 diavolumes 86
Figure 75: FPLC chromatograms at 3 diavolumes 86
Figure 76: Zoomed FPLC chromatograms at 3 diavolumes 87
Figure 77: Membrane gel layer 88
Figure 78: Membrane gel layer: 100µm scale 88
Figure 79: Constant volume TFF model 90
Figure 80: FPLC chromatogram for comparison of UC protocols 91
Figure 81: FPLC chromatograms of UC and diafiltration 3 DV 92
Figure 82: Size distribution by intensity, Permeate 3µm 93
Figure 83:: Size distribution by intensity, Retentate 1.5 94
Figure 84: Size distribution by intensity, Retentate 3 DV 94
Figure 85: BCA standard curve 97

Figure 86: Zoomed HPLC chromatograms after 5 days of storage 99
Figure 87: Zoomed HPLC chromatograms after 10 days of storage 100
Figure 88: BSA standard curve from HPLC peak heights 102
Figure 89: Size distribution by intensity, Retentate 0.5 DV 119
Figure 90: Size distribution by intensity, Retentate 0.8 DV 119
Figure 91: Size distribution by intensity, Cake 0.8 DV 120

LIST OF TABLES

Table 1: EV Isolation methods summary 36
Table 2: Instruments used 48
Table 3: HPLC Calibration curve data 56
Table 4: Asymmetry factor and No of plates of Sepharose CL-2B column 60
Table 5: Tested parameters 67
Table 6: Integrated peaks of pre-treatment step 69
Table 7: Integrated peaks, 250 kDa PVDF 74
Table 8: Integrated peaks of stage filtration with 100 kDa PES 77
Table 9: Integrated peaks of 2 different buffers on same juice 79
Table 10: Integrated peaks of 0.5 diavolumes 83
Table 11: Integrated peaks of 1.5 diavolume 85
Table 12: Integrated peaks of 3 diavolume 87
Table 13: Integrated peaks of 3 diavolumes and UC protocols 92
Table 14: Detection of large size distributions 94
Table 15: Samples with exosomal size range 95
Table 16: Average particle diameter from DLS 95
Table 17: Zeta potential through DLS 96
Table 18: BCA standard curve data 96
Table 19: Total protein concentrations using BCA 97
Table 20: Integrated area after 5 days 99
Table 21:% Degradation after 5 days 99
Table 22: Integrated area after 10 days 101
Table 23: %Degradation after 10 days 101
Table 24: BSA concentrations and peak heights 102
Table 25: EV concentrations from HPLC peak heights 103

APPENDIX I

Recipe for 0.1 M PBS, pH 7.4

This buffer is used as a mobile phase for FPLC and as the diafiltration buffer.

Solution A: 13.8g of Sodium phosphate monobasic ($NaH_2PO_4.H_2O$) in 1 L deionized water

Solution B: 14.2g of di Sodium Hydrogen Phosphate anhydrous ($NaHPO_4$) in 1 L deionized water

Add solution A to B until pH is 7.4.

Recipe for 0.1 M PBS, pH 6.7 (HPLC)

Solution A: 13.8g of Sodium phosphate monobasic ($NaH_2PO_4.H_2O$), 17.53g of NaCl (analytical grade) in 1 L HPLC grade water

Solution B: 14.2g of di Sodium Hydrogen Phosphate anhydrous (NaHPO4) 17.53g of NaCl (analytical grade) in 1 L HPLC grade water

APPENDIX II

HPLC Chromatogram: 250 kDa PVDF, 5 stages

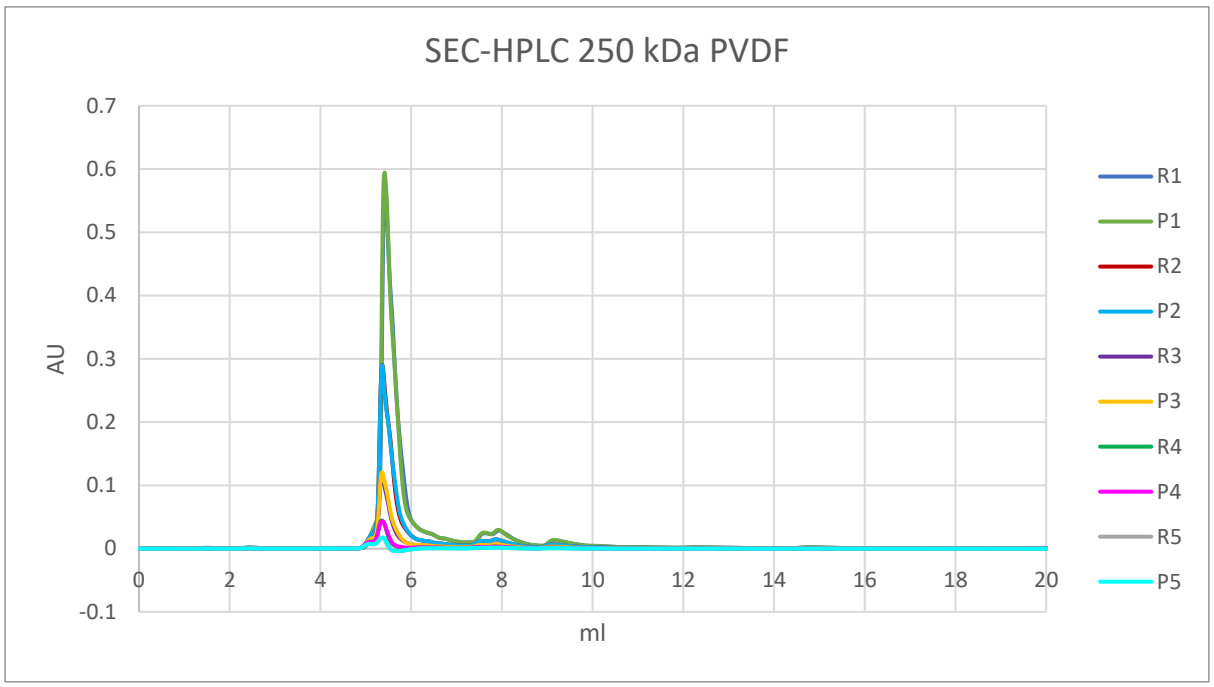

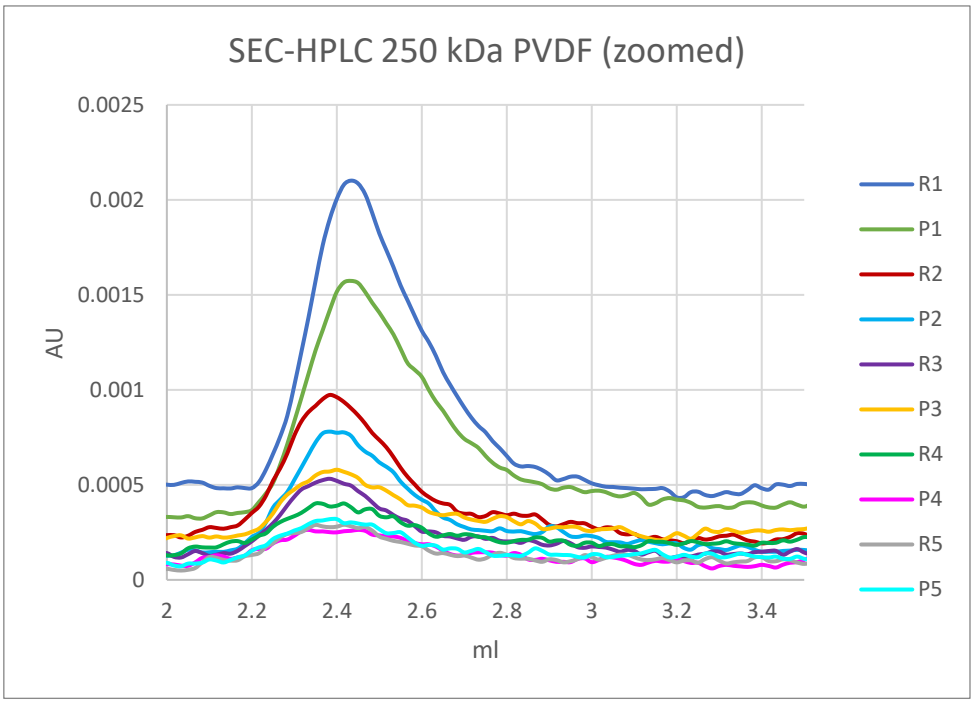

HPLC Chromatogram: 250 kDa PVDF, 2 stages

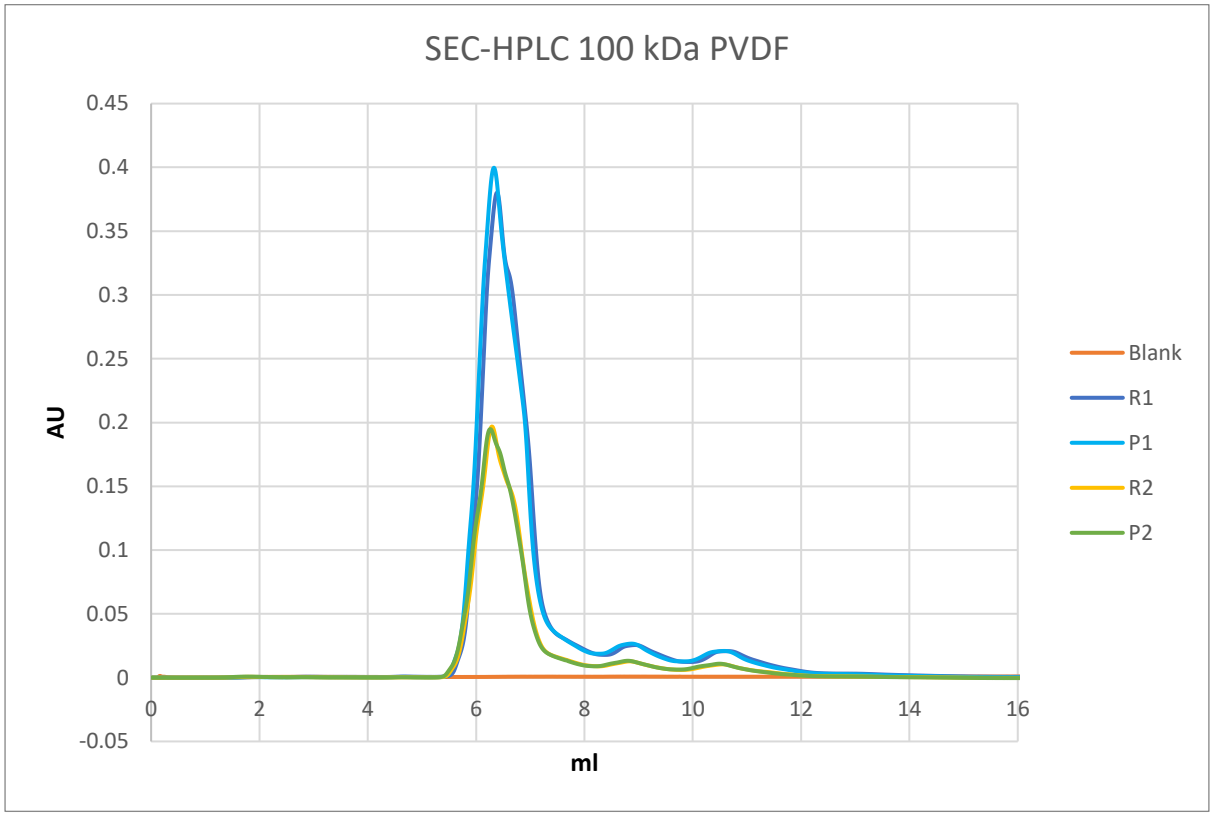

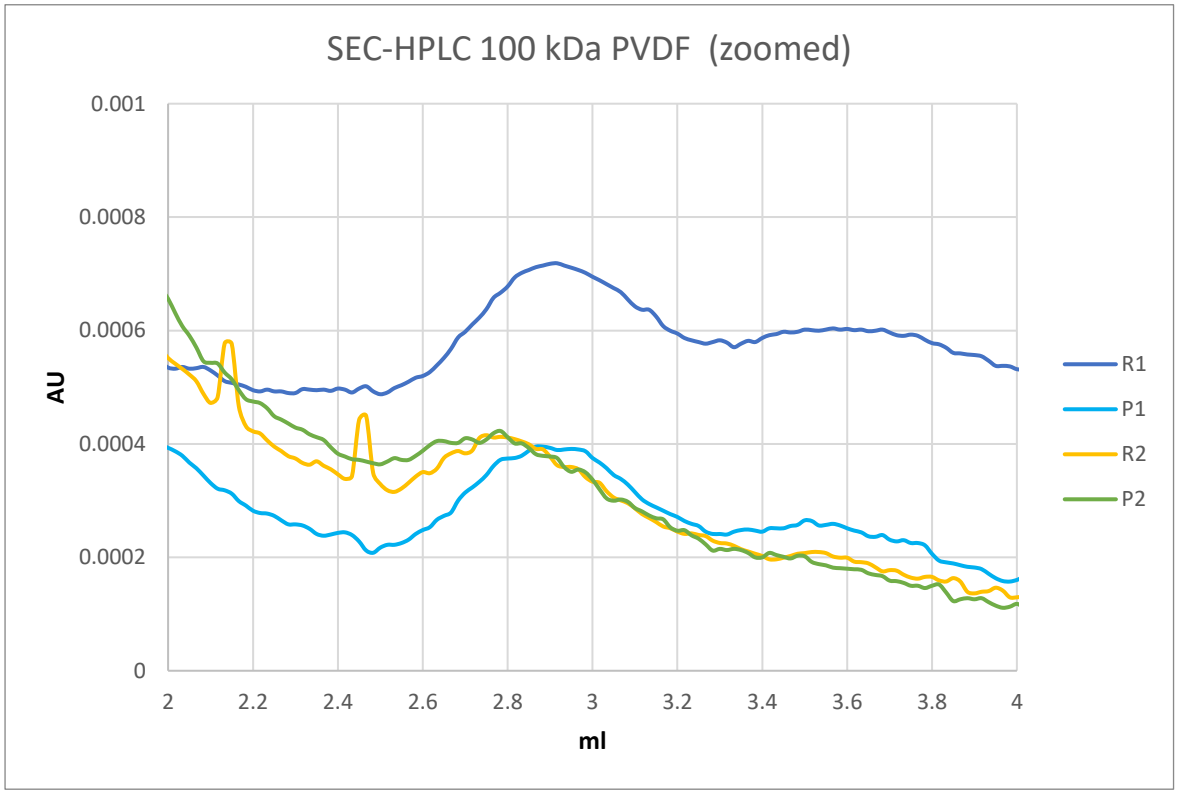

APPENDIX III

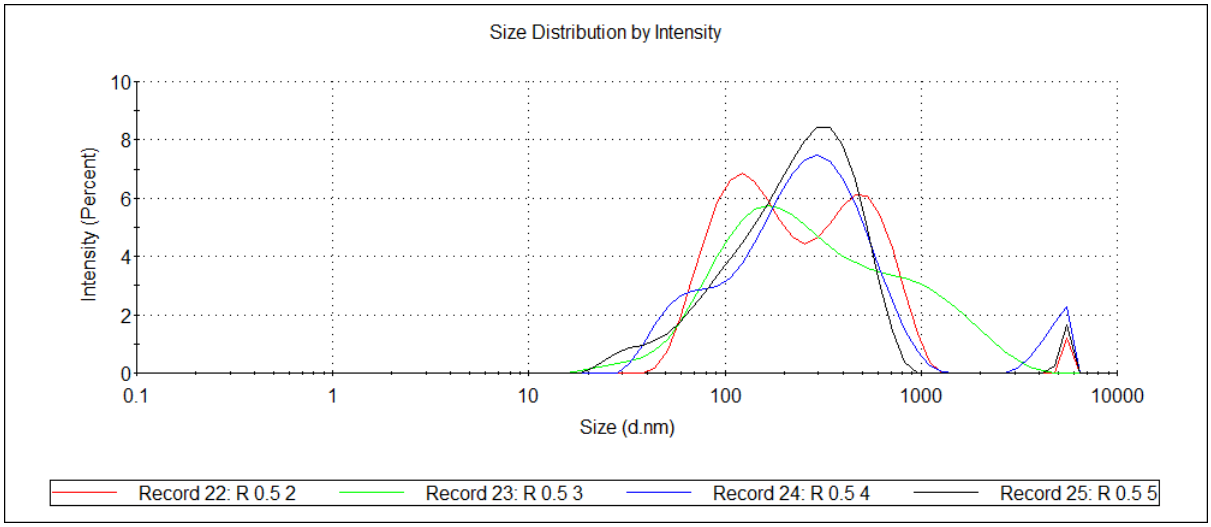

Figure 89: Size distribution by intensity, Retentate 0.5 DV

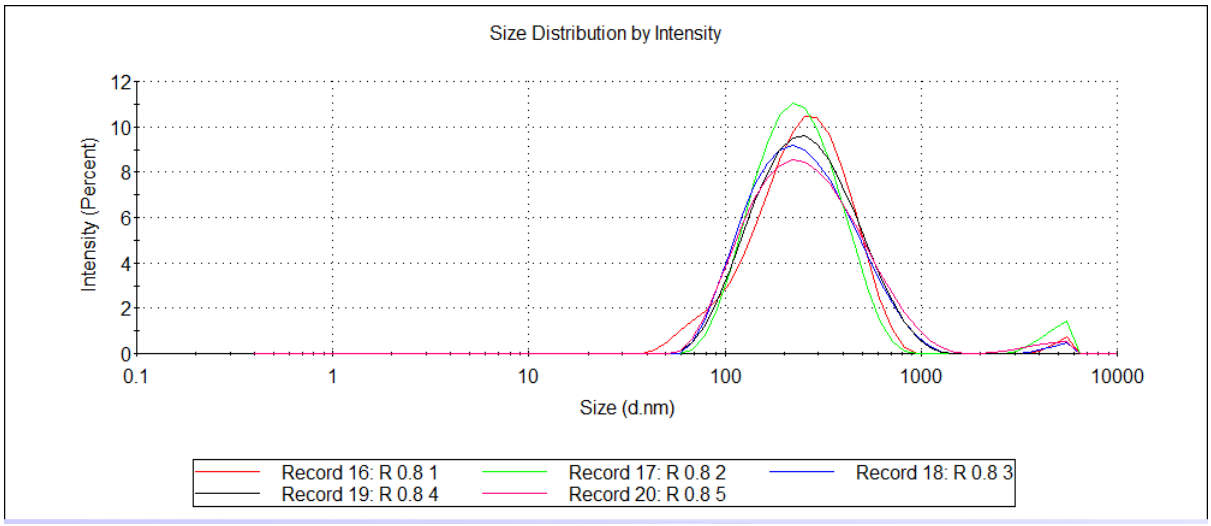

Figure 90: Size distribution by intensity, Retentate 0.8 DV

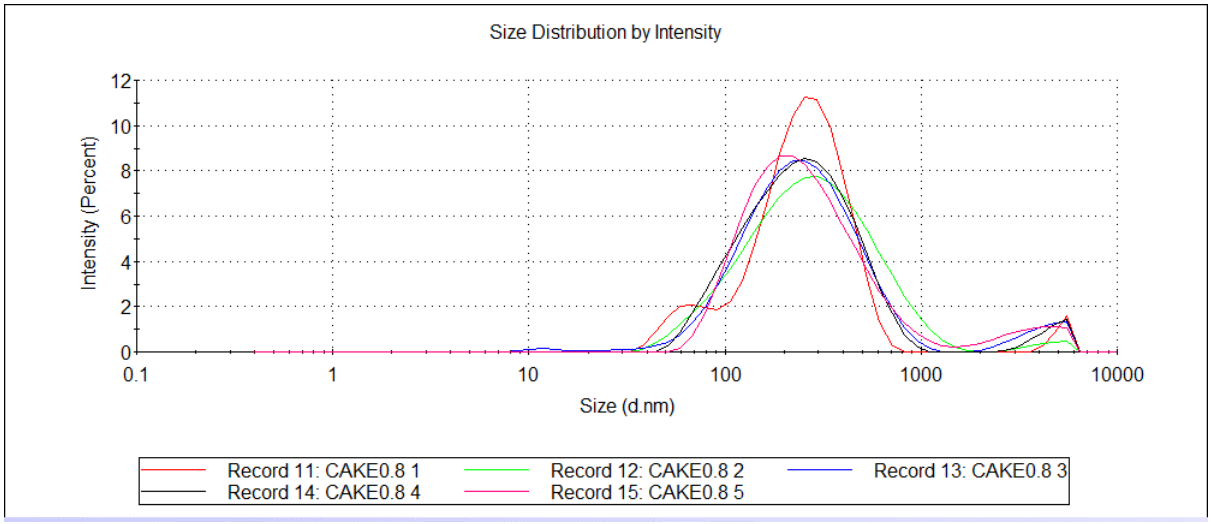

Figure 91: Size distribution by intensity, Cake 0.8 DV